

CLNS 07/1988
 EFI-06-15
 FERMILAB-PUB-07-006-T
 hep-ph/0701208
 April 12, 2007

QUARKONIA AND THEIR TRANSITIONS

Estia Eichten¹, Stephen Godfrey², Hanna Mahlke³, and Jonathan L. Rosner⁴

¹*Fermilab, P. O. Box 500, Batavia, IL 60510*

²*Ottawa Carleton Institute for Physics, Department of Physics, Carleton University,
 1125 Colonel By Drive, Ottawa, ON K1S 5B6, Canada*

³*Laboratory for Elementary-Particle Physics, Cornell University, Ithaca NY 14853*

⁴*Enrico Fermi Institute and Department of Physics, University of Chicago
 5640 South Ellis Avenue, Chicago, IL 60637*

Abstract

Valuable data on quarkonia (the bound states of a heavy quark $Q = c, b$ and the corresponding antiquark) have recently been provided by a variety of sources, mainly e^+e^- collisions, but also hadronic interactions. This permits a thorough updating of the experimental and theoretical status of electromagnetic and strong transitions in quarkonia. We discuss $Q\bar{Q}$ transitions to other $Q\bar{Q}$ states, with some reference to processes involving $Q\bar{Q}$ annihilation.

PACS numbers: 13.20.Gd, 13.25.Gv, 14.40.Gx, 13.40.Hq

Contents

1	INTRODUCTION	3
2	OVERVIEW OF QUARKONIUM LEVELS	3
3	THEORETICAL UNDERPINNINGS	5
3.1	Quarks and potential models	5
3.1.1	Validity of nonrelativistic description	5
3.1.2	Role of leptonic partial widths: $ \Psi(0) ^2$	5
3.1.3	Spin-dependent interactions	6
3.2	QCD on the lattice	7
3.3	Electromagnetic transitions	8
3.3.1	Magnetic dipole transitions	8
3.3.2	Electric dipole transitions	9
3.3.3	Higher multipole contributions in charmonium	9
3.4	Perturbative QCD and decays involving gluons	10
3.5	Hadronic transitions $[Q\bar{Q} \rightarrow (Q\bar{Q})' + (\text{light hadrons})]$	10

4	CHARMONIUM	12
4.1	The J/ψ	12
4.1.1	$J/\psi \rightarrow \gamma\eta_c$	13
4.1.2	New measurements of leptonic branching ratios	13
4.1.3	Hadronic, $gg\gamma$, and $\gamma\gamma\gamma$ decays: Extraction of α_S	13
4.2	The η_c	14
4.3	P -wave χ_{cJ} states	15
4.3.1	Production and decay via E1 transitions	15
4.3.2	Search for M2 transitions	19
4.3.3	Hadronic and $\gamma\gamma$ decays	19
4.4	The $\psi(2S)$	20
4.4.1	Decay to $\gamma\eta_c(1S)$	21
4.4.2	Decay to $\gamma\eta_c(2S)$	21
4.4.3	Hadronic transitions from $\psi(2S)$ to J/ψ	21
4.4.4	Light-hadron decays	22
4.5	The $h_c(1^1P_1)$	23
4.5.1	Significance of h_c mass measurement	23
4.5.2	Detection in $\psi(2S) \rightarrow \pi^0 h_c \rightarrow \pi^0 \gamma \eta_c$	23
4.5.3	Detection in the exclusive process $p\bar{p} \rightarrow h_c \rightarrow \gamma \eta_c \rightarrow 3\gamma$	25
4.6	The $\eta_c(2S)$	25
4.7	The $\psi(3770)$	26
4.7.1	ψ'' as a “charm factory”	26
4.7.2	Leptonic width and mixing	26
4.7.3	ψ'' transitions to $\pi\pi J/\psi$	27
4.7.4	ψ'' transitions to $\gamma\chi_{cJ}$	27
4.7.5	ψ'' transitions to light-hadron final states	27
4.8	$\psi(4040)$ and $\psi(4160)$	28
4.9	New Charmonium-like States	28
4.9.1	$X(3872)$	29
4.9.2	$Z(3930)$	32
4.9.3	$Y(3940)$	33
4.9.4	$X(3940)$	34
4.9.5	$Y(4260)$	36
4.9.6	A state in $\pi^+\pi^-\psi(2S)$	39
5	BOTTOMONIUM	40
5.1	Overview	40
5.2	$\Upsilon(1S, 2S, 3S)$	41
5.2.1	Leptonic branching ratios and partial widths	41
5.2.2	$\gamma gg/ggg$ ratios	42
5.3	E1 transitions between $\chi_{bJ}(nP)$ and S states	42
5.4	D -wave states	43
5.5	New hadronic transitions	46
5.5.1	$\chi'_{b1,2} \rightarrow \omega\Upsilon(1S)$	46
5.5.2	$\chi'_{b1,2} \rightarrow \chi_{b1,2}$	46

5.5.3	Searches for $\Upsilon(2S, 3S) \rightarrow \eta\Upsilon(1S)$	46
5.6	Searches for spin-singlets	47
5.7	$\Upsilon(4S)$	47
6	INTERPOLATION: $b\bar{c}$ LEVELS	48
7	SUMMARY	48

1 INTRODUCTION

Quarkonium spectroscopy has celebrated a great resurgence in the past few years thanks to a wealth of new information, primarily from electron-positron colliders, but also from hadronic interactions. Transitions between quarkonium states shed light on aspects of quantum chromodynamics (QCD), the theory of the strong interactions, in both the perturbative and the non-perturbative regimes. In the present article we review the new information on these states and their transitions and indicate theoretical implications, updating earlier discussions such as those in Refs. [1–9] (which may be consulted for explicit formulae).

We shall deal with states composed of a heavy quark $Q = c$ or b and the corresponding antiquark \bar{Q} . We shall discuss $Q\bar{Q}$ transitions primarily to other $Q\bar{Q}$ states, with some reference to processes involving $Q\bar{Q}$ annihilation, and will largely bypass decays to open flavor (treated, for example, in Refs. [7–11]).

A brief overview of the data on the charmonium and Υ systems is provided in Section 2. We then review theoretical underpinnings in Section 3, discussing quarks and potential models, lattice gauge theory approaches, perturbative QCD and decays involving gluons, and hadronic transitions of the form $Q\bar{Q} \rightarrow (Q\bar{Q})' + (\text{light hadrons})$. Section 4 is devoted to charmonium and Section 5 to the $b\bar{b}$ levels. Interpolation to the $b\bar{c}$ system is briefly mentioned in Section 6, while Section 7 summarizes.

2 OVERVIEW OF QUARKONIUM LEVELS

Since the discovery of the J/ψ more than thirty years ago, information on quarkonium levels has grown to the point that more is known about the $c\bar{c}$ and $b\bar{b}$ systems than about their namesake positronium, the bound state of an electron and a positron. The present status of charmonium ($c\bar{c}$) levels is shown in Fig. 1, while that of bottomonium ($b\bar{b}$) levels is shown in Fig. 2.

The levels are labeled by S , P , D , corresponding to relative orbital angular momentum $L = 0, 1, 2$ between quark and antiquark. (No candidates for $L \geq 3$ states have been seen yet.) The spin of the quark and antiquark can couple to either $S = 0$ (spin-singlet) or $S = 1$ (spin-triplet) states. The parity of a quark-antiquark state with orbital angular momentum L is $P = (-1)^{L+1}$; the charge-conjugation eigenvalue is $C = (-1)^{L+S}$. Values of J^{PC} are shown at the bottom of each figure. States are

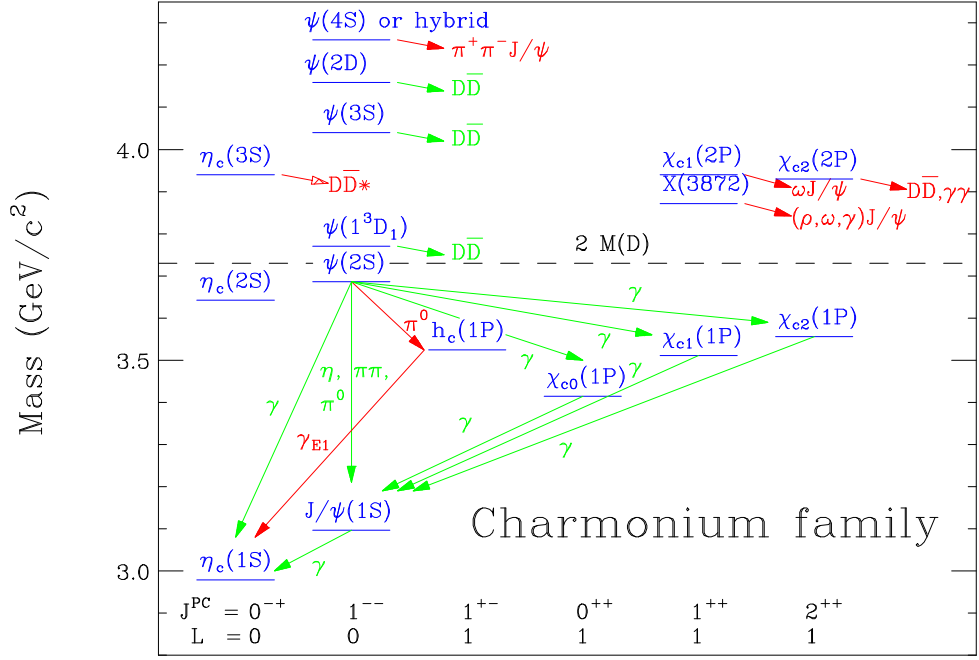


Figure 1: Transitions among charmonium states. Red (dark) arrows denote recent observations.

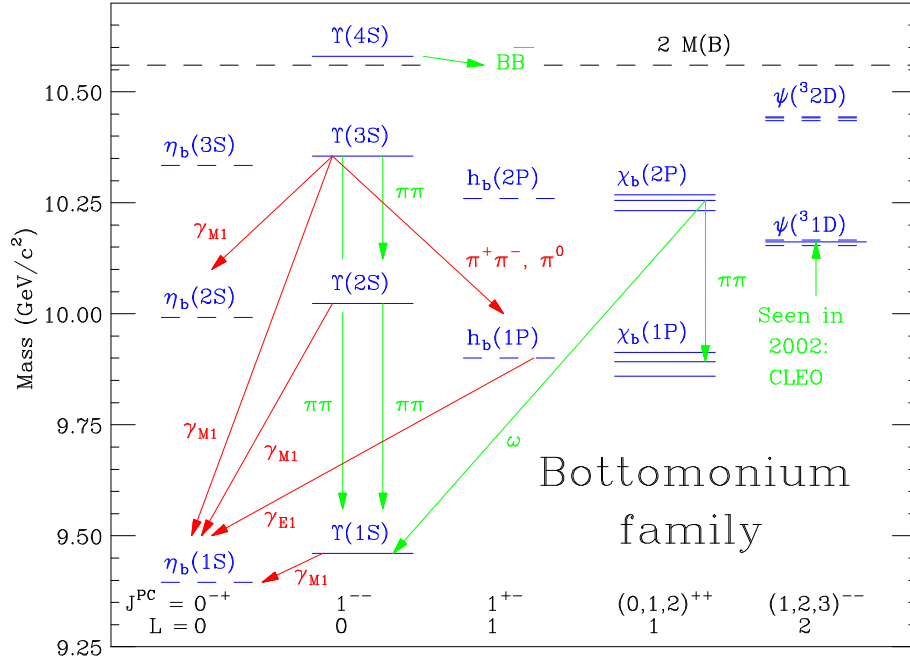


Figure 2: Transitions among $b\bar{b}$ levels. There are also numerous electric dipole transitions $S \leftrightarrow P \leftrightarrow D$ (not shown). Red (dark) arrows denote objects of recent searches.

often denoted by ${}^{2S+1}[L]_J$, with $[L] = S, P, D, \dots$. Thus, $L = 0$ states can be 1S_0 or 3S_1 ; $L = 1$ states can be 1P_1 or ${}^3P_{0,1,2}$; $L = 2$ states can be 1D_2 or ${}^3D_{1,2,3}$, and so on.

3 THEORETICAL UNDERPINNINGS

3.1 Quarks and potential models

An approximate picture of quarkonium states may be obtained by describing them as bound by an interquark force whose short-distance behavior is approximately Coulombic (with an appropriate logarithmic modification of coupling strength to account for asymptotic freedom) and whose long-distance behavior is linear to account for quark confinement. An example of this approach is found in Ref. [12]; early reviews may be found in Refs. [13–16]. Reference [17] presents more recent results.

3.1.1 Validity of nonrelativistic description

In order to estimate whether a nonrelativistic (NR) quarkonium description makes sense, “cartoon” versions of $c\bar{c}$ and $b\bar{b}$ spectra may be constructed by noting that the level spacings are remarkably similar in the two cases. They would be exactly equal if the interquark potential were of the form $V(r) = C \log(r/r_0)$ [18], which may be regarded as a phenomenological interpolation between the short-distance $\sim -1/r$ and long-distance $\sim r$ behaviors expected from QCD. In such a potential the expectation value of the kinetic energy $\langle T \rangle = (r/2)(dV/dr)$ is just $C/2 \simeq 0.37$ GeV with $C = 0.733$ as found in Ref. [15]. Since $\langle T \rangle = 2 \cdot (1/2)m_Q \langle v^2 \rangle$, one has $\langle v^2 \rangle \simeq 0.5$ for a charmed quark of mass $m_c \simeq 1.5$ GeV/ c^2 (roughly half the J/ψ mass), and $\langle v^2 \rangle \simeq 0.15$ for a b quark of mass $m_b \simeq 4.9$ GeV/ c^2 (roughly half the $\Upsilon(1S)$ mass). Thus a nonrelativistic description for charmonium is quite crude, whereas it begins to be accurate at the 15% level for $b\bar{b}$ states.

3.1.2 Role of leptonic partial widths: $|\Psi(0)|^2$

The partial widths for 3S_1 states to decay to a lepton pair through a virtual photon are a probe of the squares $|\Psi_n(0)|^2$ of the relative $n{}^3S_1$ wave functions at the origin through the relation [19]

$$\Gamma(n{}^3S_1 \rightarrow e^+e^-) = \frac{16\pi\alpha^2 e_Q^2 |\Psi_n(0)|^2}{M_n^2} \left(1 - \frac{16\alpha_S}{3\pi} + \dots \right), \quad (1)$$

where $e_Q = 2/3$ or $-1/3$ is the quark charge, M_n is the mass of the $n{}^3S_1$ state, and the last term is a QCD correction (see [3]). Thus leptonic partial widths are a probe of the compactness of the quarkonium system, and provide important information complementary to level spacings. Indeed, for the phenomenologically adequate potential $V(r) = C \log(r/r_0)$, a change in the quark mass m_Q can be compensated by a change in r_0 without affecting quarkonium mass predictions (r_0 can be viewed as setting the overall energy scale), whereas a larger quark mass will lead to a spatially more compact bound state and hence to an increased value of $|\Psi(0)|^2$ for each state. A more

general form is the power-law potential, $V(r) \sim \text{sgn}(\nu)r^\nu$, which approaches the logarithmic potential in the limit of $\nu \rightarrow 0$. One can show that in the power-law potential lengths scale as $m_Q^{-1/(2+\nu)}$ and hence $|\Psi(0)|^2$ scales as $m_Q^{3/(2+\nu)}$, or $\sim m_Q^3, m_Q^{3/2}, m_Q$ for $\nu = -1, 0, 1$ [15]. (In charmonium and bottomonium the ground states have sizes of about 0.4–0.5 fm and 0.2 fm, respectively [20].) Thus the effective quark mass in a potential description is constrained by measured leptonic widths. One can expect that in more fundamental descriptions (such as lattice gauge theories, to be discussed in Section 3.2), similar constraints will hold.

The scaling of leptonic widths from the charmonium to the bottomonium family can be roughly estimated using the above discussion, assuming an effective power $\nu \simeq 0$. In that case the leptonic width for each n scales as $\Gamma_{ee}(nS) \propto e_Q^2 |\Psi(0)|^2 / m_Q^2 \propto e_Q^2 / m_Q^{1/2}$. As the QCD correction in Eq. (1) is appreciable [as are relativistic corrections, particularly for charmonium], this is only an approximate rule.

The important role of leptonic widths is particularly evident in constructions of the interquark potential based on inverse-scattering methods [20, 21]. The reduced radial wave functions $u_{nS}(r) = r\Psi_{nS}(r)$ on the interval $0 \leq r < \infty$ for an S -wave Schrödinger equation with central potential $V(r)$ may be regarded as the odd-parity levels (since they must vanish at $r = 0$) in a symmetric potential $V(-r) = V(r)$ on the interval $-\infty < r < \infty$. The information one would normally require from the masses of the fictitious even-parity levels [with $u(0) \neq 0$] is provided by the leptonic widths of the nS levels, which provide the quantities $|\Psi(0)| = |u'_{nS}(0)|$. Thus, if QCD and relativistic corrections can be brought under control, leptonic widths of the S -wave levels are every bit as crucial as their masses.

A recent prediction of the leptonic width ratio $\Gamma_{ee}[\Upsilon(2S)]/\Gamma_{ee}[\Upsilon(1S)] = 0.43 \pm 0.05$ in lattice QCD [22] raises the question of what constitutes useful measurement and prediction precisions, both for ratios and for absolute leptonic widths. (For comparison, the CLEO Collaboration has measured this ratio to be 0.457 ± 0.006 [23].) Potential models have little trouble in predicting ratios $\Gamma_{ee}(n'S)/\Gamma_{ee}(nS)$ to an accuracy of a few percent, and one would thus hope for lattice approaches eventually to be capable of similar accuracy. Much more uncertainty is encountered by potential modes in predicting *absolute* leptonic widths as a result of QCD and relativistic corrections (see, for example, the inverse-scattering approach of Ref. [20]). Measurements with better than a few percent accuracy, such as those in Ref. [23] and others to be discussed presently, thus outstrip present theoretical capabilities.

3.1.3 Spin-dependent interactions

Hyperfine and fine-structure splittings in quarkonium are sensitive to the Lorentz structure of the interquark interaction [1, 7, 13, 14]. One may regard the effective potential $V(r)$ as the sum of Lorentz vector V_V and Lorentz scalar V_S contributions. The spin-spin interaction is due entirely to the Lorentz vector:

$$V_{SS}(r) = \frac{\sigma_Q \cdot \sigma_{\bar{Q}}}{6m_Q^2} \nabla^2 V_V(r) \quad , \quad (2)$$

where σ_Q and $\sigma_{\bar{Q}}$ are Pauli matrices acting on the spins of the quark and antiquark, respectively. For a Coulomb-like potential $\sim -1/r$ the Laplacian is proportional to $\delta^3(r)$, so that $V_{SS}(r)$ contributes to hyperfine splittings only for S waves, whose wave functions are non-zero at the origin. In QCD the coupling constant undergoes slow (logarithmic) variation with distance, leading to small non-zero contributions to hyperfine splittings for $L > 0$ states. Relativistic corrections also result in small non-zero contributions to these splittings.

Both spin-orbit and tensor forces affect states with $L > 0$. The spin-orbit potential is

$$V_{LS}(r) = \frac{L \cdot S}{2m_Q^2 r} \left(3 \frac{dV_V}{dr} - \frac{dV_S}{dr} \right) , \quad (3)$$

where L is the relative orbital angular momentum of Q and \bar{Q} , while S is the total quark spin. The tensor potential is [17, 24]

$$V_T(r) = \frac{S_T}{12m_Q^2} \left(\frac{1}{r} \frac{dV_V}{dr} - \frac{d^2V_V}{dr^2} \right) , \quad (4)$$

with $S_T \equiv 2[3(S \cdot \hat{r})(S \cdot \hat{r}) - S^2]$ (where $S = S_Q + S_{\bar{Q}}$ is the total spin operator and \hat{r} is a unit vector) has non-zero expectation values only for $L > 0$ [e.g., $-4, 2, -2/5$ for ${}^3P_{0,1,2}$ states].

3.2 QCD on the lattice

At momentum scales less than about 2 GeV/ c (distance scales greater than about 0.1 fm) the QCD coupling constant $\alpha_S(Q^2)$ becomes large enough that perturbation theory cannot be used. The value $\alpha_S(m_\tau^2) = 0.345 \pm 0.010$ [25, 26] is just about at the limit of usefulness of perturbation theory, and $\alpha_S(Q^2)$ increases rapidly below this scale. One must resort to non-perturbative methods to describe long-distance hadronic interactions.

If space-time is discretized, one can overcome the dependence in QCD on perturbation theory. Quark confinement is established using this lattice gauge theory approach. An accurate description of the heavy quarkonium spectrum can be obtained once one takes account of degrees of freedom associated with the production of pairs of light (u, d, s) quarks [27].

Lattice QCD also provides a theoretical underpinning for the phenomenological potential model approach. The well-measured static energy between a heavy quark-antiquark pair justifies the form of the nonrelativistic potential [28]. Recently, high-accuracy lattice calculations of the spin-dependent potentials have also been made [29]. This approach allows the direct determination of the spin-orbit, spin-spin and tensor potentials as well.

We shall quote lattice QCD predictions for several quantities throughout this article.

3.3 Electromagnetic transitions

The theory of electromagnetic (EM) transitions between quarkonium states is straightforward with terminology and techniques familiar from the study of EM transitions in atomic and nuclear systems. Although electromagnetic transition amplitudes can be computed from first principles in lattice QCD these calculations are in their infancy. At the present time only potential model approaches provide the detailed predictions that can be compared to experimental results. In this approach the spatial dependence of EM transition amplitudes reduces to functions of quark position and momentum between the initial and final state wave functions. Expanding the matrix elements in powers of photon momentum generates the electric and magnetic multipole moments and is also an expansion in powers of velocity. The leading order transition amplitudes are electric dipole (E1) and magnetic dipole (M1). In what follows we shall take $m_c = 1.5 \text{ GeV}/c^2$ and $m_b = 4.9 \text{ GeV}/c^2$ [3], which are considered “constituent-quark” values, appropriate to the non-perturbative regime found in charmonium and bottomonium.

3.3.1 Magnetic dipole transitions

Magnetic dipole transitions flip the quark spin, so their amplitudes are proportional to the quark magnetic moment and therefore inversely proportional to the constituent quark mass. At leading order the magnetic dipole (M1) amplitudes between S -wave states are independent of the potential model: The orthogonality of states guarantees that the spatial overlap is one for states within the same multiplet and zero for transitions between multiplets which have different radial quantum numbers.

Including relativistic corrections due to spin dependence in the Hamiltonian spoils this simple scenario and induces a small overlap between states with different radial quantum numbers. Such $n \neq n'$ transitions are referred to as “hindered”. Including finite size corrections the rates are given by [12]

$$\left\{ \begin{array}{l} \Gamma(n^3 S_1 \rightarrow n'^1 S_0 + \gamma) \\ \Gamma(n^1 S_0 \rightarrow n'^3 S_1 + \gamma) \end{array} \right\} = 4\alpha e_Q^2 k^3 (2J_f + 1) |\langle f | j_0(kr/2) | i \rangle|^2 / 3m_Q^2 \quad , \quad (5)$$

where $e_Q = 2/3$ or $-1/3$ is the quark charge, k is the photon energy, $j_0(x) = \sin x/x$, and m_Q is the quark mass. The only M1 transitions between quarkonia states so far observed occur in charmonium, but the corresponding transitions in $b\bar{b}$ systems are the objects of current searches. For small k , $j_0(kr/2) \rightarrow 1$, so that transitions with $n' = n$ have favored matrix elements, though the corresponding partial decay widths are suppressed by smaller k^3 factors.

Numerous papers have studied these M1 transitions including full relativistic corrections [4, 30–35]. They depend explicitly on the Lorentz structure of the nonrelativistic potential. Several sources of uncertainty make M1 transitions particularly difficult to calculate. In addition to issues of relativistic corrections and what are known as “exchange currents,” there is the possibility of an anomalous magnetic moment of the quark (κ_Q). Furthermore, the leading-order results depend explicitly on the constituent quark masses, and corrections depend on the Lorentz structure of the potential.

3.3.2 Electric dipole transitions

The partial widths for electric dipole (E1) transitions between states $^{2S+1}3L_{iJ_i}$ and $^{2S+1}L_{fJ_f}$ are given by [12]

$$\Gamma(n^{2S+1}L_{iJ_i} \rightarrow n'^{2S+1}L_{fJ_f} + \gamma) = \frac{4\alpha e_Q^2 k^3}{3} (2J_f + 1) \mathcal{S}_{if} |\langle f|r|i \rangle|^2 \quad . \quad (6)$$

The statistical factor \mathcal{S}_{if} is

$$\mathcal{S}_{if} = \mathcal{S}_{fi} = \max(L_i, L_f) \begin{Bmatrix} J_i & 1 & J_f \\ L_f & S & L_i \end{Bmatrix} \quad . \quad (7)$$

For transitions between spin-triplet S -wave and P -wave states, $\mathcal{S}_{if} = \frac{1}{9}$. Expressions for $P \leftrightarrow D$ transitions, which have also been observed both in charmonium and in the $b\bar{b}$ system, are given, for example, in Ref. [2].

The leading corrections for electric dipole corrections have been considered by a number of authors [30–32, 34–41]. A general form was derived by Grotch, Owen and Sebastian [31]. There are three main types of corrections: relativistic modification of the nonrelativistic wave functions, relativistic modification of the electromagnetic transition operator, and finite-size corrections. In addition to these there are additional corrections arising from the quark anomalous magnetic moment. For the $^3P_J \leftrightarrow ^3S_1$ transitions in which we are primarily interested, the dominant relativistic corrections arise from modifications of the wavefunctions and are included by the quarkonium analog of Siegert's theorem [40, 42]. We will find that differences in theoretical assumptions of the various potential models make it difficult to draw sharp conclusions from the level of agreement of a particular model with experimental data. However, there is usually very little model variation in the NR predictions if the models are fit to the same states [2]. The only exceptions are transitions where the dipole matrix element exhibits large dynamical cancellations, for instance when higher radial excitations are involved which have nodes in their wavefunctions.

3.3.3 Higher multipole contributions in charmonium

Magnetic quadrupole (M2) amplitudes are higher order in v^2/c^2 . They are of interest because they provide an indirect measure of the charmed quark's magnetic moment [43] and are sensitive to D -wave admixtures in S -wave states, providing another means of studying the $1^3D_1 - 2^3S_1$ mixing in the $\psi'' - \psi'$ states [44, 45]. They affect angular distributions in decays such as $\psi' \rightarrow \chi_{cJ} + \gamma$ and $\chi_{cJ} \rightarrow J/\psi + \gamma$ and become experimentally accessible through interference with the dominant E1 amplitudes.

The $\chi_{cJ} \rightarrow \gamma J/\psi$ or $\psi' [= \psi(2S)] \rightarrow \gamma \chi_{cJ}$ decays may be described by the respective helicity amplitudes A_λ or A'_λ , in which λ labels the projection of the spin of the χ_{cJ} parallel (for A_λ) or antiparallel (for A'_λ) to the photon, which is assumed to have helicity +1. The radiative widths are given in terms of these amplitudes by

$$\Gamma(\psi' \rightarrow \gamma \chi_{cJ}) = \frac{E_\gamma^3}{3} \sum_{\lambda \geq 0} |A'_\lambda|^2 \quad , \quad (8)$$

$$\Gamma(\chi_{cJ} \rightarrow J/\psi) = \frac{E_\gamma^3}{2J+1} \sum_{\lambda \geq 0} |A_\lambda|^2 . \quad (9)$$

In terms of a parameter $\epsilon \equiv \xi E_\gamma / (4m_c)$, where $\xi = -1$ for $\psi' \rightarrow \gamma \chi_{cJ}$ and $\xi = +1$ for $\chi_{cJ} \rightarrow \gamma J/\psi$, the predicted helicity amplitudes A_λ or A'_λ are in the relative proportions [43]:

$$\chi_{c2} : A_2 = \sqrt{6}[1 + \epsilon(1 + \kappa_c)] \quad (10)$$

$$A_1 = \sqrt{3}[1 - \epsilon(1 + \kappa_c)] \quad (11)$$

$$A_0 = [1 - 3\epsilon(1 + \kappa_c)] \quad (12)$$

$$\chi_{c1} : A_1 = \sqrt{3}[1 + \epsilon(1 + \kappa_c)] \quad (13)$$

$$A_0 = \sqrt{3}[1 - \epsilon(1 + \kappa_c)] \quad (14)$$

$$\chi_{c0} : A_0 = \sqrt{2}[1 - 2\epsilon(1 + \kappa_c)] . \quad (15)$$

Here an overall E1 amplitude has been factored out, and κ_c is the charmed quark's anomalous magnetic moment.

3.4 Perturbative QCD and decays involving gluons

Many quarkonium decays proceed through annihilation of $Q\bar{Q}$ into final states consisting of gluons and possibly photons and light-quark pairs. Expressions for partial widths of color-singlet $Q\bar{Q}$ systems are given in Ref. [3], and have been updated in Ref. [46]. In that work, annihilation rates are also given for the color-octet component of the $Q\bar{Q}$ system, which appears necessary for successful description of $Q\bar{Q}$ production in hadronic interactions. We shall confine our discussion to the effects of the color-singlet $Q\bar{Q}$ component in decays. Discrepancies between theory and experiment can be ascribed in part to neglected relativistic effects (particularly in charmonium) and in part to the neglected color-octet component.

3.5 Hadronic transitions [$Q\bar{Q} \rightarrow (Q\bar{Q})' + (\text{light hadrons})$]

A number of transitions from one $Q\bar{Q}$ state to another occur with the emission of light hadrons. So far, the observed transitions in charmonium include $\psi(2S) \rightarrow J/\psi \pi^+ \pi^-$, $\psi(2S) \rightarrow J/\psi \pi^0 \pi^0$, $\psi(2S) \rightarrow J/\psi \eta$, $\psi(2S) \rightarrow J/\psi \pi^0$, and $\psi(2S) \rightarrow h_c \pi^0$. In addition, above charm threshold a state $X(3872)$ decays to $J/\psi \pi^+ \pi^-$, and a state $Y(3940)$ decays to $J/\psi \omega$. The observed transitions in the $b\bar{b}$ system include $\Upsilon(2S) \rightarrow \Upsilon(1S) \pi \pi$, $\Upsilon(3S) \rightarrow \Upsilon(1S, 2S) \pi \pi$, $\chi'_{b1,2} \rightarrow \Upsilon(1S) \omega$, and $\chi'_{bJ} \rightarrow \chi_{bJ} \pi \pi$. Many of these transitions have been observed only in the past few years (see later sections for experimental data).

The theoretical description of hadronic transitions uses a multipole expansion for gluon emission developed in Refs. [47, 48]. Formally, it resembles the usual multipole expansion for photonic transitions discussed in Section 3.3. The interaction for color electric and magnetic emission from a heavy quark is given by

$$H_I = \int d^3x Q^\dagger(x) \mathbf{t}^a [\mathbf{x} \cdot \mathbf{E}_a(\mathbf{x}) + \boldsymbol{\sigma} \cdot \mathbf{B}_a(\mathbf{x})] Q(x) + \dots , \quad (16)$$

where \mathbf{t}^a ($a = 1, \dots, 8$) is a generator of color SU(3), and the $(\bar{Q})Q$ and \mathbf{E}, \mathbf{B} are dressed (anti)quarks and color electric and magnetic fields [48]. As usual, the multipole expansion arises from the expanding the color-electric and color-magnetic fields about their values at the center of mass of the initial quarkonium state. However, unlike EM transitions, a single interaction of H_I changes a color singlet $Q\bar{Q}$ initial state (i) into some color octet $Q\bar{Q}$ state. Therefore, a second interaction H_I is required to return to a color singlet $Q\bar{Q}$ final state (f). In the overall process at least two gluons are emitted. Assuming factorization for the quarkonium systems [49], the full transition amplitude can be expressed as a product of two subamplitudes: One that acts on the quarkonium system to produce the multipole transition and a second that creates the final light hadrons (H) from the action of the gluonic operators on the vacuum state.

In non-relativistic QCD (NRQCD) [50], the strength of the various interactions can be ordered in powers of the heavy quark velocity v . The leading behavior comes from two color-electric (E1) gluon emissions. This amplitude can be written in the factorized form [49]:

$$\sum_{\mathcal{O}} \frac{\langle i | \mathbf{r}^j \mathbf{t}^a | \mathcal{O} \rangle \langle \mathcal{O} | \mathbf{r}^k \mathbf{t}^b | f \rangle}{E_i - E_{\mathcal{O}}} \langle 0 | \mathbf{E}_a^j \mathbf{E}_b^k | H \rangle \quad (17)$$

The sum runs over allowed $Q\bar{Q}$ octet intermediate states \mathcal{O} . Phenomenological models (e.g. the Buchmüller-Tye vibrating string model [51]) are used to estimate this quarkonium overlap amplitude. The quantum numbers of the initial and final quarkonium states determine which terms in the multipole expansion may contribute. For the light hadron amplitude the states allowed are determined by the overall symmetries. In transitions between various 3S_1 quarkonium states the leading term in the multipole expansion has two color-electric (E1) interactions. The lowest-mass light hadron state allowed is a two-pion state with either an S - or D -wave relative angular momentum. The form of the light hadron amplitude is determined by chiral symmetry considerations [52]:

$$\langle 0 | \mathbf{E}_a^j \mathbf{E}_b^k | \pi(k_1) \pi(k_2) \rangle = \delta_{ab} [c_1 \delta^{jk} k_1 \cdot k_2 + c_2 (k_1^j k_2^k + k_2^j k_1^k - \frac{2}{3} \delta^{jk} k_1 \cdot k_2)]. \quad (18)$$

The two unknowns (c_1, c_2) are the coefficients of the S -wave and D -wave two-pion systems. Their values are determined from experiment. Additional terms can arise in higher orders in v [53].

Hadronic transitions which can flip the heavy quark spins first occur in amplitudes with one color-electric (E1) and one color-magnetic (M1) interaction. These transitions are suppressed by an additional power of v relative to the purely electric transitions. Transitions involving two color-magnetic interactions (M1) are suppressed by an additional power of v . Many detailed predictions for hadronic transition rates can be found in Refs. [49, 53, 54].

4 CHARMONIUM

In what follows we shall quote masses and partial widths from Ref. [55] unless otherwise noted. The masses are used to calculate photon transition energies. We shall use an electromagnetic coupling constant $\alpha = 1/137.036$ in all cases. For emission of an on-shell photon this is appropriate. For processes such as leptonic decays of vector mesons mediated by a timelike virtual photon it is a slight underestimate. For gluon emission in $Q\bar{Q}$ annihilation we shall use a momentum-dependent strong coupling constant $\alpha_S(Q^2)$ evaluated at $Q^2 = m_Q^2$. The QCD corrections to the decay widths we quote are performed for this scale choice [3]. Typical values are $\alpha_S(m_c^2) \simeq 0.3$, $\alpha_S(m_b^2) \simeq 0.2$ [3]. A different scale choice would lead to different $\mathcal{O}(\alpha_S)$ corrections [56].

4.1 The J/ψ

The J/ψ was the first charmonium state discovered, in 1974 [57, 58]. It is the lowest 3S_1 $c\bar{c}$ state and thus can couple directly to virtual photons produced in e^+e^- collisions. The most precise mass determination to date comes from the KEDR collaboration [59], $m(J/\psi) = 3096.917 \pm 0.010 \pm 0.007$ MeV, a relative uncertainty of 4×10^{-6} .

The J/ψ intrinsic width can only be determined indirectly. Recent measurements were carried out [60, 61] using the radiative return process $e^+e^- \rightarrow \gamma e^+e^- \rightarrow \gamma J/\psi \rightarrow \gamma(\mu^+\mu^-)$. The experimental observable is the radiative cross-section, a convolution of the photon emission probability and the J/ψ Breit-Wigner resonance shape. It is calculable and proportional to the coupling of the J/ψ to the annihilating e^+e^- pair and the J/ψ decay branching fraction, $\Gamma_{ee} \times \mathcal{B}(J/\psi \rightarrow \mu^+\mu^-)$. Interference with the QED process $e^+e^- \rightarrow \gamma\mu^+\mu^-$ introduces an asymmetry around the J/ψ peak in $m(\mu^+\mu^-)$ and must be taken into account. $\mathcal{B}(J/\psi \rightarrow \mu^+\mu^-)$ is known well, hence the product gives access to Γ_{ee} and, together with $\mathcal{B}(J/\psi \rightarrow \mu^+\mu^-)$, to Γ_{tot} . The current world average is $\Gamma(J/\psi) = 93.4 \pm 2.1$ keV [55].

The largest data sample now consists of 58 million J/ψ collected by the BES-II Collaboration at the Beijing Electron Synchrotron. Decays from the $\psi(2S)$ state, in particular $\psi(2S) \rightarrow \pi^+\pi^- J/\psi \rightarrow \pi^+\pi^- \text{hadrons}$, offer a very clean avenue to study J/ψ final states, yielding one $\pi^+\pi^- J/\psi$ event per three $\psi(2S)$ produced. Experimentally, this can be handled by requiring a $\pi^+\pi^-$ pair recoiling against a system of $M(J/\psi)$, without further identification of the J/ψ decay products. This path also eliminates contamination of the sample by continuum production of a final state under study, $e^+e^- \rightarrow \gamma^* \rightarrow \text{hadrons}$. Other J/ψ production mechanisms include $p\bar{p}$ collisions and radiative return from e^+e^- collisions with center-of-mass energy $> M(J/\psi)$. Many decays of J/ψ to specific states of light hadrons provide valuable information on light-hadron spectroscopy. Here we shall be concerned primarily with its decay to the $\eta_c(1^1S_0)$, the lightest charmonium state of all; its annihilation into lepton pairs; and its annihilation into three gluons, two gluons and a photon, and three photons.

4.1.1 $J/\psi \rightarrow \gamma\eta_c$

The rate predicted for the process $J/\psi \rightarrow \gamma\eta_c$ on the basis of Eq. (5) is $\Gamma(J/\psi \rightarrow \gamma\eta_c) = 2.85$ keV. Here we have taken the photon energy to be 114.3 MeV based on $M(J/\psi) = 3096.916$ MeV and $M(\eta_c) = 2980.4$ MeV, and have assumed that the matrix element of $j_0(kr/2)$ between initial and final states is 1. With $\Gamma_{\text{tot}}(J/\psi) = (93.4 \pm 2.1)$ keV, this implies a branching ratio $\mathcal{B}(J/\psi \rightarrow \gamma\eta_c) = (3.05 \pm 0.07)\%$. The branching ratio observed in Ref. [62] is considerably less, $\mathcal{B}_{\text{exp}}(J/\psi \rightarrow \gamma\eta_c) = (1.27 \pm 0.36)\%$, calling for re-examination both of theory and experiment.

One might be tempted to ascribe the discrepancy to relativistic corrections or the lack of wave function overlap generated by a relatively strong hyperfine splitting. A calculation based on lattice QCD does not yet provide a definitive answer [63], though it tends to favor a larger decay rate. Theoretical progress may also be made using a NRQCD approach [64]. Part of the ambiguity is associated with the effective value of the charmed quark mass, which we take to be $1.5 \text{ GeV}/c^2$.

4.1.2 New measurements of leptonic branching ratios

New leptonic J/ψ branching ratios were measured by the CLEO Collaboration [65] by comparing the transitions $\psi(2S) \rightarrow \pi^+\pi^-J/\psi(1S) \rightarrow \pi^+\pi^-X$ with $\psi(2S) \rightarrow \pi^+\pi^-J/\psi(1S) \rightarrow \pi^+\pi^-\ell^+\ell^-$. The results, $\mathcal{B}(J/\psi \rightarrow e^+e^-) = (5.945 \pm 0.067 \pm 0.042)\%$, $\mathcal{B}(J/\psi \rightarrow \mu^+\mu^-) = (5.960 \pm 0.065 \pm 0.050)\%$, and $\mathcal{B}(J/\psi \rightarrow \ell^+\ell^-) = (5.953 \pm 0.056 \pm 0.042)\%$, are all consistent with, but more precise than, previous measurements.

4.1.3 Hadronic, $gg\gamma$, and $\gamma\gamma\gamma$ decays: Extraction of α_S

The partial decay rate of J/ψ to hadrons through the three-gluon final state in principle provides information on $\alpha_S(m_c^2)$ through the ratio

$$\frac{\Gamma(J/\psi \rightarrow ggg)}{\Gamma(J/\psi \rightarrow \ell^+\ell^-)} = \frac{5}{18} \left[\frac{M(J/\psi)}{2m_c} \right]^2 \frac{(\pi^2 - 9)[\alpha_S(m_c^2)]^3}{\pi\alpha^2} \left[1 + 1.6 \frac{\alpha_S}{\pi} \right] . \quad (19)$$

Both processes are governed by $|\Psi(0)|^2$, the squared magnitude of the S -wave charmonium wave function at the origin. In Ref. [3] a value of $\alpha_S(m_c^2) = 0.175 \pm 0.008$ was extracted from this ratio, which at the time was measured to be 9.0 ± 1.3 . This is far below what one expects from the running of α_S down to low momentum scales ($\alpha_S(m_c^2) \simeq 0.3$ [3, 25, 26]), highlighting the importance of relativistic corrections to Eq. (19). We shall update the value of the ratio as extracted from data, but the qualitative conclusion will remain the same.

The branching ratio $\mathcal{B}(J/\psi \rightarrow ggg)$ is inferred by counting all other decays, to $\gamma\eta_c$, $\ell^+\ell^-$, $\gamma^* \rightarrow \text{hadrons}$, and γgg . As mentioned earlier, we have $\mathcal{B}(J/\psi \rightarrow \gamma\eta_c) = (1.27 \pm 0.36)\%$ [62] and $\mathcal{B}(J/\psi \rightarrow \ell^+\ell^-) = (5.953 \pm 0.056 \pm 0.042)\%$ [65] for $\ell = e, \mu$. We use the value [66] $R_{e^+e^-} = 2.28 \pm 0.04$ at $E_{\text{cm}}/c^2 = M(J/\psi)$ and the leptonic branching ratio to estimate

$$\mathcal{B}(J/\psi \rightarrow \gamma^* \rightarrow \text{hadrons}) = R_{e^+e^-} \mathcal{B}(J/\psi \rightarrow \ell^+\ell^-) = (13.6 \pm 0.3)\% . \quad (20)$$

Thus the branching ratio of J/ψ to states other than $ggg + gg\gamma$ is $[(1.27 \pm 0.36) + (2 + 2.28 \pm 0.04)(5.953 \pm 0.070) = (26.75 \pm 0.53)]\%$. Finally, we use [67] $\Gamma(J/\psi \rightarrow \gamma gg)/\Gamma(J/\psi \rightarrow ggg) = (10 \pm 4)\%$ to infer $\Gamma(J/\psi \rightarrow ggg) = (66.6 \pm 2.5)\%\Gamma_{\text{tot}}(J/\psi)$. Then

$$\frac{\Gamma(J/\psi \rightarrow ggg)}{\Gamma(J/\psi \rightarrow \ell^+\ell^-)} = \frac{66.6 \pm 2.5}{5.953 \pm 0.070} = 11.2 \pm 0.4 \quad (21)$$

implying $\alpha_S(m_c^2) = 0.188_{-0.003}^{+0.002}$. Although somewhat higher than the earlier estimate, this is still far below what we will estimate from other decays, and indicates that the small hadronic width of the J/ψ remains a problem within a nonrelativistic approach. As mentioned earlier, this could have been anticipated. In particular the contribution of color-octet $Q\bar{Q}$ components is expected to be large [46, 68]. In any event, the hadronic width of the J/ψ provides a useful testing ground for any approach which seeks to treat relativistic effects in charmonium quantitatively. The ratio

$$\frac{\Gamma(J/\psi \rightarrow \gamma gg)}{\Gamma(J/\psi \rightarrow ggg)} = \frac{16}{5} \frac{\alpha}{\alpha_S(m_c^2)} \left[1 - 2.9 \frac{\alpha_S}{\pi} \right] = (10 \pm 4)\% \quad (22)$$

itself provides information on $\alpha_S(m_c^2)$ within a much larger range, yielding $\alpha_S(m_c^2) = 0.19_{-0.05}^{+0.10}$ as found in Ref. [3].

The decay $J/\psi \rightarrow \gamma\gamma\gamma$ is also governed by $|\Psi(0)|^2$. The ratio of its rate to that for $J/\psi \rightarrow ggg$ is [3]

$$\frac{\Gamma(J/\psi \rightarrow \gamma\gamma\gamma)}{\Gamma(J/\psi \rightarrow ggg)} = \frac{54}{5} e_Q^6 \left(\frac{\alpha}{\alpha_S} \right)^2 \frac{1 - 12.7\alpha_S/\pi}{1 - 3.7\alpha_S/\pi} = \frac{128}{135} \left(\frac{\alpha}{\alpha_S} \right)^2 \frac{1 - 12.7\alpha_S/\pi}{1 - 3.7\alpha_S/\pi} . \quad (23)$$

The last ratio is a QCD correction; $e_Q = 2/3$ for the charmed quark's charge. (For the $\Upsilon(1S)$ ratio, take $e_Q = -1/3$ and replace 3.7 by 4.9 in the denominator of the QCD correction term.) With $\alpha_S(m_c^2) = 0.3$, the uncorrected ratio is 1.4×10^{-5} . The large negative QCD correction indicates that this is only a rough estimate but probably an upper bound.

4.2 The η_c

Some progress has been made in pinning down properties of the $\eta_c(1S)$, but better measurements of its mass, total width, and two-photon partial width would still be welcome. The square of the wave function at the origin cancels out in the ratio of partial widths [3],

$$\frac{\Gamma(\eta_c \rightarrow \gamma\gamma)}{\Gamma(J/\psi \rightarrow \mu^+\mu^-)} = \frac{4}{3} \left[1 + 1.96 \frac{\alpha_S}{\pi} \right] . \quad (24)$$

Using the ‘‘evaluated’’ partial widths in Ref. [55], $\Gamma(\eta_c \rightarrow \gamma\gamma) = (7.2 \pm 0.7 \pm 2.0)$ keV and $\Gamma(J/\psi \rightarrow \mu^+\mu^-) = (5.55 \pm 0.14 \pm 0.02)$ keV, one finds that $(3/4)\Gamma(\eta_c \rightarrow \gamma\gamma)/\Gamma(J/\psi \rightarrow \mu^+\mu^-) = 0.97 \pm 0.29$, which is consistent with Eq. (24) but still not precisely enough determined to test the QCD correction. A more precise test would have taken into account $M(J/\psi) \neq 2m_c$ and the running of α_S .

The total width of η_c is dominated by the gg final state. Its value has not remained particularly stable over the years, with Ref. [55] quoting $\Gamma_{\text{tot}}(\eta_c) = (25.5 \pm 3.4)$ MeV.

This value is $(3.54 \pm 1.14) \times 10^3$ that of $\Gamma(\eta_c \rightarrow \gamma\gamma)$. The $gg/\gamma\gamma$ ratio is predicted [3] to be

$$\frac{\Gamma(\eta_c \rightarrow gg)}{\Gamma(\eta_c \rightarrow \gamma\gamma)} = \frac{9[\alpha_S(m_c^2)]^2}{8\alpha^2} \left[1 + 8.2 \frac{\alpha_S}{\pi} \right] \quad , \quad (25)$$

leading to $\alpha_S(m_c^2) = 0.30_{-0.05}^{+0.03}$. This value should be regarded with caution in view of the large QCD correction factor $1 + 8.2\alpha_S/\pi \sim 1.8$.

4.3 P -wave χ_{cJ} states

The $1P$ states of charmonium, χ_{cJ} , were first seen in radiative decays from the $\psi(2S)$. The χ_{cJ} states lie 128 / 171 / 261 MeV ($J = 2/1/0$) below the $\psi(2S)$. Their masses can most accurately be determined in $p\bar{p}$ collisions [69, 70], although a precise measurement of the photon energy in $\psi(2S) \rightarrow \gamma\chi_{cJ}$ allows a mass measurement as well in principle, given that the $\psi(2S)$ mass is very well known.

BES used photon conversions $\gamma \rightarrow e^+e^-$ to improve upon the photon energy resolution [71]. The $J = 0$ state is wide, about 10 MeV, while the $J = 1$ and $J = 2$ states are narrower (0.89 ± 0.05 MeV and 2.06 ± 0.12 MeV, respectively [55]), which is below detector resolution for most exclusive χ_{cJ} decays.

4.3.1 Production and decay via E1 transitions

E1 transitions have played an important role in quarkonium physics with the initial theoretical papers describing charmonium suggesting that the triplet $1P$ states could be observed through the E1 transitions from the ψ' resonance [12, 72]. It is a great success of this picture that the initial calculations by the Cornell group [12] agree within 25% of the present experimental values.

New studies have been performed by the CLEO Collaboration of the rates for $\psi(2S) \rightarrow \gamma\chi_{c0,1,2}$ [73] and $\psi(2S) \rightarrow \gamma\chi_{c0,1,2} \rightarrow \gamma\gamma J/\psi$ [74]. We shall use these data to extract the magnitudes of electric dipole matrix elements and compare them with various predictions.

The inclusive branching ratios and inferred rates for $\psi(2S) \rightarrow \gamma\chi_{cJ}$ are summarized in Table I. Photon energies are based on masses quoted in Ref. [55]. Branching ratios are from Ref. [73]. Partial widths are obtained from these using $\Gamma_{\text{tot}}[\psi(2S)] = 337 \pm 13$ keV [55]. The E1 matrix elements $|\langle 1P|r|2S \rangle|$ extracted using the nonrelativistic expression (6) are shown in the last column.

In the nonrelativistic limit the dipole matrix elements in ${}^3S_1 \rightarrow {}^3P_J$ transitions, $|\langle r \rangle_{\text{NR}}|$, for different J values are independent of J . Predictions of specific nonrelativistic potential models sit in a small range from 2.4 to 2.7 GeV^{-1} (see Fig. 3), with a slightly larger range obtained using potentials constructed from charmonium and $b\bar{b}$ data using inverse-scattering methods [20]. However the magnitudes of the matrix elements are observed with the ordering $|\langle \chi_{c2}|r|\psi(2S) \rangle| > |\langle \chi_{c1}|r|\psi(2S) \rangle| > |\langle \chi_{c0}|r|\psi(2S) \rangle|$. This is in accord with predictions that take into account relativistic corrections [31, 32, 34, 39, 40]. Fig. 3 shows that at least some models are in good agreement with the observed rates so that we can conclude that relativistic corrections can explain the observed rates. However, it is probably premature to say that

Table I: Properties of $\psi(2S) \rightarrow \gamma\chi_{cJ}$ decays, using results from Refs. [55] and [73] as well as Eq. (6).

J	k_γ (MeV)	\mathcal{B} [73] (%)	$\Gamma[\psi(2S) \rightarrow \gamma\chi_{cJ}]$ (keV)	$ \langle 1P r 2S \rangle $ (GeV $^{-1}$)
2	127.60 \pm 0.09	9.33 \pm 0.14 \pm 0.61	31.4 \pm 2.4	2.51 \pm 0.10
1	171.26 \pm 0.07	9.07 \pm 0.11 \pm 0.54	30.6 \pm 2.2	2.05 \pm 0.08
0	261.35 \pm 0.33	9.22 \pm 0.11 \pm 0.46	31.1 \pm 2.0	1.90 \pm 0.06

Table II: Properties of the exclusive transitions $\psi(2S) \rightarrow \gamma\chi_{cJ} \rightarrow \gamma\gamma J/\psi$.

J	$\mathcal{B}_1\mathcal{B}_2$ (%) [74]	\mathcal{B}_2 (%) [55]	Γ_{tot} (MeV) [55]
2	1.85 \pm 0.04 \pm 0.07	20.1 \pm 1.0	2.06 \pm 0.12
1	3.44 \pm 0.06 \pm 0.13	35.6 \pm 1.9	0.89 \pm 0.05
0	0.18 \pm 0.01 \pm 0.02	1.30 \pm 0.11	10.4 \pm 0.7

the transitions are totally understood given the large scatter of the predictions around the observed values.

Information on the electromagnetic cascades $\psi(2S) \rightarrow \gamma\chi_{cJ} \rightarrow \gamma\gamma J/\psi$ is summarized in Table II. The products $\mathcal{B}_1\mathcal{B}_2 \equiv \mathcal{B}[\psi(2S) \rightarrow \gamma\chi_{cJ}]\mathcal{B}[\chi_{cJ} \rightarrow \gamma J/\psi]$ are taken from Ref. [74]. These and prior measurements may be combined with values of \mathcal{B}_1 from Ref. [73] and previous references to obtain the values of \mathcal{B}_2 in the Table [55]. Other important data come from the high-statistics studies of Fermilab Experiment E835 [70], who also measure total χ_{cJ} widths and present partial widths for $\chi_{cJ} \rightarrow \gamma J/\psi$.

The partial widths for $\chi_{cJ} \rightarrow \gamma J/\psi$ extracted from PDG averages for \mathcal{B}_2 and the values of $\Gamma_{\text{tot}}(\chi_{c2,1,0})$ mentioned above are summarized in Table III. The dipole matrix elements have been extracted using Eq. (6) using photon energies obtained from the χ_{cJ} and J/ψ masses in Ref. [55].

Predictions from both nonrelativistic and relativistic calculations are shown in Fig. 4. Overall the nonrelativistic calculations, with typical values of 1.9 to 2.2 GeV $^{-1}$,

Table III: Properties of the transitions $\chi_{cJ} \rightarrow \gamma J/\psi$. (Ref. [55]; Eq. (6)).

J	k_γ (MeV)	$\Gamma(\chi_{cJ} \rightarrow \gamma J/\psi)$ (keV)	$ \langle 1S r 1P \rangle $ (GeV $^{-1}$)
2	429.63 \pm 0.08	416 \pm 32	1.91 \pm 0.07
1	389.36 \pm 0.07	317 \pm 25	1.93 \pm 0.08
0	303.05 \pm 0.32	135 \pm 15	1.84 \pm 0.10

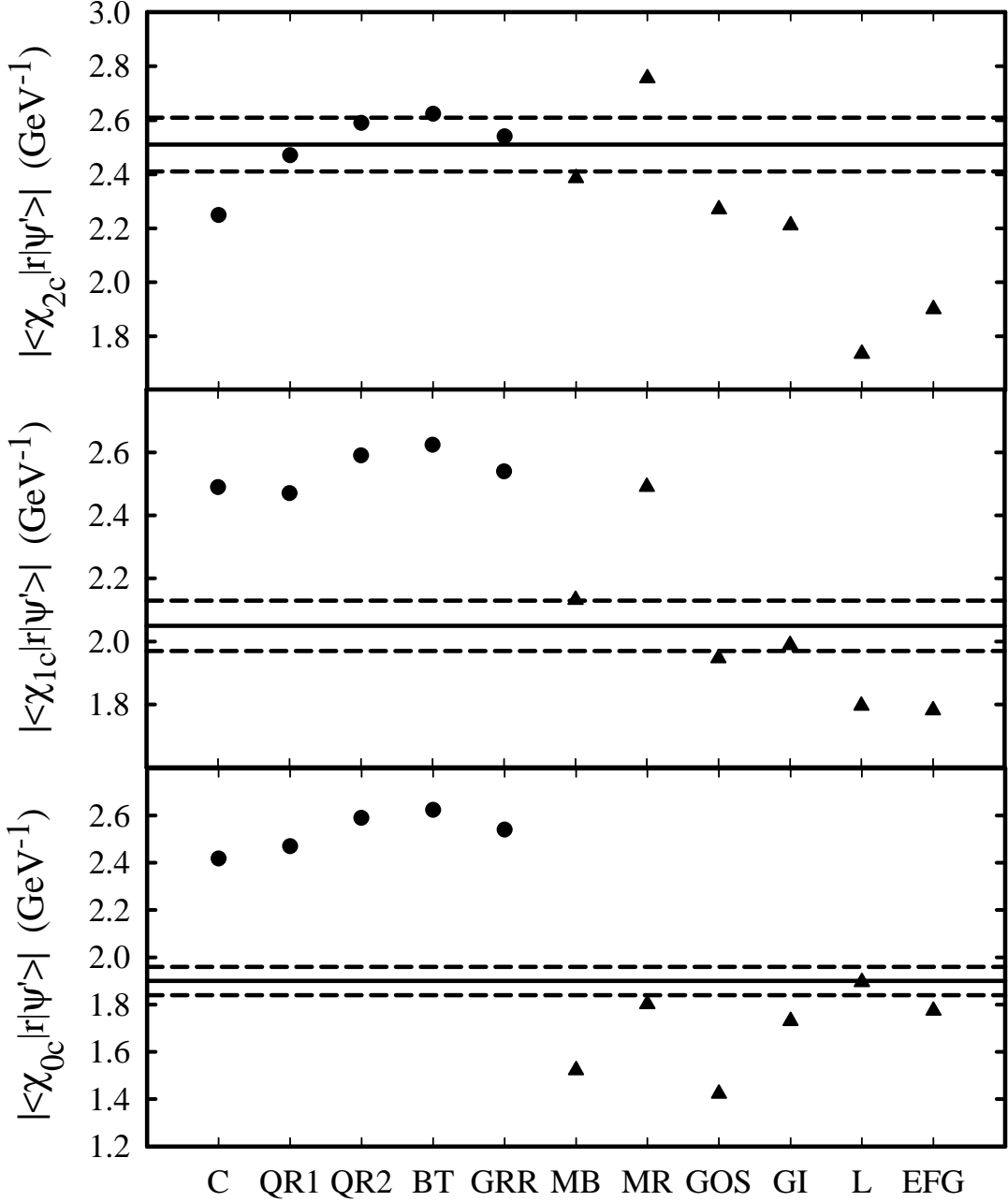


Figure 3: E1 dipole transition matrix elements for the charmonium decays $2^3S_1 \rightarrow 1^3P_J$. The horizontal bands indicate the experimental results. The circles designate nonrelativistic predictions and the triangles relativistic predictions. Within these subsets the results are given in chronological order of the publication date. The labels refer to C-Cornell Model [12], QR-Quigg Rosner, $c\bar{c}$ $\rho = 2$ and $b\bar{b}$ potentials [20], BT-Buchmüller Tye [75], GRR-Gupta Radford Repko [76], MB-McClary Byers [40], MR-Moxhay Rosner [39], GOS-Grotch Owen Sebastian [31], GI-Godfrey Isgur, calculated using the wavefunctions of Ref. [32], L-Lahde, DYN column [35], EFG-Ebert Faustov Galkin [34].

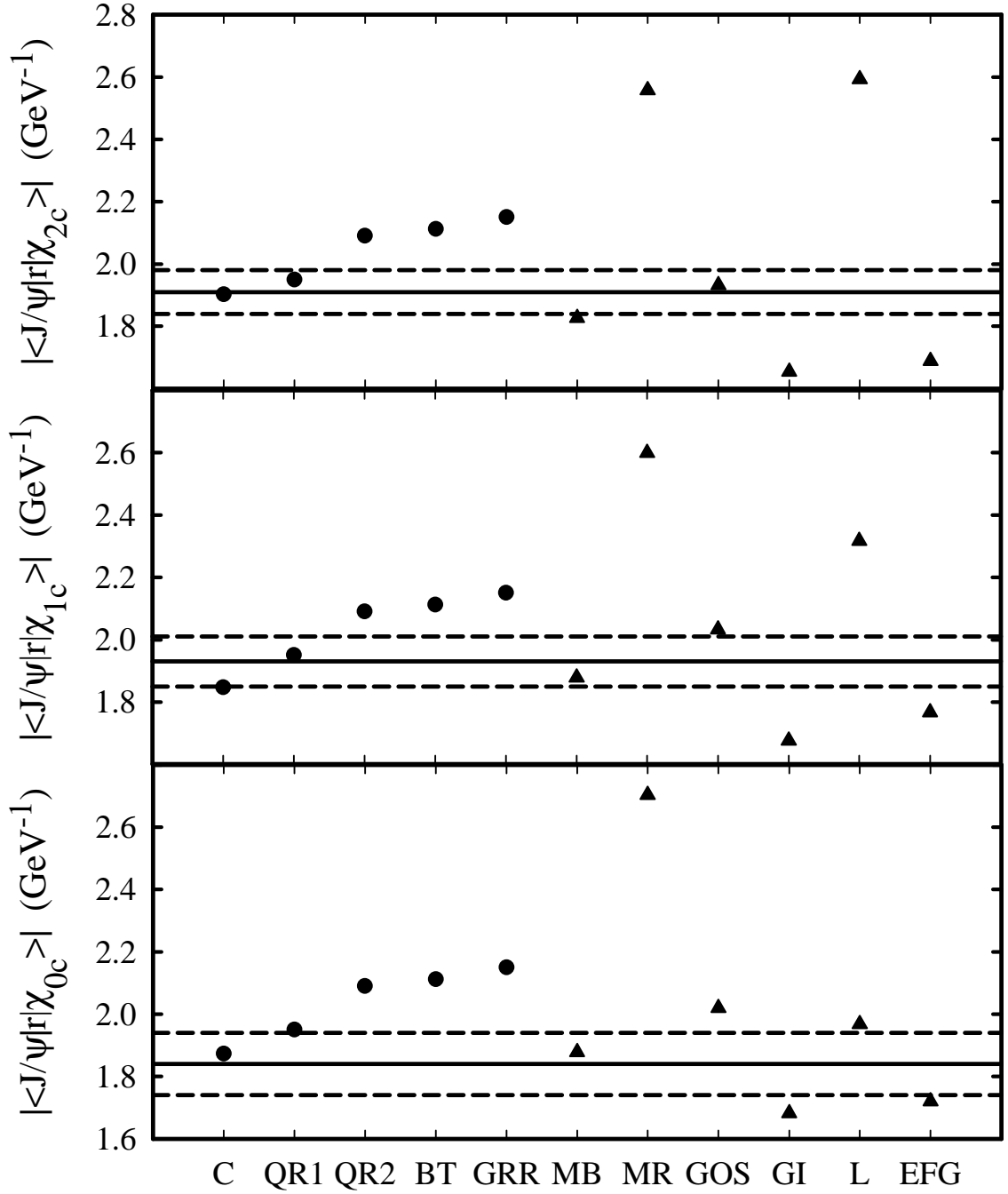


Figure 4: E1 dipole transition matrix elements for the charmonium decays $1^3P_J \rightarrow 1^3S_1$. Labels are as in Fig. 3.

Table IV: Predicted and observed $M2/(E1^2 + M2^2)^{1/2}$ ratios for the transitions $\chi_{cJ} \rightarrow \gamma J/\psi$.

State	Prediction [78]	Experiment [55]
χ_{c1}	$-0.065(1 + \kappa_c)$	$-0.002^{+0.008}_{-0.017}$
χ_{c2}	$-0.096(1 + \kappa_c)$	-0.13 ± 0.05

are in reasonable agreement with the observed values reflecting their relative J -independence. The predictions including relativistic corrections are generally poorer which is surprising because both the $1P$ and $1S$ wavefunctions have no nodes so that the integrals should be relatively insensitive to details of the calculation.

4.3.2 Search for M2 transitions

Attempts have been made to observe magnetic quadrupole (M2) transitions in charmonium through their interference with the dominant E1 amplitudes. These are not yet conclusive [77, 78]. The best prospects are expected for the most energetic photons, i.e., those in $\chi_{cJ} \rightarrow \gamma J/\psi$. Using the notation of [78], the expected normalized M2/E1 amplitude ratios a_2 for these decays are

$$a_2(\chi_{c1}) = E_{\gamma_1}(1 + \kappa_c)/(4m_c) , \quad (26)$$

$$a_2(\chi_{c2}) = (3/\sqrt{5})E_{\gamma_2}(1 + \kappa_c)/(4m_c) , \quad (27)$$

and are shown in Table IV. These values are based on averages [55] of those in Refs. [77] and [78]. We note that a comparison between the *ratios* of the two decays would yield a more stringent test due to the cancellation of the charm quark mass (theory) and possible systematic uncertainties (experiment).

4.3.3 Hadronic and $\gamma\gamma$ decays

In principle the measured χ_{cJ} widths [55] can be used to determine $\alpha_S(m_c^2)$ if the value of the derivative of the $L = 1$ radial wave function for zero separation, $|R'_{nP}(0)|$, is known. Potential models or lattice gauge theories can be used to estimate such quantities. However, they cancel out in ratios of partial widths to various final states. We shall concentrate on the ratios $\Gamma_{\gamma\gamma}(\chi_{cJ})/\Gamma_{gg}(\chi_{cJ})$ for $J = 2, 0$ (χ_{c1} cannot decay into two photons). These are predicted to be [3, 79]

$$\frac{\Gamma_{\gamma\gamma}(\chi_{cJ})}{\Gamma_{gg}(\chi_{cJ})} = \frac{8\alpha^2}{9[\alpha_S(m_c^2)]^2} C_J ; \quad C_2 = \frac{1 - (16\alpha_S)/(3\pi)}{1 - (2.2\alpha_S)/\pi} , \quad C_0 = \frac{1 + (0.2\alpha_S)/\pi}{1 + (9.5\alpha_S)/\pi} . \quad (28)$$

Here we have exhibited the corrections separately to the $\gamma\gamma$ partial widths (numerators) and gg partial widths (denominators).

CLEO has reported a new measurement of $\Gamma(\chi_{c2} \rightarrow \gamma\gamma) = 559 \pm 57 \pm 48 \pm 36$ eV based on 14.4 fb^{-1} of e^+e^- data at $\sqrt{s} = 9.46\text{--}11.30$ GeV [80]. The result is compatible

with other measurements when they are corrected for CLEO's new $\mathcal{B}(\chi_{c2} \rightarrow \gamma J/\psi)$ and $\mathcal{B}(J/\psi \rightarrow \ell^+\ell^-)$. The errors given are statistical, systematic, and $\Delta\mathcal{B}(\chi_{c2} \rightarrow \gamma J/\psi)$. One can average the CLEO measurement with a corrected Belle result [81] to obtain $\Gamma(\chi_{c2} \rightarrow \gamma\gamma) = 565 \pm 62$ eV. Using $\Gamma_{\text{tot}}(\chi_{c2}) = 2.06 \pm 0.12$ MeV [55] and $\mathcal{B}(\chi_{c2} \rightarrow \gamma J/\psi) = (20.2 \pm 1.0)\%$ [55] one finds $\Gamma(\chi_{c2} \rightarrow gg) \approx \Gamma(\chi_{c2} \rightarrow \text{light hadrons}) = 1.64 \pm 0.10$ MeV. This can be compared to $\Gamma(\chi_{c2} \rightarrow \gamma\gamma)$, taking account of the QCD radiative corrections noted above, to obtain $\alpha_S(m_c^2) = 0.296_{-0.019}^{+0.016}$.

The decay $\chi_{c0} \rightarrow \gamma\gamma$ also has been measured. Important contributions from the Fermilab E835 Collaboration [82, 83] are combined with other data to yield $\mathcal{B}(\chi_{c0} \rightarrow \gamma\gamma) = (2.76 \pm 0.33) \times 10^{-4}$ [55], or, with $\Gamma_{\text{tot}}(\chi_{c0}) = 10.4 \pm 0.7$ MeV [55], $\Gamma(\chi_{c0} \rightarrow \gamma\gamma) = (2.87 \pm 0.39)$ keV. Taking account of the $(1.30 \pm 0.11)\%$ branching ratio of χ_{c0} to $\gamma J/\psi$ [55] one estimates $\Gamma(\chi_{c0} \rightarrow gg) = 10.3 \pm 0.7$ MeV and hence $\mathcal{B}(\chi_{c0} \rightarrow \gamma\gamma)/\mathcal{B}(\chi_{c0} \rightarrow gg) = (2.80 \pm 0.42) \times 10^{-4}$. Using Eq. (28) one then finds $\alpha_S(m_c^2) = 0.32 \pm 0.02$, compatible both with the value found from the corresponding χ_{c2} ratio and with a slightly higher value obtained by extrapolation from higher momentum scales [25, 26].

4.4 The $\psi(2S)$

The $\psi(2S)$ resonance was discovered at SLAC in e^+e^- collisions within days after the announcement of the J/ψ [84].

The most precise $\psi(2S)$ mass measurement to date comes, as for the J/ψ , from KEDR [59], at a relative uncertainty of 7×10^{-6} . The current world average is $m(\psi(2S)) = 3686 \pm 0.034$ MeV.

The total $\psi(2S)$ width has been determined in direct $p\bar{p}$ production (E760 from the shape of the resonance curve [85]) as well as in e^+e^- collisions (BES [86] from a fit to the cross-sections $\psi(2S) \rightarrow \text{hadrons}$, $\pi^+\pi^-J/\psi$, and $\mu^+\mu^-$ to obtain the corresponding partial widths; the total width is computed as the sum of hadronic and leptonic widths). The PDG average of these two ‘‘direct’’ measurements is 277 ± 22 MeV. (Not included in the average is a recent value of $290 \pm 25 \pm 4$ MeV based on a measurement of the shape of the resonance curve by Fermilab Experiment E835 [87].) Another estimation comes from the PDG's global fit [55], which among many other measurements takes a measurement of Γ_{ee} into account. As for the J/ψ , the radiative return process can be used [88]; the decay chain presented there is $e^+e^- \rightarrow \gamma\psi(2S) \rightarrow \gamma(X + J/\psi)$, which holds for any decay $\psi(2S) \rightarrow XJ/\psi$. The observed cross-section is proportional to $\Gamma_{ee}(\psi(2S)) \times \mathcal{B}(J/\psi \rightarrow XJ/\psi)$, where $X = \pi^+\pi^-$, $\pi^0\pi^0$, η were used. The result of the global fit is 337 ± 13 MeV.

The two largest modern on-resonance samples are 29 M $\psi(2S)$ decays from the CLEO detector and a 14 M sample collected with the BES II detector. We have already discussed the transitions $\psi(2S) \rightarrow \gamma\chi_{cJ}$ in the previous subsection. Here we treat a variety of other electromagnetic and hadronic transitions of the $\psi(2S)$. We also briefly comment on $\psi(2S)$ decay via $c\bar{c}$ annihilation.

4.4.1 Decay to $\gamma\eta_c(1S)$

The decay $\psi(2S) \rightarrow \gamma\eta_c(1S)$ is a forbidden magnetic dipole (M1) transition, which would vanish in the limit of zero photon energy because of the orthogonality of 1S and 2S wave functions. The photon energy is 638 MeV, leading to a non-zero matrix element $\langle 1S|j_0(kr/2)|2S\rangle$. The decay was first observed by the Crystal Ball Collaboration [62] in the inclusive photon spectrum of $\psi(2S)$ decays with branching ratio $(2.8 \pm 0.6) \times 10^{-3}$. The CLEO collaboration measures $\mathcal{B}[\psi(2S) \rightarrow \gamma\eta_c(1S)] = (3.2 \pm 0.4 \pm 0.6) \times 10^{-3}$, also using the inclusive $\psi(2S)$ photon spectrum. We note that the yield fit depends considerably on the η_c width. The Crystal Ball Collaboration arrived at a width that is substantially below more recent experimental data, 11.5 ± 4.5 MeV as opposed to about 25 MeV. CLEO's result is for a nominal width of 24.8 ± 4.9 MeV; rescaled to the width found by Crystal Ball the CLEO result becomes $\mathcal{B}[\psi(2S) \rightarrow \gamma\eta_c(1S)] = (2.5 \pm 0.6) \times 10^{-3}$ for the Crystal Ball width. We average the two primary results and arrive at $(3.0 \pm 0.5) \times 10^{-3}$. When combined with $\Gamma_{\text{tot}}[\psi(2S)] = (337 \pm 13)$ keV, this implies $\Gamma[\psi(2S) \rightarrow \gamma\eta_c(1S)] = (1.00 \pm 0.16)$ keV, and hence [via Eq. (5)] $|\langle 1S|j_0(kr/2)|2S\rangle| = 0.045 \pm 0.004$. While this result is in agreement with some quark model predictions, for example Ref. [12] and [34] give 0.053 and 0.042 respectively, there is a wide scatter of predictions [30–33, 35, 38]. It would therefore be useful to have a prediction from lattice QCD for this matrix element, as well as for corresponding forbidden matrix elements in the $b\bar{b}$ system.

4.4.2 Decay to $\gamma\eta_c(2S)$

The decay $\psi(2S) \rightarrow \gamma\eta_c(2S)$ is an allowed M1 transition and thus should be characterized by a matrix element $\langle 2S|j_0(kr/2)|2S\rangle$ of order unity in the limit of small k . One may estimate the branching ratio $\mathcal{B}[\psi(2S) \rightarrow \gamma\eta_c(2S)]$ by scaling from $J/\psi \rightarrow \gamma\eta_c(1S)$.

With $\mathcal{B}(J/\psi \rightarrow \gamma\eta_c) = (1.27 \pm 0.36)\%$ [62] and $\Gamma_{\text{tot}}(J/\psi) = (93.4 \pm 2.1)$ keV [55], one has $\Gamma(J/\psi \rightarrow \gamma\eta_c) = (1.19 \pm 0.34)$ keV. Assuming that the matrix elements for $\psi(2S) \rightarrow \gamma\eta'_c(2S)$ and $J/\psi(1S) \rightarrow \gamma\eta_c(1S)$ are equal, the $2S \rightarrow 2S$ rate should be $[E_\gamma(2S \rightarrow 2S)/E_\gamma(1S \rightarrow 1S)]^3$ times that for $1S \rightarrow 1S$. With photon energies of 47.8 MeV for $2S \rightarrow 2S$ and 114.3 MeV for $1S \rightarrow 1S$, this factor is 0.073, giving a predicted partial width $\Gamma[\psi(2S) \rightarrow \gamma\eta'_c(2S)] = (87 \pm 25)$ eV (compare, for example with 170 – 210 eV in Ref. [11]). Using $\Gamma_{\text{tot}}(\psi(2S)) = (337 \pm 13)$ keV [55], one then finds $\mathcal{B}[\psi(2S) \rightarrow \gamma\eta'_c(2S)] = (2.6 \pm 0.7) \times 10^{-4}$.

4.4.3 Hadronic transitions from $\psi(2S)$ to J/ψ

The transitions $\psi(2S) \rightarrow \pi^+\pi^-J/\psi$ and $\psi(2S) \rightarrow \pi^0\pi^0J/\psi$ are thought to proceed via electric dipole emission of a pair of gluons followed by hadronization of the gluon pair into $\pi\pi$ [47]. In addition, the hadronic transitions $\psi(2S) \rightarrow \eta J/\psi$ and $\psi(2S) \rightarrow \pi^0 J/\psi$ have been observed. Recent CLEO measurements of the branching ratios for these transitions [74] are summarized in Table V. (We have already quoted the branching ratios to J/ψ via the χ_{cJ} states in Table II.)

Table V: Branching ratios for hadronic transitions $\psi(2S) \rightarrow J/\psi X$ [74].

Channel	\mathcal{B} (%)
$\pi^+\pi^- J/\psi$	$33.54 \pm 0.14 \pm 1.10$
$\pi^0\pi^0 J/\psi$	$16.52 \pm 0.14 \pm 0.58$
$\eta J/\psi$	$3.25 \pm 0.06 \pm 0.11$
$\pi^0 J/\psi$	$0.13 \pm 0.01 \pm 0.01$
$X J/\psi$	$59.50 \pm 0.15 \pm 1.90$

Isospin predicts the $\pi^0\pi^0$ rate to be one-half that of $\pi^+\pi^-$. CLEO determines $\mathcal{B}(\pi^0\pi^0 J/\psi)/\mathcal{B}(\pi^+\pi^- J/\psi) = (49.24 \pm 0.47 \pm 0.86)\%$ [74], taking cancellations of common uncertainties into account. Two other direct measurements of this ratio are: $(57.0 \pm 0.9 \pm 2.6)\%$ (BES [89]), $(57.1 \pm 1.8 \pm 4.4)\%$ (E835 [90]); the PDG fit result is $(51.7 \pm 1.8)\%$ [55]. The π^0/η ratio is $(4.1 \pm 0.4 \pm 0.1)\%$, somewhat higher than theoretical expectations, for example Ref. [91] based on [92] (1.6%) or Ref. [93] (3.4%). The inclusive branching ratio for $\psi(2S) \rightarrow J/\psi X$, $\mathcal{B} = (59.50 \pm 0.15 \pm 1.90)\%$, is to be compared with the sum of known modes $(58.9 \pm 0.2 \pm 2.0)\%$. Thus there is no evidence for any “missing” modes. The results imply $\mathcal{B}[\psi(2S) \rightarrow \text{light hadrons}] = (16.9 \pm 2.6)\%$, whose significance will be discussed presently.

4.4.4 Light-hadron decays

Decays to light hadrons proceed via annihilation of the $c\bar{c}$ pair into either three gluons or a virtual photon. This includes production of baryons. Such studies can receive substantial background due to continuum production of the same final state, $e^+e^- \rightarrow \gamma^* \rightarrow \text{hadrons}$. When interpreting the observed rate on the $\psi(2S)$, interference effects between on-resonance and continuum production can complicate the picture.

CLEO-c has collected a sample of 20.7 pb^{-1} at $\sqrt{s} = 3.67 \text{ GeV}$, while BES’s below- $\psi(2S)$ continuum data, 6.6 pb^{-1} , were taken at $\sqrt{s} = 3.65 \text{ GeV}$. At the two center-of-mass energies, the $\psi(2S)$ tail is of order 1/1000 [1/5000] compared to the peak cross-section for the two experiments (this number depends on the collider’s beam energy spread).

One expects $Q \equiv \mathcal{B}[\psi(2S) \rightarrow f]/\mathcal{B}(J/\psi \rightarrow f)$ to be comparable to $\mathcal{B}[\psi(2S) \rightarrow \ell^+\ell^-]/\mathcal{B}(J/\psi \rightarrow \ell^+\ell^-) = (12.4 \pm 0.3)\%$ (the “12% rule”), since light-quark decays are presumably governed by $|\Psi(0)|^2$ as are leptonic decays. In fact, Q is much smaller than 12% for most VP and VT modes, where P=pseudoscalar, V=vector, T=tensor, and severely so in some cases [94, 95]. For example, $Q(\rho\pi) = (1.9 \pm 0.6) \times 10^{-3}$, with a similar suppression for $K^{*\pm}K^\mp$. Many models have been brought forward to explain this behavior. Another interesting observation is that the Dalitz plot for the decay to $\pi^+\pi^-\pi^0$ looks quite different for J/ψ , $\psi(2S)$, and the continuum below the $\psi(2S)$ [96]: In the case of the J/ψ , the ρ bands dominate, while at the two higher energies the $m(\pi\pi)$ distributions tend towards higher values. Studies of $\psi(2S) \rightarrow VP$ states by CLEO [94] and BES [97–99] show that the 12% rule is much-better obeyed for

VP decays forbidden by G-parity and hence proceeding via electromagnetism (e.g., $\psi(2S) \rightarrow \omega\pi^0, \rho\eta, \rho\eta'$).

Investigation of decays of the kind $\psi(2S) \rightarrow PP$ for $P = \pi^+, K^+$, and K^0 allow one to extract the relative phase and strength ratio between the $\psi(2S) \rightarrow ggg$ and $\psi(2S) \rightarrow \gamma^*$ amplitudes. This has been done by the CLEO and BES collaborations (see [100] and references therein).

CLEO has studied many exclusive multi-body final states of $\psi(2S)$ [101], several of which have not been reported before. Mode by mode, deviations from the 12% rule rarely amount to more than a factor of two. Moreover, the ratio of $\mathcal{B}[\psi(2S) \rightarrow \text{light hadrons}] = (16.9 \pm 2.6)\%$ to $\mathcal{B}[J/\psi \rightarrow \text{light hadrons}] = (86.8 \pm 0.4)\%$ [55] is $(19.4 \pm 3.1)\%$, which *exceeds* the corresponding ratio of $(12.4 \pm 0.3)\%$ for J/ψ by 2.3σ . The suppression of hadronic $\psi(2S)$ final states thus appears to be confined to certain species such as $\rho\pi, K^*\bar{K}$.

The CLEO Collaboration has measured decays of $\psi(2S)$ to baryon-antibaryon pairs [102], as has the BES Collaboration [103]. The branching ratios indicate that flavor SU(3) seems approximately valid for octet-baryon pair production. In all measured channels, the values of Q are either compatible with or greater than the expected 12% value.

No clear pattern emerges, with some channels obeying the 12% rule while others fail drastically, and so the conclusion at this point is that the simplified picture as painted by the 12% rule is not adequate, and more refined models are necessary.

4.5 The $h_c(1^1P_1)$

The $h_c(1^1P_1)$ state of charmonium has been observed by CLEO [104,105] via $\psi(2S) \rightarrow \pi^0 h_c$ with $h_c \rightarrow \gamma\eta_c$. These transitions are denoted by red (dark) arrows in Fig. 5 [106]. It has also been seen by Fermilab Experiment E835 [107] in the reaction $\bar{p}p \rightarrow h_c \rightarrow \gamma\eta_c \rightarrow \gamma\gamma\gamma$, with 13 candidate events. A search for the decay $B^\pm \rightarrow h_c K^\pm$ by the Belle Collaboration, however, has resulted only in an upper limit on the branching ratio [108] $\mathcal{B}(B^\pm \rightarrow h_c K^\pm) < 3.8 \times 10^{-5}$ for $M(h_c) = 3527$ MeV and $\mathcal{B}(h_c \rightarrow \gamma\eta_c) = 0.5$. Attempts at previous observations are documented in Ref. [105].

4.5.1 Significance of h_c mass measurement

Hyperfine splittings test the spin-dependence and spatial behavior of the $Q\bar{Q}$ force. Whereas these splittings are $M(J/\psi) - M(\eta_c) = 116.5 \pm 1.2$ MeV for 1S and $M(\psi') - M(\eta'_c) = 48 \pm 4$ MeV for 2S levels, P -wave splittings should be less than a few MeV since the potential is proportional to $\delta^3(\vec{r})$ for a Coulomb-like $c\bar{c}$ interaction. Lattice QCD [109] and relativistic potential [34] calculations confirm this expectation. One expects $M(h_c) \equiv M(1^1P_1) \simeq \langle M(^3P_J) \rangle = 3525.36 \pm 0.06$ MeV.

4.5.2 Detection in $\psi(2S) \rightarrow \pi^0 h_c \rightarrow \pi^0 \gamma\eta_c$

In the CLEO data, both inclusive and exclusive analyses saw a signal near $\langle M(^3P_J) \rangle$. The exclusive analysis reconstructed η_c in 7 decay modes, while no η_c reconstruction

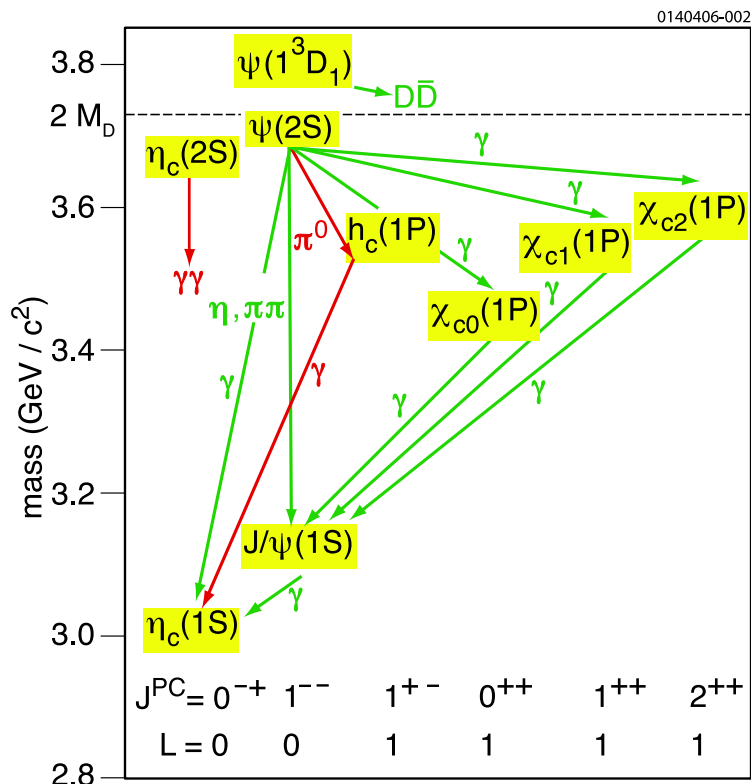


Figure 5: Transitions among low-lying charmonium states. From Ref. [106].

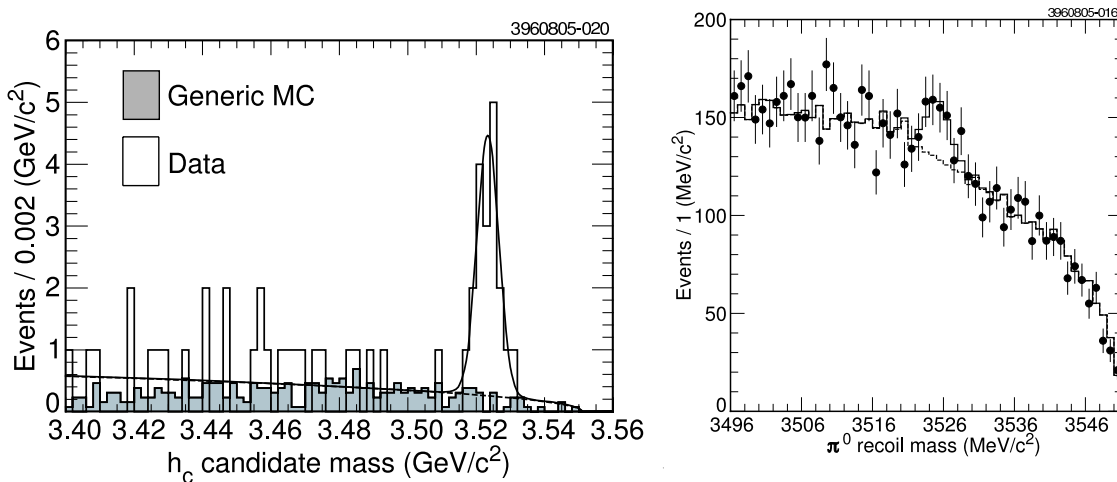


Figure 6: Left: Exclusive h_c signal from CLEO (3 million $\psi(2S)$ decays). Data events correspond to open histogram; Monte Carlo background estimate is denoted by shaded histogram. The signal shape is a double Gaussian, obtained from signal Monte Carlo. The background shape is an ARGUS function. Right: Inclusive h_c signal from CLEO (3 million $\psi(2S)$ decays). The curve denotes the background function based on generic Monte Carlo plus signal. The dashed line shows the contribution of background alone. Both figures are from Ref. [105].

was performed in the inclusive analysis. The exclusive signal is shown on the left in Fig. 6. A total of 19 candidates were identified, with a signal of 17.5 ± 4.5 events above background. The result of one of two inclusive analyses is shown on the right in Fig. 6. Combining exclusive and inclusive results yields $M(h_c) = (3524.4 \pm 0.6 \pm 0.4)$ MeV, $\mathcal{B}_1\mathcal{B}_2 = (4.0 \pm 0.8 \pm 0.7) \times 10^{-4}$. The h_c mass is $(1.0 \pm 0.6 \pm 0.4)$ MeV below $\langle M(^3P_J) \rangle$, barely consistent with the (nonrelativistic) bound [110] $M(h_c) \geq \langle M(^3P_J) \rangle$ and indicating little P -wave hyperfine splitting in charmonium. The value of $\mathcal{B}_1\mathcal{B}_2$ agrees with theoretical estimates [6] of $(10^{-3} \cdot 0.4)$.

4.5.3 Detection in the exclusive process $p\bar{p} \rightarrow h_c \rightarrow \gamma\eta_c \rightarrow 3\gamma$

The Fermilab E835 Collaboration [107] studied a number of charmonium resonances accessible in the direct $\bar{p}p$ channel using the carefully controlled \bar{p} energy of the Fermilab Accumulator ring and a gas-jet fixed target. The signal of 13 events sits above an estimated background of 3 events and corresponds to a mass $M(h_c) = 3525.8 \pm 0.2 \pm 0.2$ MeV. The signal strength is evaluated to be $\Gamma_{\bar{p}p}\mathcal{B}_{\eta_c\gamma} = (10.0 \pm 3.5, 12.0 \pm 4.5)$ eV for $\Gamma_{\text{tot}}(h_c) = (0.5, 1.0)$ MeV. With $\mathcal{B}_{\eta_c\gamma} = 0.4$ this would correspond to $\Gamma_{h_c \rightarrow \bar{p}p} = (25, 30)$ eV. (Kuang, Tuan, and Yan predicted $\Gamma_{h_c \rightarrow \bar{p}p} = 186$ eV [111].) For comparison the partial widths of $\eta_c, J/\psi, \chi_{c0,1,2}$, and $\psi(2S)$ to $\bar{p}p$ are roughly (33 ± 11) keV, (203 ± 9) eV, (2.25 ± 0.25) keV¹, (60 ± 6) eV, (136 ± 13) eV, and (89 ± 8) eV, where we have used branching ratios and total widths from Ref. [55].

4.6 The $\eta_c(2S)$

The claim by the Crystal Ball Collaboration [112] for the first radial excitation of the η_c , the $\eta'_c = \eta_c(2S)$, at a mass of 3594 ± 5 MeV, remained unconfirmed for 20 years. Then, the Belle Collaboration observed a candidate for $\eta_c(2S)$ in $B \rightarrow K(K_S K \pi)$ [113] and $e^+e^- \rightarrow J/\psi + X$ [114] at a significantly higher mass. An upper limit on the decay $\psi(2S) \rightarrow \gamma\eta_c(2S)$ by the CLEO Collaboration [73] failed to confirm the Crystal Ball state at 3594 MeV. The Belle result stimulated a study of what other charmonium states could be produced in B decays [115].

By studying its production in photon-photon collisions, CLEO [116] confirmed the presence of the new $\eta_c(2S)$ candidate, as did the BaBar Collaboration [117]. The mass of the $\eta_c(2S)$ is found to be only 48 ± 4 MeV/ c^2 below the corresponding spin-triplet $\psi(2S)$ state, a hyperfine splitting which is considerably less than the 116.5 ± 1.2 MeV/ c^2 difference seen in the 1S charmonium states (*i.e.*, between the J/ψ and the $\eta_c(1S)$). While potential models predict the $\psi(2S) - \eta_c(2S)$ splitting to be less than the $J/\psi - \eta_c$ splitting due to the smaller wavefunction at the origin for the 2S state compared to the 1S state, most models (e.g., Refs. [34, 118–120]), but not all [32, 121], predict a much larger splitting than what is observed. It is likely that the proximity of the charmed meson pair threshold, which can lower the $\psi(2S)$ mass by tens of MeV/ c^2 [8, 10, 122], plays an important role in the $\psi(2S) - \eta_c(2S)$ splitting.

The CLEO Collaboration found that the product $\Gamma(\eta_c(2S) \rightarrow \gamma\gamma)\mathcal{B}(\eta_c(2S) \rightarrow K_S K \pi)$ is only $0.18 \pm 0.05 \pm 0.02$ times the corresponding product for $\eta_c(1S)$. This

¹Using $\mathcal{B}(\chi_{c0} \rightarrow p\bar{p}) = (2.16 \pm 0.19) \times 10^{-4}$.

could pose a problem for descriptions of charmonium if the branching ratios to $K_S K \pi$ are equal. More likely, the heavier $\eta_c(2S)$ has more decay modes available to it, so its branching ratio to $K_S K \pi$ is likely to be less than that of the $\eta_c(1S)$.

4.7 The $\psi(3770)$

The $\psi'' = \psi(3770)$ is primarily a 1^3D_1 state with small admixtures of n^3S_1 states [notably $\psi(2S)$] [8, 10, 123]. It is most easily produced in e^+e^- collisions, where it appears at 3770 MeV as a broad resonance (23.0 ± 2.7 MeV [55]). Both Belle [124] and BaBar [125] observed $\psi(3770)$ in B decay. The broadness of the state is due to the fact that decay to open charm $D\bar{D}$ is kinematically available and also allowed by quantum numbers. Final states involving D^* and D_s are not accessible at this energy. The mass and width have are most accurately determined in a scan. Ref. [126] achieves uncertainties of below 1 MeV for the mass and below 10% relative on the width. The leptonic width can be determined via a hadron production rate measurement as the cross-section is proportional to the coupling, Γ_{ee} . The BES detector in China has been studying its decays to charmed and non-charmed final states (see, e.g., Ref. [127]), and for the past few years it has been the subject of dedicated studies by the CLEO Collaboration [128].

4.7.1 ψ'' as a “charm factory”

The fact that ψ'' lies so close to charm threshold [only about 40 MeV above $2M(D^0)$] makes it a well-defined source of charmed particle pairs (without additional pions) in e^+e^- collisions. An interesting question is whether the total cross section $\sigma(e^+e^- \rightarrow \psi'')$ is nearly saturated by $D\bar{D}$. If not, there could be significant non- $D\bar{D}$ decays of the ψ'' [123]. A new CLEO measurement [129], $\sigma(\psi'') = (6.38 \pm 0.08^{+0.41}_{-0.30})$ nb, appears very close to the CLEO value $\sigma(D\bar{D}) = (6.39 \pm 0.10^{+0.17}_{-0.08})$ nb [130], leaving little room for non- $D\bar{D}$ decays. Some question has nonetheless been raised by new BES analyses [126, 131, 132] in which a significant non- $D\bar{D}$ component could still be present.

As a result of the difference between D^0 and D^- masses, the ψ'' decays to $D^0\bar{D}^0$ more frequently than to D^+D^- . For example, Ref. [130] finds $\sigma(e^+e^- \rightarrow \psi'' \rightarrow D^+D^-)/\sigma(e^+e^- \rightarrow \psi'' \rightarrow D^0\bar{D}^0) = 0.776 \pm 0.024^{+0.014}_{-0.006}$. This ratio reflects not only the effect of differing phase space, but also different final-state electromagnetic interactions [133], and is expected to vary somewhat as center-of-mass energy is varied over the resonance peak.

4.7.2 Leptonic width and mixing

The CLEO measurement of $\sigma(\psi'')$ mentioned above [129] also leads to a new, more precise value for the ψ'' leptonic width, $\Gamma_{ee}(\psi'') = (0.204 \pm 0.003^{+0.041}_{-0.027})$ keV. This enters into the quoted average [55] of $(0.242^{+0.027}_{-0.024})$ keV. Subsequent results are $(0.251 \pm 0.026 \pm 0.011)$ keV [126] and $(0.279 \pm 0.011 \pm 0.013)$ keV [132] from BES-II. These improvements allow a more precise estimate for the angle ϕ describing the mixing

between $1D$ and $2S$ states in $\psi'(3686)$ [the state we have previously referred to as $\psi(2S)$] and $\psi''(3770)$:

$$\psi' = -\sin\phi|1^3D_1\rangle + \cos\phi|2^3S_1\rangle \quad , \quad \psi'' = \cos\phi|1^3D_1\rangle + \sin\phi|2^3S_1\rangle \quad . \quad (29)$$

This mixing affects the ratio $R_{\psi''/\psi'}$ of leptonic widths of ψ' and ψ'' and their predicted rates for E1 transitions to the χ_{cJ} states [134, 135]. A previous analysis based on $\Gamma_{ee}(\psi'') = 0.26 \pm 0.04$ keV [123] gave $\phi = (12 \pm 2)^\circ$, while the present leptonic width will give smaller errors on ϕ . The large present and anticipated CLEO-c $\psi''(3770)$ data sample will further constrain this value. A solution with negative ϕ consistent with $R_{\psi''/\psi'}$ gives an unphysically large rate for $\psi' \rightarrow \gamma\chi_{c0}$.

As noted earlier, the nonrelativistic predictions for the ψ' rates are generally too high, indicating the limitations of a nonrelativistic approach. We shall see that the predicted rate for $\psi'' \rightarrow \gamma\chi_{c0}$, which has recently been observed by the CLEO Collaboration [136], is also a factor of 2 too high in a nonrelativistic approach but is satisfactory when relativistic and coupled-channel effects are taken into account.

4.7.3 ψ'' transitions to $\pi\pi J/\psi$

The rates for transitions of ψ'' to $\pi\pi J/\psi$ have been predicted on the assumption that it is mainly a D -wave state with a small S -wave admixture as in the above example [137]. (The sign convention for the mixing angle in Ref. [137] is opposite to ours.) A wide range of partial widths, $\Gamma(\psi'' \rightarrow \pi^+\pi^- J/\psi) = 26$ to 147 keV, corresponding to branching ratios ranging from about 0.1% to 0.7%, is predicted.

The BES Collaboration [138] finds $\mathcal{B}(\psi'' \rightarrow \pi^+\pi^- J/\psi) = (0.34 \pm 0.14 \pm 0.09)\%$. The CLEO Collaboration has measured a number of branching ratios for $\psi'' \rightarrow XJ/\psi$ [88]: $\mathcal{B}(\psi'' \rightarrow \pi^+\pi^- J/\psi) = (0.189 \pm 0.020 \pm 0.020)\%$, $\mathcal{B}(\psi'' \rightarrow \pi^0\pi^0 J/\psi) = (0.080 \pm 0.025 \pm 0.016)\%$, $\mathcal{B}(\psi'' \rightarrow \eta J/\psi) = (0.087 \pm 0.033 \pm 0.022)\%$, and $\mathcal{B}(\psi'' \rightarrow \pi^0 J/\psi) < 0.028\%$. Together these account for less than 1/2% of the total ψ'' decays.

4.7.4 ψ'' transitions to $\gamma\chi_{cJ}$

CLEO has recently reported results on $\psi'' \rightarrow \gamma\chi_{cJ}$ partial widths, based on the exclusive process $\psi'' \rightarrow \gamma\chi_{c1,2} \rightarrow \gamma\gamma J/\psi \rightarrow \gamma\gamma\ell^+\ell^-$ [139] and reconstruction of exclusive χ_{cJ} decays [136]. The results are shown in Table VI, implying $\sum_J \mathcal{B}(\psi'' \rightarrow \gamma\chi_{cJ}) = \mathcal{O}(1\%)$. Recent calculations [8, 11] including relativistic corrections are in good agreement with these measurements while nonrelativistic treatments overestimate $\Gamma(\psi'' \rightarrow \gamma\chi_{c0})$.

4.7.5 ψ'' transitions to light-hadron final states

Several searches for $\psi''(3770) \rightarrow$ (light hadrons), including VP [140, 141], $K_L K_S$ [142, 143], and multi-body [144] final states have been performed. No evidence was seen for any light-hadron ψ'' mode above expectations from continuum production except for a marginally significant branching ratio $\mathcal{B}(\psi'' \rightarrow \phi\eta) = (3.1 \pm 0.7) \times 10^{-4}$, indicating no obvious signature of non- $D\bar{D}$ ψ'' decays.

Table VI: Radiative decays $\psi'' \rightarrow \gamma\chi_{cJ}$: energies, predicted and measured partial widths. Theoretical predictions of Ref. [8] are (a) without and (b) with coupled-channel effects; nonrelativistic (c) and relativistic (d) predictions of Ref. [11]; (e) shows predictions of Ref. [134].

Mode	E_γ (MeV) [55]	Predicted (keV)					CLEO (keV) [136]
		(a)	(b)	(c)	(d)	(e)	
$\gamma\chi_{c2}$	208.8	3.2	3.9	4.9	3.3	24 ± 4	< 21
$\gamma\chi_{c1}$	251.4	183	59	125	77	73 ± 9	70 ± 17
$\gamma\chi_{c0}$	339.5	254	225	403	213	523 ± 12	172 ± 30

4.8 $\psi(4040)$ and $\psi(4160)$

The $\psi(4040)$ and $\psi(4160)$ resonances appear as elevations in the measurement of $R = \sigma(\text{hadrons})/\sigma(\mu^+\mu^-)$. They are commonly identified with the $3S$ and $2D$ states of charmonium (Fig. 1). Their parameters have undergone some refinement as a result of a recent analysis in Ref. [145]. The error on the mass of $\psi(4040)$ has shrunk considerably, with $M = (4040 \pm 10)$ MeV/ c^2 in 2004 (Ref. [146]) replaced with (4039 ± 1) MeV/ c^2 in 2006 (Ref. [55]). The width is now quoted as (80 ± 10) MeV/ c^2 , up from (52 ± 10) MeV/ c^2 . Similarly, the mass and width of the $\psi(4160)$ are now quoted as (4153 ± 3) MeV/ c^2 and (108 ± 8) MeV/ c^2 , replacing (4159 ± 20) MeV/ c^2 and (78 ± 20) MeV/ c^2 . Data taken at the $\psi(4040)$ and the $\psi(4160)$ can be useful to search for the $2P$ states through radiative decays $\psi(4160) \rightarrow \gamma\chi'_{c0,1,2}$. Identifying the transition photon in the inclusive photon spectrum requires excellent background suppression and is therefore a challenge. The E1 branching fractions listed in [147] are, calculated for χ'_{cJ} masses chosen to be² 3929/3940/3940 MeV for $J = 2/1/0$:

$$\begin{aligned} \psi(4040) &\rightarrow \gamma\chi'_{c2,1,0}: & 0.7/0.3/0.1 \times 10^{-3}, \\ \psi(4160) &\rightarrow \gamma\chi'_{c2,1,0}: & 0.1/1.3/1.7 \times 10^{-3}. \end{aligned}$$

The $J = 0$ and $J = 1$ states can be distinguished since the decays $\chi_{c0} \rightarrow D\bar{D}$ and $\chi_{c1} \rightarrow D\bar{D}^*$ are possible but not the reverse. χ'_{c2} can decay to either, where the relative rate depends on the amount of phase space, which in turn depends on the mass. Exclusive decays to charmonium have not been observed, though CLEO has set upper limits on a number of final states involving charmonium [148].

4.9 New Charmonium-like States

Many new charmonium states above $D\bar{D}$ threshold have recently been observed. While some of these states appear to be consistent with conventional $c\bar{c}$ states, others do not. Here we give a brief survey of the new states and their possible interpretations. Reviews may be found in Refs. [149–151]. In all cases, the picture is not entirely clear. This situation could be remedied by a coherent search of the decay pattern to $D\bar{D}^{(*)}$, search for production in two-photon fusion and ISR, the study of radiative decays of

² The motivation for this choice will become apparent in Section 4.9.

Table VII: Summary of the $X(3872)$ decay modes and searches. The two entries for $D^0\bar{D}^0\pi^0$ are both from Belle and are based on samples of 88 fb^{-1} and 414 fb^{-1} , respectively.

final state	$X(3872)$ branching fraction	reference
$\pi^+\pi^-J/\psi$	$(11.6 \pm 1.9) \times 10^{-6}/\mathcal{B}_{B^+\rightarrow X(3872)K^+} (> 10\sigma)$	[158]
$\pi^-\pi^0J/\psi$	not seen	[156]
$\gamma\chi_{c1}$	$< 0.9 \times \mathcal{B}_{\pi^+\pi^-J/\psi}$	[152]
$\gamma J/\psi$	$(3.3 \pm 1.0 \pm 0.3) \times 10^{-6}/\mathcal{B}_{B\rightarrow X(3872)K^+} (> 4\sigma)$	[159]
	$(0.14 \pm 0.05) \times \mathcal{B}_{X(3872)\rightarrow\pi^+\pi^-J/\psi} (4.0\sigma)$	[160]
$\eta J/\psi$	$< 7.7 \times 10^{-6}/\mathcal{B}_{B\rightarrow X(3872)K^+}$	[161]
$\pi^+\pi^-\pi^0J/\psi$	$(1.0 \pm 0.4 \pm 0.3) \times \mathcal{B}_{X(3872)\rightarrow\pi^+\pi^-J/\psi} (4.3\sigma)$	[160]
$D^0\bar{D}^0$	$< 6 \times 10^{-5}/\mathcal{B}_{B^+\rightarrow X(3872)K^+}$	[124]
D^+D^-	$< 4 \times 10^{-5}/\mathcal{B}_{B^+\rightarrow X(3872)K^+}$	[124]
$D^0\bar{D}^0\pi^0$	$< 6 \times 10^{-5}/\mathcal{B}_{B^+\rightarrow X(3872)K^+}$	[124]
	$(12.2 \pm 3.1^{+2.3}_{-3.0}) \times 10^{-5}/\mathcal{B}_{B^+\rightarrow X(3872)K^+}^a (6.4\sigma)$	[162]

^a Belle report the quoted number as branching fraction at the peak. They find a peak position that is slightly above that seen by other experiments for other $X(3872)$ decays.

$\psi(4160)$, and of course tighter uncertainties by way of improved statistical precision upon the current measurements.

4.9.1 $X(3872)$

The $X(3872)$, discovered by Belle in B decays [152] and confirmed by BaBar [153] and in hadronic production by CDF [154] and D0 [155], is a narrow state of mass 3872 MeV that was first seen decaying to $J/\psi\pi^+\pi^-$. No signal at this mass was seen in $B \rightarrow X^-K$, $X^- \rightarrow \pi^-\pi^0J/\psi$ [156], which would have implied a charged partner of $X(3872)$. It was not observed in two-photon production or initial state radiation [157]. Subsequent studies focused on determining the mass, width, and decay properties in order to establish its quantum numbers and possible position in the charmonium system of states. To date, decays to $\pi^+\pi^-J/\psi$, $\gamma J/\psi$, $\pi^+\pi^-\pi^0J/\psi$ and possibly $D^0\bar{D}^0\pi^0$ have been reported. Results on decay modes of $X(3872)$ are summarized in Table VII.

The averaged mass of this state is $M = 3871.2 \pm 0.5\text{ MeV}$ [55]; the width is determined to be $\Gamma < 2.3\text{ MeV}$ (90% C.L.) [152], below detector resolution. Signal distributions from two experiments are shown in Figure 7, and mass measurements (including $M(D^0) + M(D^{*0})$ [163]) are compared in Figure 8.

The combined branching fraction product from Belle and BaBar is $\mathcal{B}[B^+ \rightarrow K^+X(3872)] \times \mathcal{B}[X(3872) \rightarrow \pi^+\pi^-J/\psi] = (11.4 \pm 2.0) \times 10^{-6}$ [55]. After setting a limit of $\mathcal{B}[B^+ \rightarrow K^+X(3872)] < 3.2 \times 10^{-4}$ (90% C.L.), BaBar [158] derives $\mathcal{B}[X(3872) \rightarrow \pi^+\pi^-J/\psi] > 4.2\%$ (90% C.L.). For comparison, examples of other states above open flavor threshold are $\mathcal{B}[\psi(3770) \rightarrow \pi^+\pi^-J/\psi] = (1.93 \pm 0.28) \times 10^{-3}$ [55] (partial width 46 keV) and limits $\mathcal{B}[\psi(4040, 4160) \rightarrow \pi^+\pi^-J/\psi]$ of order 10^{-3} [55]

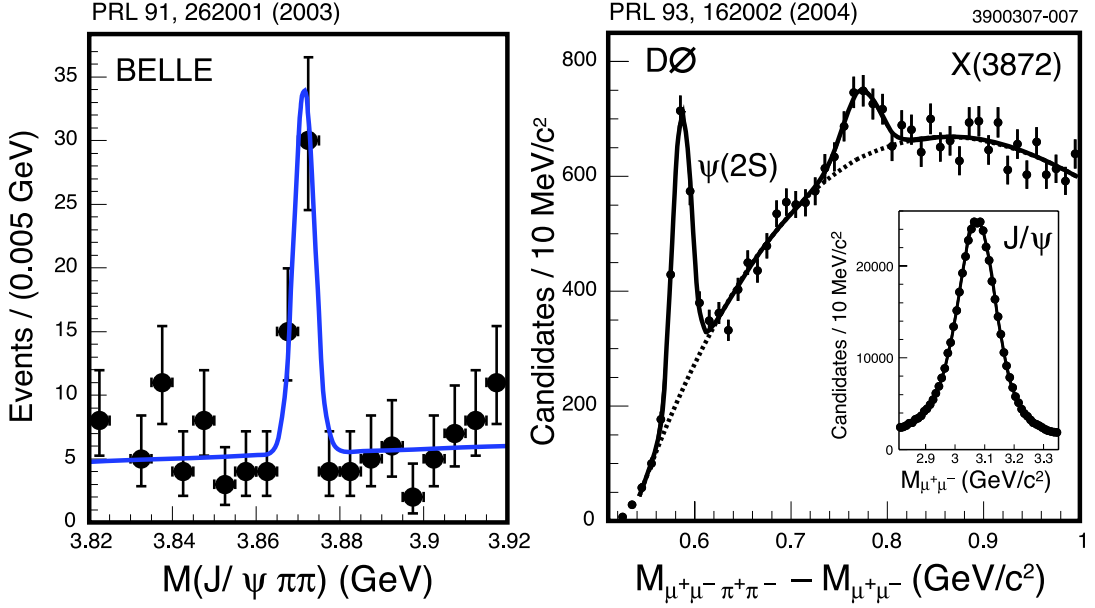


Figure 7: Observation of $X(3872) \rightarrow \pi^+\pi^-J/\psi$ in B decay (example from Belle [152]) and in $p\bar{p}$ collisions (example from D0 [155]).

(partial widths ~ 100 keV).

Regular charmonium states that cannot decay to D pairs are expected to have a narrow width also; however, in these cases, E1 transitions to the χ_{cJ} states are preferred. This is not borne out by the data for $X(3872)$ [152]. This result also disfavors the interpretation as a $1^{1,3}D_2$ state.

Decay into a pair of D mesons has not been observed, and upper limits on the rate are in the range of a few times that for $\pi^+\pi^-J/\psi$ [124]. A signal in $B \rightarrow (D^0\bar{D}^0\pi^0)K$ with $m(D^0\bar{D}^0\pi^0)$ in the right range is the first candidate for open-charm decays of $X(3872)$. The observed rate is an order of magnitude above that for $\pi^+\pi^-J/\psi$.

The dipion mass distribution favors high $m(\pi^+\pi^-)$ values. This is not untypical for charmonium states (*cf.* $\psi(2S) \rightarrow \pi^+\pi^-J/\psi$), but could be an indication that the pion pair might even be produced in a ρ configuration; if that were indeed the case the $X(3872)$ could not be a charmonium state. A search for $X(3872) \rightarrow \pi^0\pi^0J/\psi$ would be most helpful to clarify this aspect (as well as to determine the $\pi^0\pi^0J/\psi : \pi^+\pi^-J/\psi$ ratio) because the decay chain $X(3872) \rightarrow \rho^0J/\psi \rightarrow \pi^0\pi^0J/\psi$ would be forbidden. Observation of $X(3872) \rightarrow \pi^0\pi^0J/\psi$ would therefore rule out the hypothesis of an intermediate ρ state. The decay $X(3872) \rightarrow \pi^+\pi^-\pi^0J/\psi$ was observed at a rate comparable to that of $\pi^+\pi^-J/\psi$ [160] (preliminary). The $m(\pi^+\pi^-\pi^0)$ distribution is concentrated at the highest values, coinciding with the kinematic limit, which spurred speculations that the decay might proceed through (the low-side tail of) an ω .

Since the $X(3872)$ lies well above $D\bar{D}$ threshold but is narrower than experimental resolution, unnatural $J^P = 0^-, 1^+, 2^-$ is favored. An angular distribution analysis by the Belle collaboration, utilizing in part suggestions in Ref. [164], favors $J^{PC} = 1^{++}$ [165], although a higher-statistics analysis by CDF cannot distinguish between

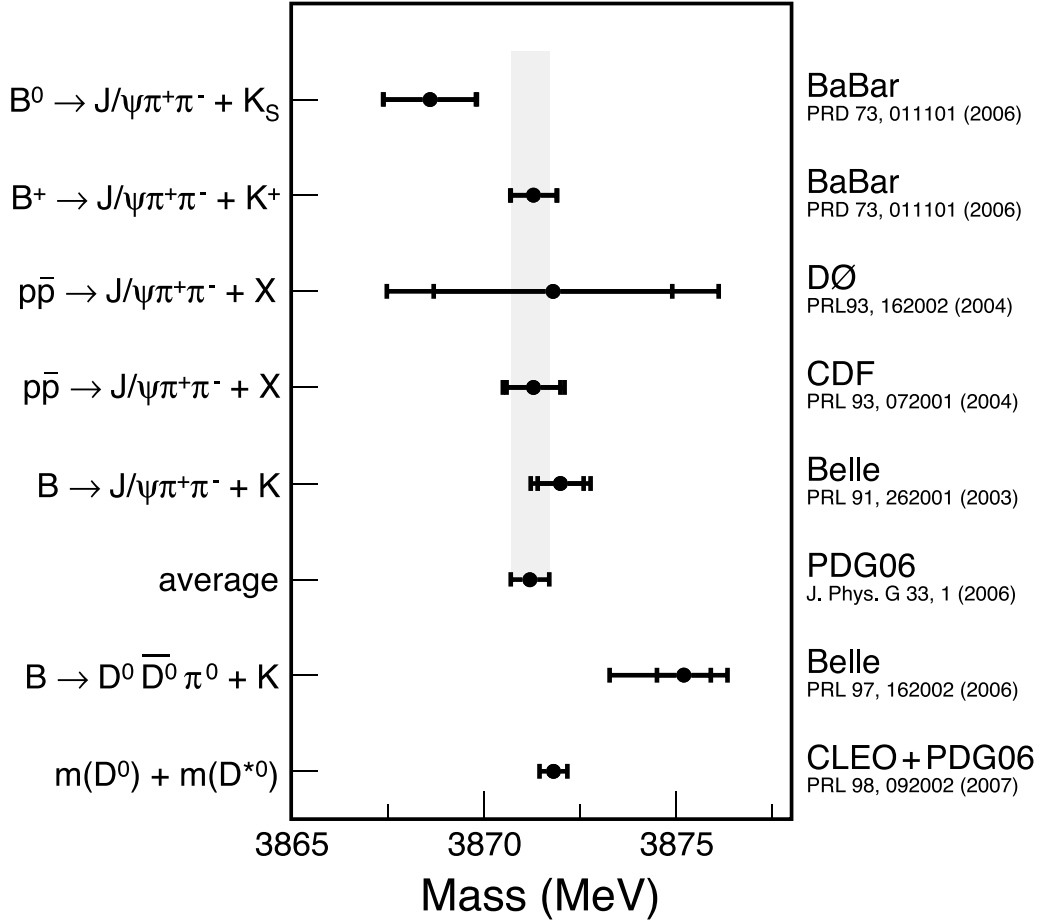


Figure 8: Comparison of mass determinations: From $X(3872) \rightarrow \pi^+ \pi^- J/\psi$, their weighted average as computed by PDG, an observed threshold enhancement in $B \rightarrow D^0 \bar{D}^0 \pi^0 + K$ (at 2σ deviation from the average), and the sum of the D^0 and D^* mass [163].

$J^{PC} = 1^{++}$ or 2^{-+} [166] (see also [151, 167, 168]). $J^{PC} = 2^{-+}$ is disfavored by Belle's observation [162] of $X \rightarrow D^0 \bar{D}^0 \pi^0$, which would require at least two units of relative orbital angular momentum in the three-body state, very near threshold.

Of conventional $c\bar{c}$ states only the $1D$ and $2P$ multiplets are nearby in mass. Taking into account the angular distribution analysis only the $J^{PC} = 1^{++} 2^3P_1$ and $2^{-+} 1^1D_2$ assignments are possible. The decay $X(3872) \rightarrow \gamma J/\psi$ is observed at a rate about a quarter or less of that for $X(3872) \rightarrow \pi^+ \pi^- J/\psi$ [159, 160]. This would be an E1 transition for 2^3P_1 but a more suppressed higher multipole for 2^{-+} , and therefore the $J^{PC} = 1^{++}$ interpretation appears more likely assuming $c\bar{c}$ content. For a 1^{++} state the only surviving candidate is the 2^3P_1 . However, we will see that the identification of the $Z(3931)$ with the 2^3P_2 implies a 2^3P_2 mass of ~ 3930 MeV, which is inconsistent with the 2^3P_1 interpretation of $X(3872)$ if the $2^3P_2 - 2^3P_1$ mass splittings are decidedly lower than 50 MeV [10, 11]. This favors the conclusion that

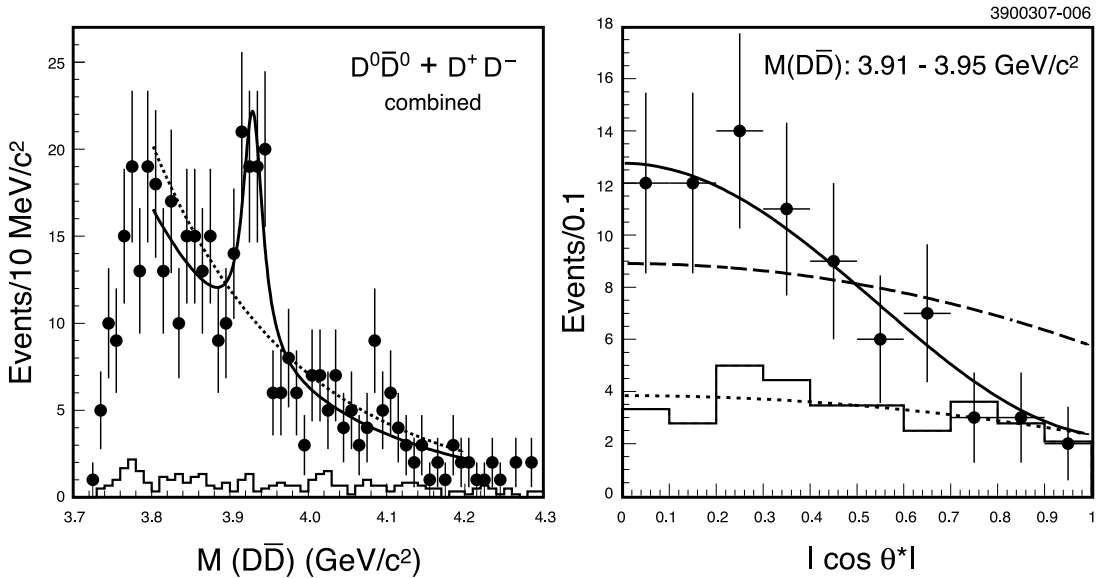


Figure 9: Belle’s χ'_{c2} candidate [171]: Left: The invariant mass $m(D\bar{D})$ distribution in two-photon production of the $Z(3930)$, D^+D^- and $D^0\bar{D}^0$ combined. The signal yield is 64 ± 18 events. The two curves are fits with and without a resonance component. Right: $\cos \theta^*$, the angle of the D meson relative to the beam axis in the $\gamma\gamma$ center-of-mass frame for events with $3.91 < M(D\bar{D}) < 3.95$ GeV; the data (circles) are compared with predictions for $J = 2$ (solid) and $J = 0$ (dashed). The background level can be judged from the solid histogram or the interpolated smooth dotted curve.

the $X(3872)$ may be a $D^0\bar{D}^{*0}$ molecule or “tetraquark” [169] state. It has many features in common with an S -wave bound state of $(D^0\bar{D}^{*0} + \bar{D}^0D^{*0})/\sqrt{2} \sim c\bar{c}u\bar{u}$ with $J^{PC} = 1^{++}$ [170]. Its simultaneous decay to $\rho J/\psi$ and $\omega J/\psi$ with roughly equal branching ratios is a consequence of this “molecular” assignment. The upper limit on $X(3872) \rightarrow \eta J/\psi$ [161] is consistent with expectations for a charmonium state as well as a hybrid. A new measurement of $M(D^0) = 1864.847 \pm 0.150 \pm 0.095$ MeV/ c^2 [163] implies $M(D^0\bar{D}^{*0}) = 3871.81 \pm 0.36$ MeV/ c^2 and hence a binding energy of 0.6 ± 0.6 MeV (see also Fig. 8).

4.9.2 $Z(3930)$

Belle has reported a candidate for a $2^3P_2(\chi'_{c2})$ state in $\gamma\gamma$ collisions [171], decaying to $D\bar{D}$. The state appears as an enhancement in the $m(D\bar{D})$ distribution at a statistical significance of 5.3σ . The relative D^+D^- and $D^0\bar{D}^0$ rates are consistent with expectations based on isospin invariance and the $D^+ - D^0$ mass difference. Combining charged and neutral modes, a fit shown in the left-hand panel of Fig. 9 yields mass and width $M = 3929 \pm 5 \pm 2$ MeV and $\Gamma = 29 \pm 10 \pm 2$ MeV. Although in principle the D -pair could be produced from $D^*\bar{D}$, the observed transverse momentum spectrum of the $D\bar{D}$ pair is consistent with no contribution from $D^*\bar{D}$.

The observation of decay to $D\bar{D}$ makes it impossible for $Z(3930)$ to be the $\eta_c(3S)$ state. Both χ'_{c0} and χ'_{c2} are expected to decay to $D\bar{D}$ (χ'_{c1} is not; it only decays to $D^*\bar{D}$). To distinguish between the two remaining hypotheses, the distribution in θ^* , which is the angle of the D -meson relative to the beam axis in the $\gamma\gamma$ center-of-mass frame, is examined. This distribution is consistent with $\sin^4\theta^*$ as expected for a state with $J = 2, \lambda = \pm 2$ (right-hand panel of Fig. 9). The two-photon width is, under the assumption of a tensor state, measured to be $\Gamma_{\gamma\gamma} \cdot \mathcal{B}_{D\bar{D}} = 0.18 \pm 0.05 \pm 0.03$ keV.

BaBar has searched for $Z(3930)$ decay into $\gamma J/\psi$ [159], and set an upper limit $\mathcal{B}(B \rightarrow Z(3930) + K) \times \mathcal{B}(Z(3930) \rightarrow \gamma J/\psi) < 2.5 \times 10^{-6}$.

The predicted mass of the χ'_{c2} is 3972 MeV and the predicted partial widths and total width assuming $M[2^3P_2(c\bar{c})] = 3930$ MeV are [10, 172]

$$\begin{aligned}\Gamma(\chi'_{c2} \rightarrow D\bar{D}) &= 21.5 \text{ MeV}, \\ \Gamma(\chi'_{c2} \rightarrow D\bar{D}^*) &= 7.1 \text{ MeV and} \\ \Gamma_{\text{total}}(\chi'_{c2}) &= 28.6 \text{ MeV},\end{aligned}$$

in good agreement with the experimental measurement. Furthermore, using $\Gamma(\chi'_{c2} \rightarrow \gamma\gamma) = 0.67$ keV [173] times $\mathcal{B}(\chi'_{c2} \rightarrow D\bar{D}) = 70\%$ implies $\Gamma_{\gamma\gamma} \cdot \mathcal{B}_{D\bar{D}} = 0.47$ keV, which is within a factor of 2 of the observed number, fairly good agreement considering the typical reliability of two-photon partial width predictions.

The observed $Z(3930)$ properties are consistent with those predicted for the χ'_{c2} $2^3P_2(c\bar{c})$ state. So far, the only mild surprise is the observed mass, which is 40 – 50 MeV below expectations. Adjusting that, all other properties observed so far can be accommodated within the framework of [10, 172]. The χ'_{c2} interpretation could be confirmed by observation of the $D\bar{D}^*$ final state. We also note that the χ'_{c2} is predicted to undergo radiative transitions to $\psi(2S)$ with a partial width of $\mathcal{O}(100 \text{ keV})$ [10, 11].

4.9.3 $Y(3940)$

The $Y(3940)$ is seen by Belle in the $\omega J/\psi$ subsystem in the decay $B \rightarrow K\omega(\rightarrow \pi^+\pi^-\pi^0)J/\psi$ [174]. The final state is selected by kinematic constraints that incorporate the parent particle mass $m(B)$ and the fact that the B -meson pair is produced with no additional particles. Background from decays such as $K_1(1270) \rightarrow \omega K$ is reduced by requiring $m(\omega J/\psi) > 1.6$ GeV. The $K\omega J/\psi$ final state yield is then further examined in bins of $m(\omega J/\psi)$. A threshold enhancement is observed, shown in Figure 10, which is fit with a threshold function suitable for phase-space production of this final state and an S -wave Breit-Wigner shape. The reported mass and width of the enhancement are $M = 3943 \pm 11 \pm 13$ MeV and $\Gamma = 87 \pm 22 \pm 26$ MeV. A fit without a resonance contribution gives no good description of the data.

The mass and width of $Y(3940)$ suggest a radially excited P -wave charmonium state. The combined branching ratio is $\mathcal{B}(B \rightarrow KY) \cdot \mathcal{B}(Y \rightarrow \omega J/\psi) = (7.1 \pm 1.3 \pm 3.1) \times 10^{-5}$. One expects that $\mathcal{B}(B \rightarrow K\chi'_{cJ}) < \mathcal{B}(B \rightarrow K\chi_{cJ}) = 4 \times 10^{-4}$. This implies that $\mathcal{B}(Y \rightarrow \omega J/\psi) > 12\%$, which is unusual for a $c\bar{c}$ state above open charm threshold.

For the χ'_{c1} $2^3P_1(c\bar{c})$ we expect $D\bar{D}^*$ to be the dominant decay mode with a predicted width of 140 MeV [147], which is consistent with that of the $Y(3940)$ within the theoretical and experimental uncertainties. Furthermore, the χ_{c1} is also

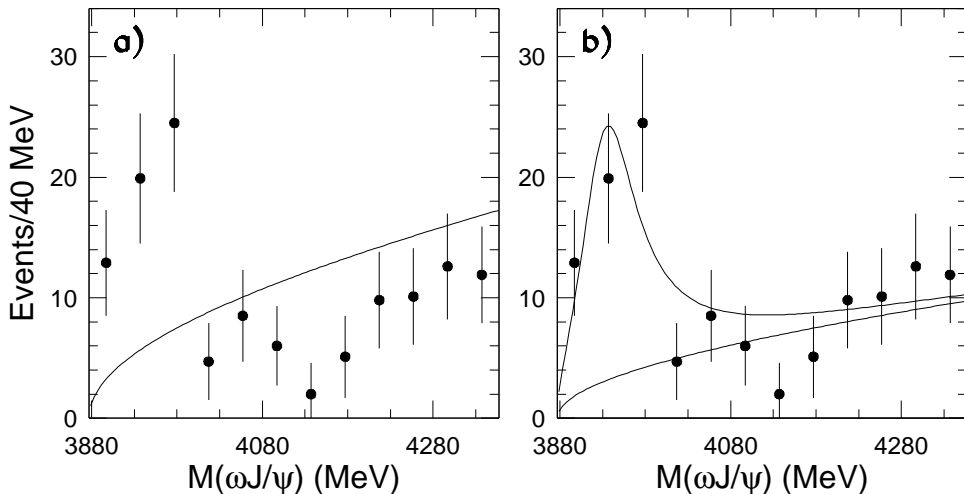


Figure 10: Belle’s χ'_{c1} candidate [174]: The invariant mass $m(\omega J/\psi)$ distribution in $m(B \rightarrow K\omega J/\psi)$ decay. The signal yield is 58 ± 11 events. The two curves are fits without (left) and including (right) a resonance component.

seen in B -decays. Although the decay $1^{++} \rightarrow \omega J/\psi$ is unusual, the corresponding decay $\chi'_{b1} \rightarrow \omega \Upsilon(1S)$ has also been seen [175]. One possible explanation for this unusual decay mode is that rescattering through $D\bar{D}^*$ is responsible: $1^{++} \rightarrow D\bar{D}^* \rightarrow \omega J/\psi$. Another contributing factor might be mixing with the possible molecular state tentatively identified with the $X(3872)$.

BaBar has searched for $Y(3940)$ decay into $\gamma J/\psi$ [159], and set an upper limit $\mathcal{B}(B \rightarrow Y(3940) + K) \times \mathcal{B}(Y(3940) \rightarrow \gamma J/\psi) < 1.4 \times 10^{-5}$.

The χ'_{c1} assignment can be tested by searching for the $D\bar{D}$ and $D\bar{D}^*$ final states and by studying their angular distributions. With the present experimental data, a χ'_{c0} assignment cannot be ruled out.

4.9.4 $X(3940)$

Belle studied double-charmonium production and $e^+e^- \rightarrow J/\psi + X$ near the $\Upsilon(4S)$ [176] and observed enhancements for the well-known charmonium states η_c , χ_{c0} , and $\eta_c(2S)$, at rates and masses consistent with other determinations. In addition, a peak at a higher energy was found. The mass and width were measured to be $M = 3936 \pm 14 \pm 6$ MeV and $\Gamma = 39 \pm 26$ (stat) MeV.

To further examine the properties of this enhancement, Belle searched for exclusive decays $J/\psi \rightarrow D\bar{D}^{(*)}$, given that these decays are kinematically accessible. The J/ψ recoil mass for the cases $D\bar{D}$ and $D\bar{D}^*$ are also shown in Figure 11. An enhancement at the $X(3940)$ mass is seen for $D\bar{D}^*$, but not for $D\bar{D}$. The mass and width determined in this study are $M = (3943 \pm 6 \pm 6)$ MeV, $\Gamma < 52$ MeV (90% c.l.). Note that the inclusive and exclusive samples have some overlap, and thus the two mass measurements are not statistically independent. The overlap has been eliminated for

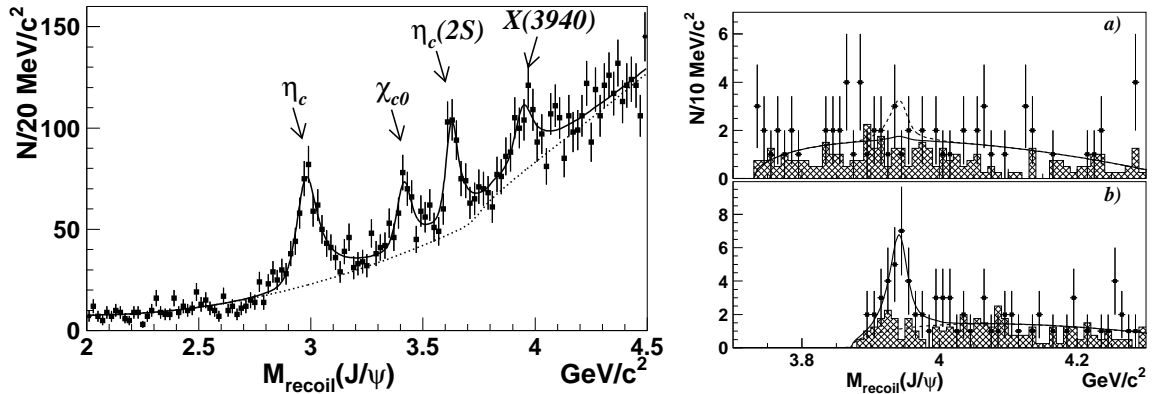


Figure 11: Belle’s $X(3940)$ [176], sighted in $e^+e^- \rightarrow J/\psi + X$: Left: The mass of the system recoiling against the J/ψ . The excess at $X(3940)$ contains 266 ± 63 events and has a statistical significance of 5.0σ . Right: Study of $X(3940)$ decay into D mesons, $e^+e^- \rightarrow J/\psi + DD^*$. Top: DD , no signal is seen at 3940 MeV. Bottom: DD^* , the signal amounts to 24.5 ± 6.9 events (5.0σ).

Table VIII: Properties of the $X(3940)$ [176].

Mass	$3936 \pm 14 \pm 6 \text{ MeV (incl.)}$ $3943 \pm 6 \pm 6 \text{ MeV } (DD^*)$
Total width	$< 52 \text{ MeV}$
$\mathcal{B}(X(3940) \rightarrow DD^*)$	$(96_{-32}^{+45} \pm 22)\%$, $> 45\% (90\% \text{ C.L.})$
$\mathcal{B}(X(3940) \rightarrow DD)$	$< 41\% (90\% \text{ CL})$
$\mathcal{B}(X(3940) \rightarrow \omega J/\psi)$	$< 26\% (90\% \text{ CL})$

the branching fraction determination. A signal of 5.0σ significance was seen for DD^* , but none for DD . In addition, the $X(3940)$ did not show a signal for a decay $\omega J/\psi$, unlike the $Y(3940)$. The findings are summarized in Table VIII.

If confirmed, the decay to DD^* but not DD suggests the $X(3940)$ has unnatural parity. The lower mass η_c and η'_c are also produced in double charm production. One is therefore led to try an η''_c assignment, although this state is expected to have a somewhat higher mass [11]. The predicted width for a 3^1S_0 state with a mass of 3943 MeV is $\sim 50 \text{ MeV}$ [10], which is in not too bad agreement with the measured $X(3940)$ width.

Another possibility due to the dominant DD^* final states is that the $X(3940)$ is the $2^3P_1(c\bar{c}) \chi'_1$ state. It is natural to consider the $2P(c\bar{c})$ since the 2^3P_J states are predicted to lie in the 3920–3980 MeV mass region and the widths are predicted to be in the range $\Gamma(2^3P_J) = 30\text{--}165 \text{ MeV}$ [11]. The dominant DD^* mode would then suggest that the $X(3940)$ is the $2^3P_1(c\bar{c})$ state. The problems with this interpretation are (1) there is no evidence for the $1^3P_1(c\bar{c})$ state in the same data, (2) the predicted

Table IX: Comparison of parameters of $Y(4260)$ as measured by the BaBar [177], CLEO [178], and Belle [179] Collaborations. The average has been calculated using the total error as a weight (in case of asymmetric errors, the one leaning towards the average), and a PDG-style S -factor has been applied to the uncertainty on the average.

Collab.	Mass (MeV/ c^2)	Γ (MeV/ c^2)	$\Gamma_{ee} \times \mathcal{B}(Y(4260) \rightarrow \pi^+\pi^-J/\psi)$ (eV)
BaBar	$4259 \pm 8_{-6}^{+2}$	$88 \pm 23_{-4}^{+6}$	$5.5 \pm 1.0_{-0.7}^{+0.8}$
CLEO	$4284_{-16}^{+17} \pm 4$	$73_{-25}^{+39} \pm 5$	$8.9_{-3.1}^{+3.9} \pm 1.8$
Belle	$4295 \pm 10_{-3}^{+10}$	$133 \pm 26_{-6}^{+13}$	$8.7 \pm 1.1_{-0.9}^{+0.3}$
Average	4274 ± 12	102 ± 17	7.1 ± 1.1
“ S -factor”	2.0	1.1	1.2

width of the $2^3P_1(c\bar{c})$ is 140 MeV (assuming $M(2^3P_1(c\bar{c})) = 3943$ MeV) [147], and (3) there is another candidate for the $1^3P_1(c\bar{c})$ state, the $Y(3940)$.

The most likely interpretation of the $X(3940)$ is that it is the $3^1S_0(c\bar{c}) \eta_c''$ state. Tests of this assignment are to study the angular distribution of the $D\bar{D}^*$ final state and to observe it in $\gamma\gamma \rightarrow D\bar{D}^*$.

4.9.5 $Y(4260)$

Perhaps the most intriguing of the recently discovered states is the $Y(4260)$ reported by BaBar as an enhancement in the $\pi\pi J/\psi$ subsystem in the radiative return reaction $e^+e^- \rightarrow \gamma_{\text{ISR}} J/\psi \pi\pi$ [177], where “ISR” stands for “initial state radiation.” This and subsequent independent confirmation signals [178, 179] are shown in Fig. 12. The measured mass, width, and leptonic width times $\mathcal{B}(Y \rightarrow J/\psi \pi^+\pi^-)$ are summarized in the first row of Table IX. Further evidence was seen by BaBar in $B \rightarrow K(\pi^+\pi^- J/\psi)$ [180].

The CLEO Collaboration has confirmed the $Y(4260)$, both in a direct scan [148] and in radiative return [178]. Results from the scan are shown in Fig. 13, including signals for $Y(4260) \rightarrow \pi^+\pi^- J/\psi$ (11σ), $\pi^0\pi^0 J/\psi$ (5.1σ), and $K^+K^- J/\psi$ (3.7σ). There are also weak signals for $\psi(4160) \rightarrow \pi^+\pi^- J/\psi$ (3.6σ) and $\pi^0\pi^0 J/\psi$ (2.6σ), consistent with the $Y(4260)$ tail, and for $\psi(4040) \rightarrow \pi^+\pi^- J/\psi$ (3.3σ). Reference [178] determines the resonance parameters shown in the second row of Table IX. The Belle Collaboration reported preliminary results [179], based on the study of ISR events at $\Upsilon(4S)$ energy, shown in the third row of Table IX. A comparison of the measured quantities reported by the three collaborations reveals some spread; while the uncertainties on the total width and the coupling are large, the masses differ substantially from each other. This is particularly important in connection with a state at higher energy observed by BaBar (see Section 4.9.6), which is distinctly separate from the $Y(4260)$ in the BaBar mass assignment, but much less so in the Belle measurement.

A variety of ratios between channels have been measured now [148, 181–184], which

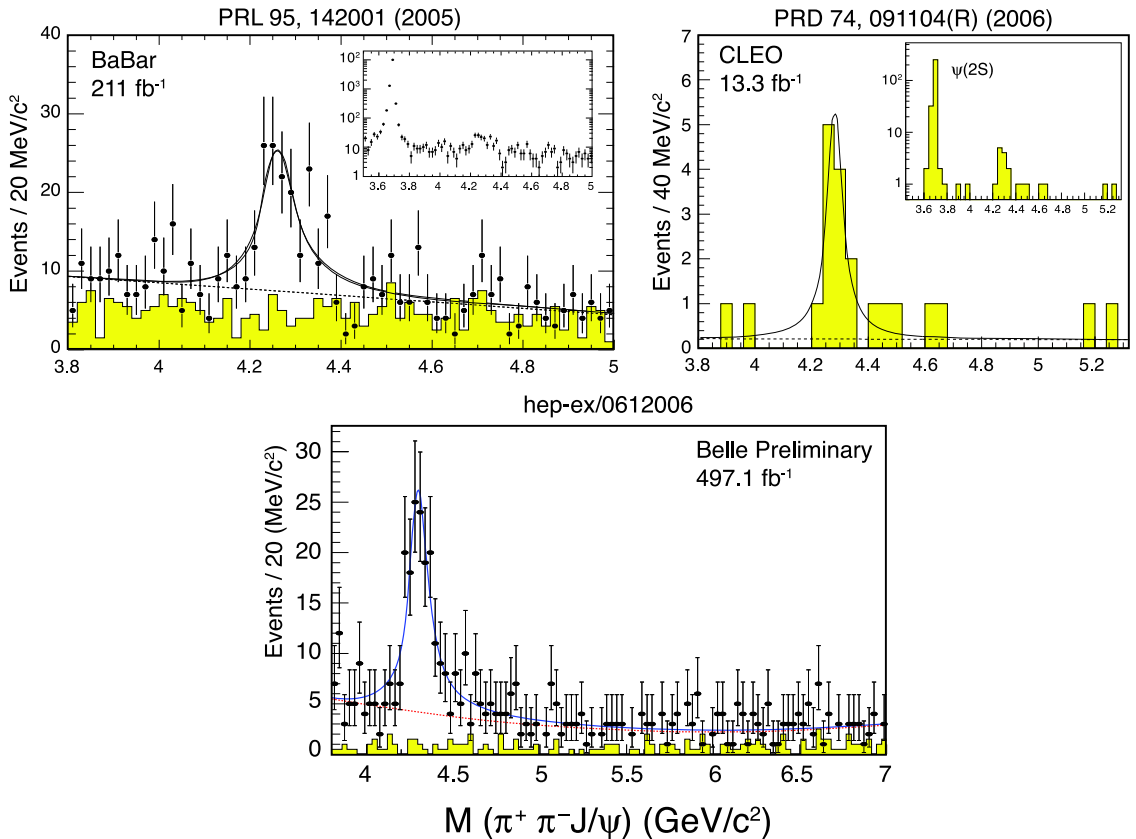


Figure 12: $Y(4260)$ signal in ISR from the $Y(4S)$ by BaBar [177], CLEO [178], and Belle [179]. The fit parameters are given in Table IX.

should help narrow down the possible explanations of $Y(4260)$. They are listed in Table X. The preliminary upper limit for the ratio of $D\bar{D}$ to $\pi^+\pi^-J/\psi$ of 7.6 may not seem particularly tight at first glance, but is to be compared, for example, with the same ratio for the $\psi(3770)$, where it is about 500.

A number of explanations have appeared in the literature: $\psi(4S)$ [185], $c\bar{s}c\bar{s}$ tetraquark [186], and $c\bar{c}$ hybrid [187–189]. In some models the mass of the $Y(4260)$ is consistent with the $4S(c\bar{c})$ level [185]. Indeed, a $4S$ charmonium level at $4260 \text{ MeV}/c^2$ was anticipated on exactly this basis [18]. With this assignment, the nS levels of charmonium and bottomonium are remarkably congruent to one another. However, other calculations using a linear plus Coulomb potential identify the $4^3S_1(c\bar{c})$ level with the $\psi(4415)$ state (e.g., Ref. [11]). If this is the case the first unaccounted-for $1^{--}(c\bar{c})$ state is the $\psi(3^3D_1)$. Quark models estimate its mass to be $M(3^3D_1) \simeq 4500 \text{ MeV}$ which is much too heavy to be the $Y(4260)$. The $Y(4260)$ therefore represents an overpopulation of the expected 1^{--} states. The absence of open charm production also argues against it being a conventional $c\bar{c}$ state.

The hybrid interpretation of $Y(4260)$ is appealing. The flux tube model predicts that the lowest $c\bar{c}$ hybrid mass is $\sim 4200 \text{ MeV}$ [190] with lattice gauge theory having

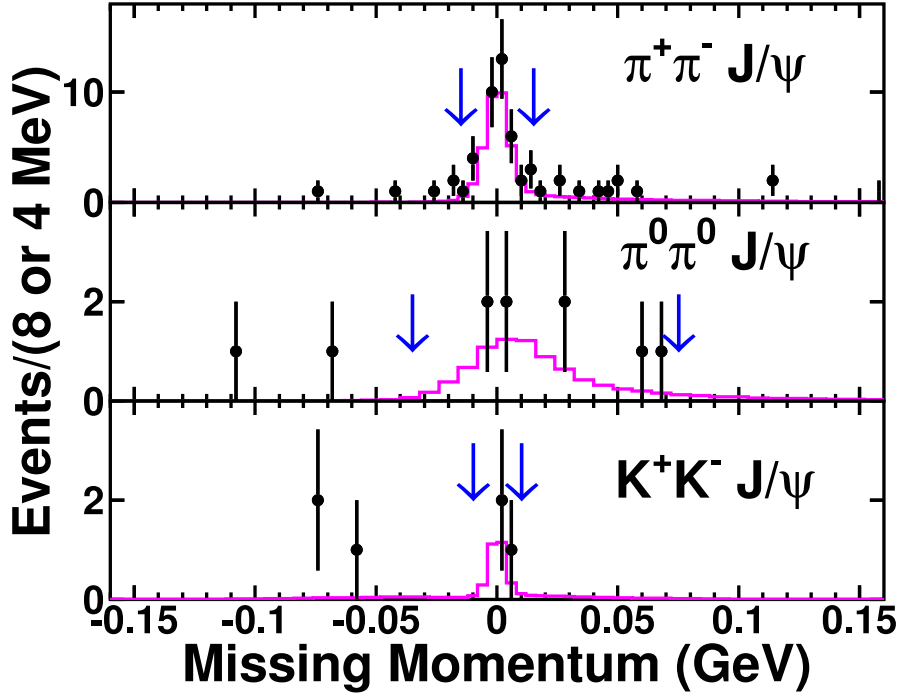


Figure 13: Evidence for $Y(4260)$ from a direct scan by CLEO [148].

similar expectations [191]. Models of hybrids typically expect the wavefunction at the origin to vanish implying a small e^+e^- width in agreement with the observed value. Lattice gauge theory found that the $b\bar{b}$ hybrids have large couplings to closed flavor channels [192] which is similar to the BaBar observation of $Y \rightarrow J/\psi\pi^+\pi^-$; the branching ratio of $\mathcal{B}(Y \rightarrow J/\psi\pi^+\pi^-) > 8.8\%$ combined with the observed width implies that $\Gamma(Y \rightarrow J/\psi\pi^+\pi^-) > 7.7 \pm 2.1$ MeV. This is much larger than the typical charmonium transition widths of, for example, $\Gamma(\psi(3770) \rightarrow J/\psi\pi^+\pi^-) \sim 80$ keV. And the Y is seen in this mode while the conventional states $\psi(4040)$, $\psi(4160)$, and $\psi(4415)$ are not.

One predicted consequence of the hybrid hypothesis is that the dominant hybrid charmonium open-charm decay modes are expected to be a meson pair with an S -wave (D , D^* , D_s , D_s^*) and a P -wave (D_J , D_{sJ}) in the final state [188]. The dominant decay mode is expected to be $D\bar{D}_1 + \text{c.c.}$. (Subsequently we shall omit “+c.c.” in cases where it is to be understood). Evidence for a large $D\bar{D}_1$ signal would be strong evidence for the hybrid interpretation. A complication is that $D\bar{D}_1$ threshold is 4287 MeV/ c^2 if we consider the lightest D_1 to be the narrow state noted in Ref. [55] at 2422 MeV/ c^2 . The possibility also exists that the $Y(4260)$ could be a $D\bar{D}_1$ bound state. It would decay to $D\pi\bar{D}^*$, where the D and π are not in a D^* . Note that the dip in $R_{e^+e^-}$ occurs just below $D\bar{D}_1$ threshold, which may be the first S -wave meson pair accessible in $c\bar{c}$ fragmentation [188,193]. In addition to the hybrid decay modes given above, lattice gauge theory suggests that we search for other closed charm modes with $J^{PC} = 1^{--}$: $J/\psi\eta$, $J/\psi\eta'$, $\chi_{cJ}\omega$ and more. Distinguishing among the interpretations

Table X: Experimental results on $Y(4260)$ decay. The last column gives the relative rate compared to $\pi^+\pi^-J/\psi$ for each channel. Unless indicated otherwise, data are from Refs. [148] and [181], and upper limits are at 90% CL.

Channel	cross-section (pb)	$\mathcal{B}/\mathcal{B}_{\pi^+\pi^-J/\psi}$
$\pi^+\pi^-J/\psi$	$58_{-10}^{+12} \pm 4$	1
	51 ± 12 [182]	1
$\pi^0\pi^0J/\psi$	$23_{-8}^{+12} \pm 1$	$0.39_{-0.15}^{+0.20} \pm 0.02$
K^+K^-J/ψ	$9_{-5}^{+9} \pm 1$	$0.15_{-0.08}^{+0.10} \pm 0.02$
$\eta J/\psi$	< 32	< 0.6
$\pi^0 J/\psi$	< 32	< 0.2
$\eta' J/\psi$	< 19	< 0.3
$\pi^+\pi^-\pi^0 J/\psi$	< 7	< 0.1
$\eta\eta J/\psi$	< 44	< 0.8
$\pi^+\pi^-\psi(2S)$	< 20	< 0.3
$\eta\psi(2S)$	< 25	< 0.4
$\omega\chi_{c0}$	< 234	< 4.0
$\gamma\chi_{c1}$	< 30	< 0.5
$\gamma\chi_{c2}$	< 90	< 1.6
$\pi^+\pi^-\pi^0\chi_{c1}$	< 46	< 0.8
$\pi^+\pi^-\pi^0\chi_{c2}$	< 96	< 1.7
$\pi^+\pi^-\phi$	< 5	< 0.1 (also [183])
$D\bar{D}$		< 7.6 (95%CL) [184]
$p\bar{p}$		< 0.13 (90%CL) [182]

of the $Y(4260)$ will likely require careful measurement of several decay modes.

If the $Y(4260)$ is a hybrid it is expected to be a member of a multiplet consisting of eight states with masses in the 4.0 to 4.5 GeV mass range with lattice gauge theory preferring the higher end of the range [194]. It would be most convincing if some of these partners were found, especially the J^{PC} exotics. In the flux-tube model the exotic states have $J^{PC} = 0^{+-}, 1^{-+},$ and 2^{+-} while the non-exotic low-lying hybrids have $0^{-+}, 1^{+-}, 2^{-+}, 1^{++},$ and 1^{--} .

4.9.6 A state in $\pi^+\pi^-\psi(2S)$

In the radiative return process $e^+e^- \rightarrow \gamma + X$, the BaBar Collaboration [184, 195] reports a broad structure decaying to $\pi^+\pi^-\psi(2S)$, where $\psi(2S) \rightarrow \pi^+\pi^-J/\psi$. A single-resonance hypothesis with $M(X) = (4324 \pm 24)$ MeV/ c^2 and $\Gamma(X) = (172 \pm 33)$ MeV is adequate to fit the observed mass spectrum.

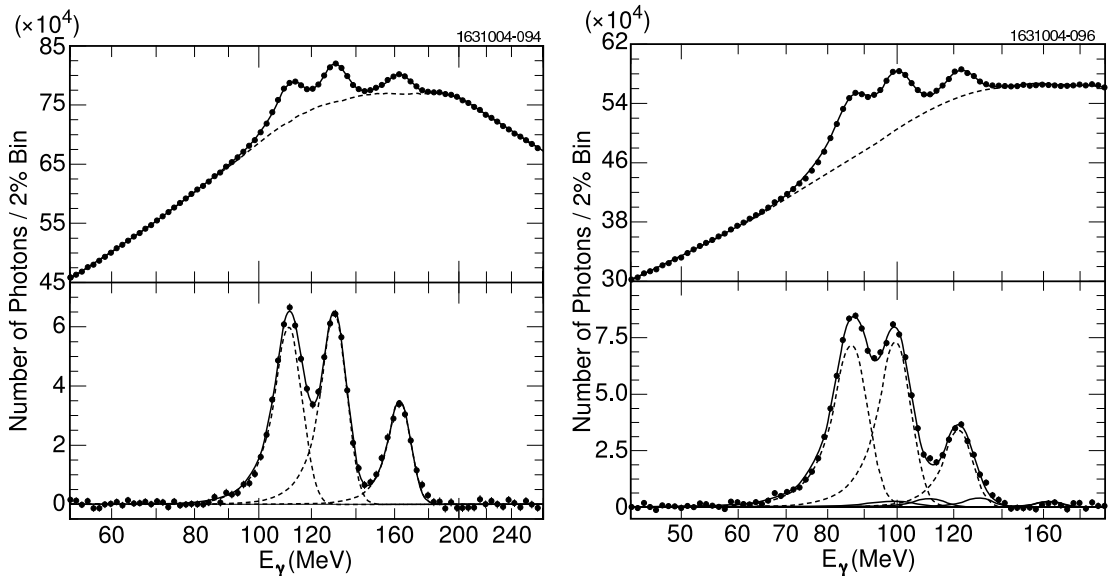


Figure 14: From Ref. [196]: Inclusive photon spectrum in $\Upsilon(nS) \rightarrow \gamma X$, for $n = 2$ (left) and $n = 3$ (right), before and after background subtraction. In the upper plots, the dashed line indicates the background level; in the lower plots, the fit contribution for each resonance is delineated. The low-lying solid curves in the lower right plot show two background contributions. The three peaks corresponding to the $\chi_{bJ}(')$ are clearly visible. The peak position determines the $\chi_{bJ}(')$ masses. The signal area is used to determine the $\Upsilon(nS) \rightarrow \gamma\chi_{bJ}(')$ branching fraction.

5 BOTTOMONIUM

5.1 Overview

Some properties and decays of the $\Upsilon(b\bar{b})$ levels are summarized in Fig. 2. The measured masses of the Υ states below open flavor threshold have accuracies comparable to those in charmonium since similar techniques are used. Experimentally, the situation is more difficult due to the larger multiplicities involved and due to the increased continuum background compared to the charmonium region.

Modern data samples are CLEO's 22M, 9M, 6M $\Upsilon(1, 2, 3S)$ decays (with smaller off-resonance samples in addition) and Belle's $\Upsilon(3S)$ sample of 11M $\Upsilon(3S)$.

The $\chi_{bJ}(')$ states are reached through E1 transitions; branching fractions for $n \rightarrow n - 1$ range from 4-14%. Their masses are determined from the transition photon energies. Their intrinsic widths are not known. Examples of fits to the inclusive photon spectrum that led to $\chi_{bJ}(')$ mass determinations [196] are shown in Fig. 14. Exclusive hadronic decays of the $\chi_{bJ}(')$ states have not been reported; information exists only on transitions within the bottomonium spectrum. An $\Upsilon(1D)$ candidate has been observed; the singlets $\eta_b(')$ and $h_b(')$ have thus far escaped detection.

Mass differences within the bottomonium spectrum are in agreement with unquenched lattice QCD calculations [197]. Direct photons have been observed in 1S,

Table XI: Comparison of observed (a) and predicted (b) partial widths for $2S \rightarrow 1P_J$ and $3S \rightarrow 2P_J$ transitions in $b\bar{b}$ systems.

	Γ (keV), $2S \rightarrow 1P_J$ transitions			Γ (keV), $3S \rightarrow 2P_J$ transitions		
	$J = 0$	$J = 1$	$J = 2$	$J = 0$	$J = 1$	$J = 2$
(a)	1.20 ± 0.18	2.22 ± 0.23	2.32 ± 0.23	1.38 ± 0.19	2.95 ± 0.30	3.21 ± 0.33
(b)	1.39	2.18	2.14	1.65	2.52	2.78

$2S$, and $3S$ decays, leading to estimates of the strong fine-structure constant α_S consistent with others [198]. The transitions $\chi_b(2P) \rightarrow \pi\pi\chi_b(1P)$ have been seen [199]. BaBar has observed $\Upsilon(4S) \rightarrow \pi^+\pi^-\Upsilon(1S, 2S)$ transitions [200], while Belle has seen $\Upsilon(4S) \rightarrow \pi^+\pi^-\Upsilon(1S)$ [201].

Decays to light hadrons proceed, as in the case of the charmonium states, via annihilation of the heavy quarks into ggg , $gg\gamma$ or γ^* , which subsequently hadronize. At higher energies, fragmentation into low-multiplicity states is suppressed, and so the second step makes it difficult to arrive at a simple scaling prediction to translate bottomonium and charmonium results into each other. Comparing the Υ states with each other, for example by constructing a prescription akin to the 12% rule in charmonium, is possible, but to date only a few exclusive radiative decays to light mesons, but no exclusive non-radiative decays to light mesons, have been observed.

5.2 $\Upsilon(1S, 2S, 3S)$

5.2.1 Leptonic branching ratios and partial widths

New values of $\mathcal{B}[\Upsilon(1S, 2S, 3S) \rightarrow \mu^+\mu^-] = (2.49 \pm 0.02 \pm 0.07, 2.03 \pm 0.03 \pm 0.08, 2.39 \pm 0.07 \pm 0.10)\%$ [202], when combined with new measurements $\Gamma_{ee}(1S, 2S, 3S) = (1.252 \pm 0.004 \pm 0.019, 0.581 \pm 0.004 \pm 0.009, 0.413 \pm 0.004 \pm 0.006)$ keV [23], imply total widths $\Gamma_{\text{tot}}(1S, 2S, 3S) = (50.28 \pm 1.66, 28.62 \pm 1.30, 17.28 \pm 0.61)$ keV. The values of $\Gamma_{\text{tot}}(2S, 3S)$ changed considerably with respect to previous world averages. Combining with previous data, the Particle Data Group [55] now quotes $\Gamma_{\text{tot}}(1S, 2S, 3S) = (54.02 \pm 1.25, 31.98 \pm 2.63, 20.32 \pm 1.85)$ keV, which we shall use in what follows. This will lead to changes in comparisons of predicted and observed transition rates. As one example, the study of $\Upsilon(2S, 3S) \rightarrow \gamma X$ decays [196] has provided new branching ratios for E1 transitions to $\chi_{bJ}(1P)$, $\chi_{bJ}(2P)$ states. These may be combined with the new total widths to obtain updated partial decay widths [line (a) in Table XI], which may be compared with one set of nonrelativistic predictions [2] [line (b)]. The suppression of transitions to $J = 0$ states by 10–20% with respect to nonrelativistic expectations agrees with relativistic predictions [39, 40, 203]. The partial width for $\Upsilon(3S) \rightarrow \gamma 1^3P_0$ is found to be 61 ± 23 eV, about nine times the highly-suppressed value predicted in Ref. [2]. That prediction is very sensitive to details of wave functions; the discrepancy indicates the importance of relativistic distortions.

Table XII: Ratio $R_{\tau\tau} \equiv \mathcal{B}[\Upsilon(nS) \rightarrow \tau\tau]/\mathcal{B}[\Upsilon(nS) \rightarrow \mu\mu]$ and $\mathcal{B}[\Upsilon(nS) \rightarrow \tau\tau]$ [204].

	$R_{\tau\tau}$	$\mathcal{B}[\Upsilon(nS) \rightarrow \tau\tau]$ (%)
$\Upsilon(1S)$	$1.02 \pm 0.02 \pm 0.05$	$2.54 \pm 0.04 \pm 0.12$
$\Upsilon(2S)$	$1.04 \pm 0.04 \pm 0.05$	$2.11 \pm 0.07 \pm 0.13$
$\Upsilon(3S)$	$1.05 \pm 0.08 \pm 0.05$	$2.52 \pm 0.19 \pm 0.15$

Table XIII: Predicted [2] and measured [55] branching ratios for $\chi_{bJ}(2P) = 2^3P_J$ radiative E1 decays.

Level	Final state	Predicted \mathcal{B} (%) [2]	Measured \mathcal{B} (%) [55]
2^3P_0	$\gamma + 1S$	0.96	0.9 ± 0.6
	$\gamma + 2S$	1.27	4.6 ± 2.1
2^3P_1	$\gamma + 1S$	11.8	8.5 ± 1.3
	$\gamma + 2S$	20.2	21 ± 4
2^3P_2	$\gamma + 1S$	5.3	7.1 ± 1.0
	$\gamma + 2S$	18.9	16.2 ± 2.4

The branching ratios $\mathcal{B}[\Upsilon(1S, 2S, 3S) \rightarrow \tau^+\tau^-]$ have been measured by the CLEO Collaboration [204], and are shown in Table XII. They are consistent with lepton universality and represent the first measurement of the $\Upsilon(3S) \rightarrow \tau\tau$ branching ratio.

5.2.2 $\gamma gg/ggg$ ratios

The direct photon spectrum in $1S, 2S, 3S$ decays has been measured using CLEO III data [198]. The ratios $R_\gamma \equiv \mathcal{B}(gg\gamma)/\mathcal{B}(ggg)$ are found to be $R_\gamma(1S) = (2.70 \pm 0.01 \pm 0.13 \pm 0.24)\%$, $R_\gamma(2S) = (3.18 \pm 0.04 \pm 0.22 \pm 0.41)\%$, $R_\gamma(3S) = (2.72 \pm 0.06 \pm 0.32 \pm 0.37)\%$. $R_\gamma(1S)$ is consistent with an earlier CLEO value of $(2.54 \pm 0.18 \pm 0.14)\%$.

5.3 E1 transitions between $\chi_{bJ}(nP)$ and S states

We have already discussed the inclusive branching ratios for the transitions $\Upsilon(2S) \rightarrow \gamma\chi_{bJ}(1P)$, $\Upsilon(3S) \rightarrow \gamma\chi_{bJ}(1P)$, and $\Upsilon(3S) \rightarrow \gamma\chi_{bJ}(2P)$. When these are combined with branching ratios for exclusive transitions where the photons from $\chi_{bJ} \rightarrow \gamma\Upsilon(1S)$ and $\chi_{bJ}(2P) \rightarrow \gamma\Upsilon(1S, 2S)$ and the subsequent decays $\Upsilon(1S, 2S) \rightarrow \ell^+\ell^-$ also are observed, one can obtain branching ratios for the radiative E1 decays of the $\chi_{bJ}(1P)$ and $\chi_{bJ}(2P)$ states. The $\chi_{bJ}(1P)$ branching ratios have not changed since the treatment of Ref. [2], and are consistent with the predictions quoted there. There has been some improvement in knowledge of the $\chi_{bJ}(2P)$ branching ratios, as summarized in Table XIII.

The dipole matrix elements for $\Upsilon(2S) \rightarrow \gamma\chi_{bJ}(1P)$ and $\Upsilon(3S) \rightarrow \gamma\chi_{bJ}(2P)$ are shown in Figs. 15 and 16, along with predictions of various models. The dipole matrix element predictions are in generally good agreement with the observed values.

As already pointed out, the most notable exceptions are the matrix elements $\langle 3^3S_1|r|1^3P_J \rangle$. In the NR limit this overlap is less than 5% of any other $S - P$ overlap, and its suppression occurs for a broad range of potential shapes [206]. This dynamical accident makes these transition rates very sensitive to the details of wave functions and relativistic corrections which are not known to this level of precision. This sensitivity is shown most clearly looking at the signs of the matrix elements as well as their magnitudes. The average experimental value for this matrix element is $\langle 3^3S_1|r|1^3P_J \rangle = 0.050 \pm 0.006 \text{ GeV}^{-1}$ [207]. Taking the predictions of Ref. [32] for comparison, the average over J values gives 0.052 GeV^{-1} which is in good agreement with the observed value. However, more detailed scrutiny gives 0.097 , 0.045 , and -0.015 GeV^{-1} for $J = 2, 1$, and 0 matrix elements respectively. Not only is there a large variation in the magnitudes but the sign also changes, highlighting how sensitive the results for this particular transition are to details of the model due to delicate cancellations in the integral.

The branching ratios can also be used to measure the ratios of various E1 matrix elements which can then be compared to potential model predictions. CLEO [207] obtained the following values for ratios:

$$\begin{aligned} \frac{|\langle 2^3P_2|r|1^3S_1 \rangle|}{|\langle 2^3P_2|r|2^3S_1 \rangle|} &= 0.105 \pm 0.004 \pm 0.006, \\ \frac{|\langle 2^3P_1|r|1^3S_1 \rangle|}{|\langle 2^3P_1|r|2^3S_1 \rangle|} &= 0.087 \pm 0.002 \pm 0.005, \\ \frac{|\langle 2^3P_{1,2}|r|1^3S_1 \rangle|}{|\langle 2^3P_{1,2}|r|2^3S_1 \rangle|} &= 0.096 \pm 0.002 \pm 0.005, \end{aligned}$$

where the final ratio averages the results for $J = 1$ and $J = 2$. In nonrelativistic calculations the E1 matrix elements do not depend on J . The deviation of the results for $J = 1$ and $J = 2$ from each other suggests relativistic contributions to the matrix elements.

5.4 D -wave states

The precise information on the masses of S -wave and P -wave $b\bar{b}$ levels leads to highly constrained predictions for the masses and production rates for the D -wave levels [2,5]. The CLEO Collaboration [208] has presented evidence for at least one of these levels in the four-photon cascade $\Upsilon(3S) \rightarrow \gamma\chi_b(2P)$, $\chi_b(2P) \rightarrow \gamma\Upsilon(1D)$, $\Upsilon(1D) \rightarrow \gamma\chi_b(1P)$, $\chi_b(1P) \rightarrow \gamma\Upsilon(1S)$, followed by the $\Upsilon(1S)$ annihilation into e^+e^- or $\mu^+\mu^-$. CLEO III [208] finds their data are dominated by the production of one $\Upsilon(1D)$ state consistent with the $J = 2$ assignment and a mass $(10161.1 \pm 0.6 \pm 1.6) \text{ MeV}$, which is consistent with predictions from potential models and lattice QCD calculations. The signal product branching ratio obtained is $\mathcal{B}(\gamma\gamma\gamma\gamma\ell^+\ell^-)_{\Upsilon(1D)} = (2.5 \pm 0.5 \pm 0.5) \cdot 10^{-5}$ where the first error is statistical and the second one is systematic. The branching

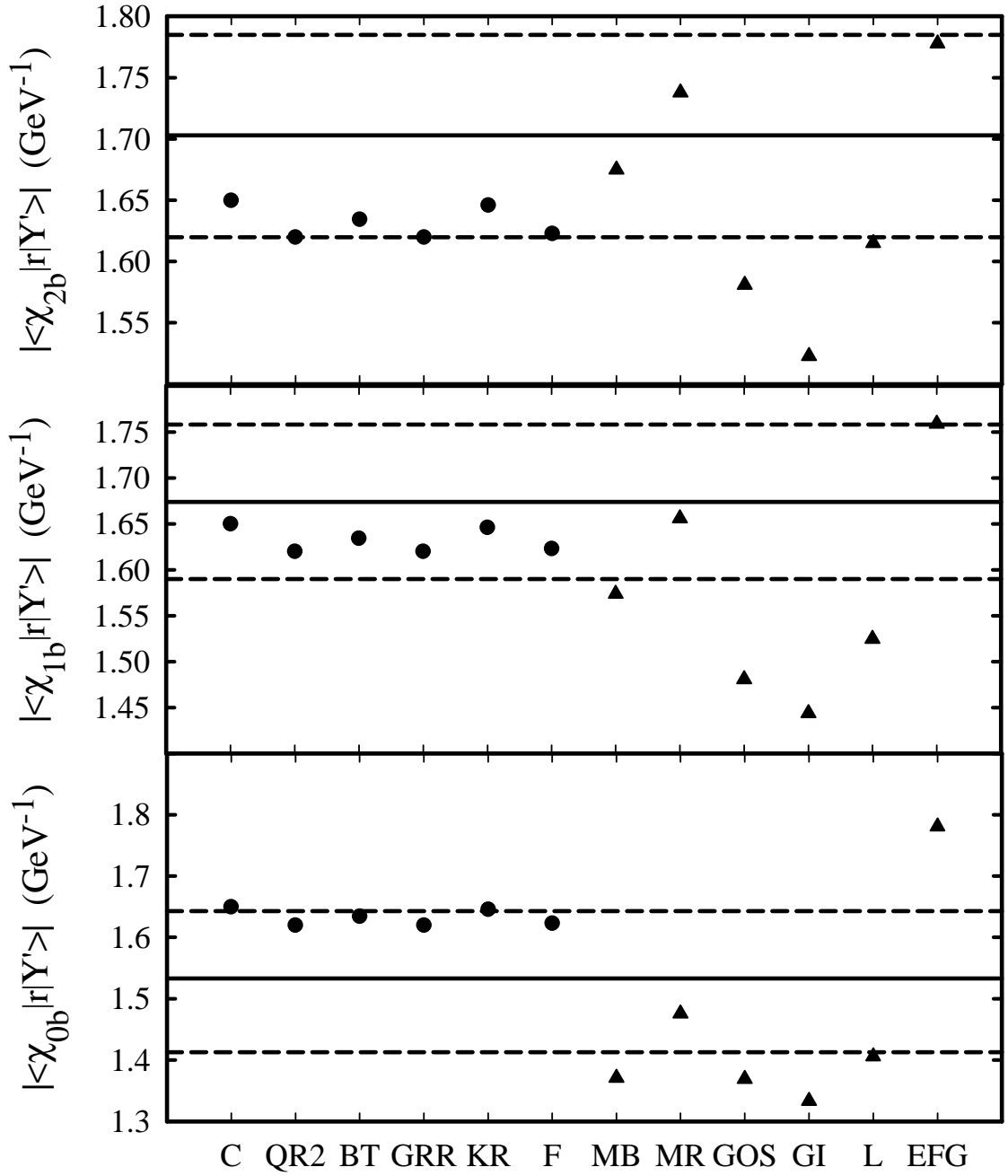


Figure 15: E1 dipole transition matrix elements for the bottomonium decays $2^3S_1 \rightarrow 1^3P_J$. The labels are the same as in Fig. 3 with the addition of two sets of predictions: KR-Kwong Rosner [2], F-Fulcher [205].

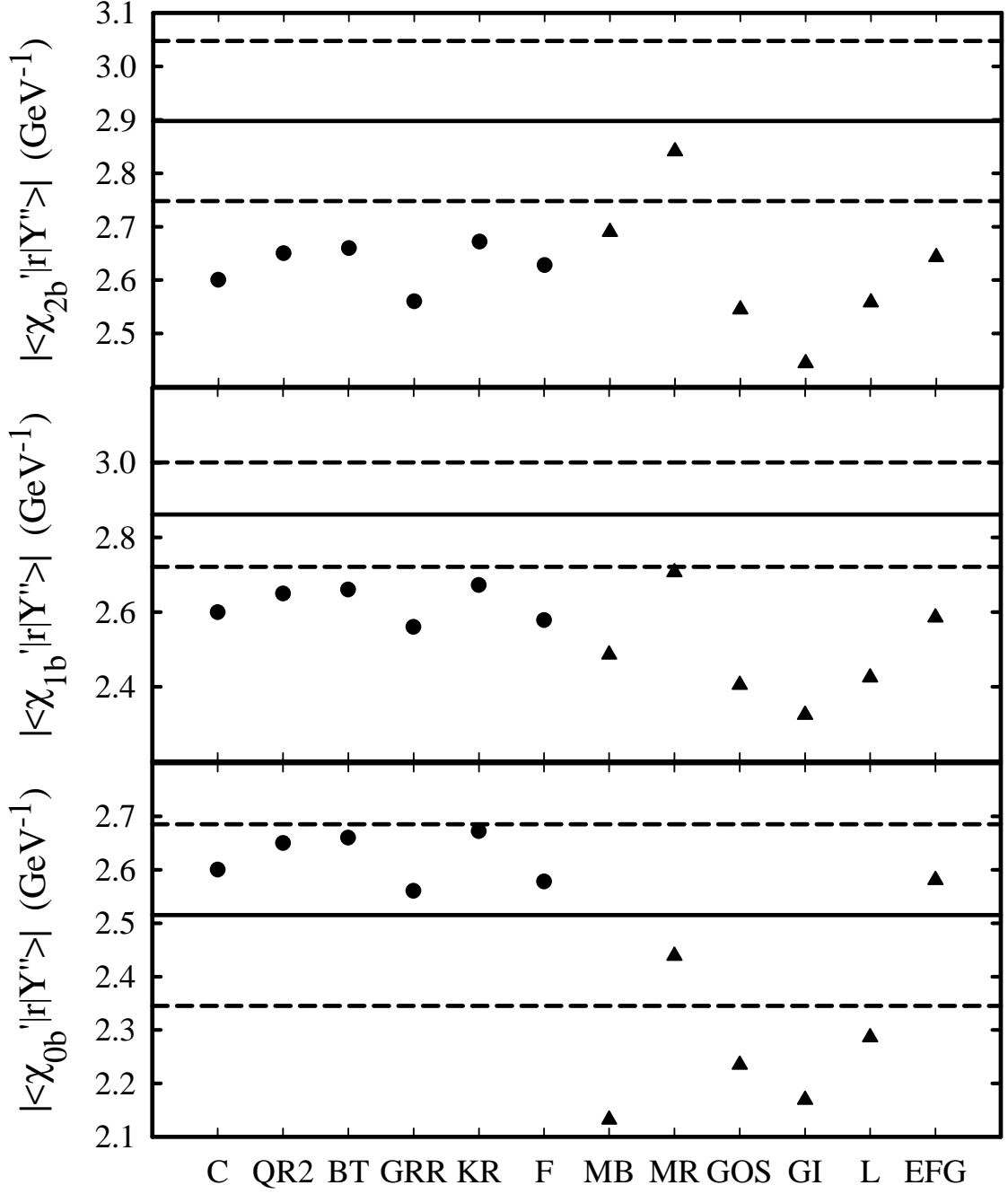


Figure 16: E1 dipole transition matrix elements for the bottomonium decays $3^3S_1 \rightarrow 2^3P_J$. The labels are the same as in Fig. 15.

ratio is consistent with the theoretical estimate of 2.6×10^{-5} [2, 5] for the $\Upsilon(1^3D_2)$ intermediate state.

5.5 New hadronic transitions

5.5.1 $\chi'_{b1,2} \rightarrow \omega\Upsilon(1S)$

The first transition of one heavy quarkonium state to another involving ω emission was reported by the CLEO Collaboration [175]: $\Upsilon(2^3P_{1,2}) \rightarrow \omega\Upsilon(1S)$, which we have already mentioned in connection with the corresponding transition for the $\chi'_{c1}(2^3P_1)$ charmonium state.

5.5.2 $\chi'_{b1,2} \rightarrow \chi_{b1,2}$

The transitions $\chi'_b \rightarrow \chi_b\pi\pi$ have been observed for the first time [199]. One looks for $\Upsilon(3S) \rightarrow \gamma\chi'_b \rightarrow \gamma\pi\pi\chi_b \rightarrow \gamma\pi\pi\gamma\Upsilon(1S)$ in CLEO data consisting of 5.8 million $3S$ events. Both charged and neutral pions are detected. Assuming that $\Gamma(\chi'_{b1} \rightarrow \pi\pi\chi_{b1}) = \Gamma(\chi'_{b2} \rightarrow \pi\pi\chi_{b2})$, both are found equal to $(0.83 \pm 0.22 \pm 0.08 \pm 0.19)$ keV, with the uncertainties being statistical, internal CLEO systematics, and common systematics from outside sources. This value is in satisfactory agreement with theoretical expectations [49].

5.5.3 Searches for $\Upsilon(2S, 3S) \rightarrow \eta\Upsilon(1S)$

The decay $\psi(2S) \rightarrow \eta J/\psi(1S)$ has been known to occur since the early decays of charmonium spectroscopy. The world average for its branching ratio is $\mathcal{B}[\psi(2S) \rightarrow \eta J/\psi(1S)] = (3.09 \pm 0.08)\%$ [55]. The corresponding $\Upsilon(2S) \rightarrow \eta\Upsilon(1S)$ process has not been seen and is represented only by the very old upper limit $\mathcal{B} < 2 \times 10^{-3}$ [209]. The corresponding upper limit for $\Upsilon(3S) \rightarrow \eta\Upsilon(1S)$ is $\mathcal{B} < 2.2 \times 10^{-3}$ [210]. However, because these transitions involve a quark spin flip, they are expected to be highly suppressed in the $b\bar{b}$ system. Defining the ratios

$$R' \equiv \frac{\Gamma[\Upsilon(2S) \rightarrow \eta\Upsilon(1S)]}{\Gamma[\psi(2S) \rightarrow \eta J/\psi(1S)]} \quad , \quad R'' \equiv \frac{\Gamma[\Upsilon(3S) \rightarrow \eta\Upsilon(1S)]}{\Gamma[\psi(2S) \rightarrow \eta J/\psi(1S)]} \quad , \quad (30)$$

Kuang [137] finds in one model $R' = 0.0025$, $R'' = 0.0013$. Combining these results with the latest total widths [55], one predicts

$$\mathcal{B}[\Upsilon(2S) \rightarrow \eta\Upsilon(1S)] = (8.1 \pm 0.8) \times 10^{-4} \quad , \quad (31)$$

$$\mathcal{B}[\Upsilon(3S) \rightarrow \eta\Upsilon(1S)] = (6.7 \pm 0.7) \times 10^{-4} \quad . \quad (32)$$

The present CLEO III samples of 9 million $\Upsilon(2S)$ and 6 million $\Upsilon(3S)$ decays could be used to test these predictions.

5.6 Searches for spin-singlets

Decays of the $\Upsilon(1S, 2S, 3S)$ states can yield $b\bar{b}$ spin-singlets, but none has been seen yet. One expects $1S$, $2S$, and $3S$ hyperfine splittings to be approximately 60, 30, 20 MeV/ c^2 [4]. The lowest P -wave singlet state (“ h_b ”) is expected to be near $\langle M(1^3P_J) \rangle \simeq 9900$ MeV/ c^2 [6].

Several searches have been performed or are under way in $1S$, $2S$, and $3S$ CLEO data. The allowed M1 transition in $\Upsilon(1S) \rightarrow \gamma\eta_b(1S)$ can be studied by reconstructing exclusive final states in $\eta_b(1S)$ decays. One may be able to dispense with the soft photon, which could be swallowed up in background. Final states are likely to be of high multiplicity.

One can search for higher-energy but suppressed M1 photons in $\Upsilon(n'S) \rightarrow \gamma\eta_b(nS)$ ($n \neq n'$) decays. Inclusive searches already exclude many models. The strongest upper limit obtained is for $n' = 3$, $n = 1$: $\mathcal{B} \leq 4.3 \times 10^{-4}$ (90% c.l.) [196]. Exclusive searches (in which η_b decay products are reconstructed) also hold some promise. Searches for η_b using the sequential processes $\Upsilon(3S) \rightarrow \pi^0 h_b(1^1P_1) \rightarrow \pi^0 \gamma \eta_b(1S)$ and $\Upsilon(3S) \rightarrow \gamma \chi'_{b0} \rightarrow \gamma \eta \eta_b(1S)$ (suggested in Ref. [211]) are being conducted. Additional searches for h_b involve the transition $\Upsilon(3S) \rightarrow \pi^+ \pi^- h_b$ [for which a typical experimental upper bound based on earlier CLEO data [210,212] is $\mathcal{O}(10^{-3})$]. The $h_b \rightarrow \gamma \eta_b$ transition is expected to have a 40% branching ratio [6], much like $h_c \rightarrow \gamma \eta_c$.

5.7 $\Upsilon(4S)$

The $\Upsilon(4S)$ is the lowest-lying bound bottomonium state above open-flavor threshold. Its mass and total width as well as electronic width have been determined in scans, most recently by BaBar [213]: $M = (10579.3 \pm 0.4 \pm 1.2)$ MeV/ c^2 , $\Gamma_{ee} = (0.321 \pm 0.017 \pm 0.029)$ keV, $\Gamma = (20.7 \pm 1.6 \pm 2.5)$ MeV. Although the $\Upsilon(4S)$ has primarily been regarded as a $B\bar{B}$ “factory,” its decays to bound $b\bar{b}$ states are beginning to be observed in the large data samples accumulated by BaBar and Belle. This is not surprising, as the corresponding first charmonium state above flavor threshold, the $\psi''(3770)$, does decay – rarely – to charmonium [55].

The BaBar Collaboration [200] measures the product branching fractions $\mathcal{B}[\Upsilon(4S) \rightarrow \pi^+ \pi^- \Upsilon(1S)] \times \mathcal{B}(\Upsilon(1S) \rightarrow \mu^+ \mu^-) = (2.23 \pm 0.25 \pm 0.27) \times 10^{-6}$ and $\mathcal{B}[\Upsilon(4S) \rightarrow \pi^+ \pi^- \Upsilon(2S)] \times \mathcal{B}(\Upsilon(2S) \rightarrow \mu^+ \mu^-) = (1.69 \pm 0.26 \pm 0.20) \times 10^{-6}$, while the Belle Collaboration [201] finds $\mathcal{B}[\Upsilon(4S) \rightarrow \pi^+ \pi^- \Upsilon(1S)] \times \mathcal{B}(\Upsilon(1S) \rightarrow \mu^+ \mu^-) = (4.4 \pm 0.8 \pm 0.6) \times 10^{-6}$. These product branching fractions, when combined with $\mathcal{B}(\Upsilon(1S)[\Upsilon(2S)] \rightarrow \mu^+ \mu^-) = (2.48 \pm 0.05)\%[(1.93 \pm 0.17)\%]$ [55] result in branching fractions of the order of 10^{-4} and partial widths of a few keV, comparable with other partial widths for dipion transitions in the Upsilon system of the same order of magnitude. An interesting feature is that the distribution of $m(\pi^+ \pi^-)$ in $\Upsilon(4S) \rightarrow \Upsilon(2S)$ looks markedly different from the Upsilon dipion transitions with $\Delta n = 1$ [$\Upsilon(3S) \rightarrow \Upsilon(2S)$, $\Upsilon(2S) \rightarrow \Upsilon(1S)$] and more resembles that of $\Upsilon(3S) \rightarrow \Upsilon(1S)$; however, the $\Upsilon(4S) \rightarrow \Upsilon(1S)$ dipion spectrum ($\Delta n = 3$) can be described by a model that suits the $\Delta n = 1$ bottomonium transitions and also the shape in $\psi(2S) \rightarrow \pi^+ \pi^- J/\psi$ [49].

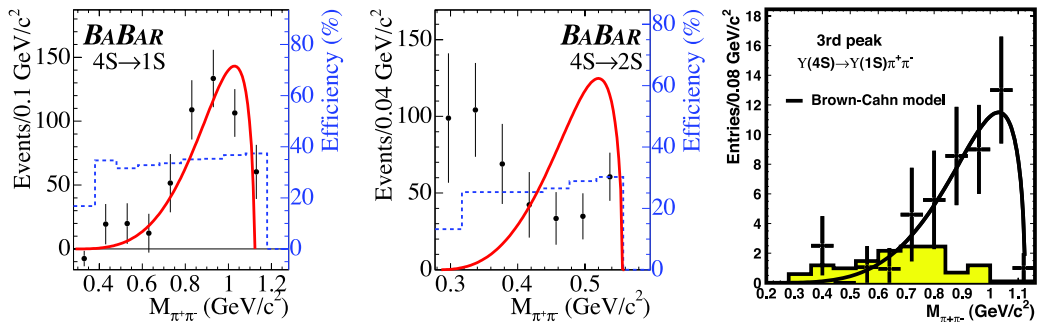


Figure 17: Invariant mass of the dipion system in $\Upsilon(4S) \rightarrow \pi^+\pi^-\Upsilon(1, 2S)$ as measured in data from BaBar [200] and Belle [201] (points), after efficiency correction. For the BaBar figures, the dotted line is the selection efficiency, and the solid line is the prediction of Ref. [49]. In the Belle plot, the shaded histogram is a background estimate, and the curve is based on the model detailed in Ref. [48, 52, 214].

The measured dipion invariant mass distributions for $\Upsilon(4S) \rightarrow \pi^+\pi^-\Upsilon(1S, 2S)$ are shown in Figure 17.

6 INTERPOLATION: $b\bar{c}$ LEVELS

The CDF Collaboration has identified events of the form $B_c \rightarrow J/\psi\pi^\pm$, allowing for the first time a precise determination of the mass: $M=(6276.5\pm 4.0\pm 2.7)$ MeV/ c^2 [215]. This is in reasonable accord with the latest lattice prediction of $6304\pm 12_{-0}^{+18}$ MeV [216].

The mass of the observed $b\bar{c}$ state can be used to distinguish among various theoretical approaches to $c\bar{c}$, $b\bar{c}$, and $b\bar{b}$ spectra. In this manner, in principle, one can obtain a more reliable prediction of the masses of unseen $b\bar{b}$ states such as $\eta_b(1S, 2S, 3S)$. For example, by comparing predictions of potential models to the measured values of the J/ψ , η_c , Υ , and B_c states one could use the prediction of the most reliable models [32, 34, 118, 119, 217] to estimate the mass of the $\eta_b(1S) = 9400 - 9410$ MeV.

7 SUMMARY

In the presence of much more accurate data, multipole expansions for both electromagnetic and hadronic transitions hold up well. The coefficients appearing in these expansions have been described in the past by a combination of potential models and perturbative QCD. As expected there are significant relativistic corrections for the charmonium system. The overall scales of these corrections are reduced for the $b\bar{b}$ system and are consistent with expectations from the NRQCD velocity expansion. Relativistic corrections are determined in the same framework as leading order terms. However, relativistic corrections have not improved markedly upon the nonrelativistic

treatments, though some qualitative patterns (such as hierarchies in electric dipole matrix elements) are reproduced.

Electromagnetic transitions for which the leading-order expansion coefficient is dynamically suppressed are particularly sensitive to relativistic corrections. For the $\Upsilon(3S) \rightarrow \chi_b(1P)$ E1 transitions there is a large cancellation in overlap amplitude because of the node in the $3S$ radial wavefunction. The result is a wide scatter of theoretical predictions. For the $\Upsilon(3S) \rightarrow \eta_b(1S)$ M1 transition, the overlap coefficient vanishes in leading order (a hindered transition). Here the experimental upper bound on the rate is smaller than expected in potential models for relativistic corrections. Modern theoretical tools (effective theories and nonperturbative lattice QCD) combined with more detailed high-statistics experimental data will help pin down the various relativistic corrections.

Decays described by perturbative QED or QCD, such as $\chi_{c0,2} \rightarrow (\gamma\gamma, gg)$, appear to behave as expected, yielding values of α_S for the most part consistent with other determinations. Exceptions (as in the case of the anomalously small J/ψ hadronic width) can be ascribed to large QCD or relativistic corrections or to neglected color-octet components of the wave function which are not yet fully under control.

Recent experiments have also observed a number of new hadronic transitions. Many details remain to be understood. The two-pion invariant mass distributions in both the $\Upsilon(3S) \rightarrow \Upsilon(1S) + 2\pi$ and $\Upsilon(4S) \rightarrow \Upsilon(2S) + 2\pi$ transitions do not show typically strong S -wave behavior. Perhaps some dynamical suppression plays a role in these transitions. To further complicate the situation, the $\Upsilon(4S) \rightarrow \Upsilon(1S) + 2\pi$ decay seems to show the usual S -wave behavior with the dipion spectrum peaked toward the highest effective masses.

Coupled-channel effects appear to be important in understanding quarkonium behavior, especially in such cases as the $X(3872)$ which lies right at the $D^0\bar{D}^{*0}$ threshold. It seems that long-awaited states such as “molecular charmonium” [with $X(3872)$ the leading candidate] and hybrids [perhaps such as $Y(4260)$] are making their appearance, and the study of their transitions will shed much light on their nature. Now that we are entering the era of precise lattice QCD predictions for low-lying quarkonium states, it is time for lattice theorists to grapple with these issues as well.

ACKNOWLEDGMENTS

Input from Frank Close, Richard Galik and Brian Heltsley is gratefully acknowledged. Fermilab is operated by Fermi Research Alliance, LLC under Contract No. DE-AC02-07CH11359 with the United States Department of Energy. This work was supported in part by the United States Department of Energy under Grant No. DE FG02 90ER40560, the Natural Sciences and Engineering Research Council of Canada, and the US National Science Foundation under cooperative agreement PHY-0202078.

References

- [1] W. Kwong, C. Quigg, and J. L. Rosner, *Ann. Rev. Nucl. Part. Sci.* **37**, 325 (1987).
- [2] W. Kwong and J. L. Rosner, *Phys. Rev. D* **38**, 279 (1988).
- [3] W. Kwong, P. B. Mackenzie, R. Rosenfeld, and J. L. Rosner, *Phys. Rev. D* **37**, 3210 (1988).
- [4] S. Godfrey and J. L. Rosner, *Phys. Rev. D* **64**, 074011 (2001). [Erratum-*ibid.* *D* **65**, 039901 (2002)].
- [5] S. Godfrey and J. L. Rosner, *Phys. Rev. D* **64**, 097501 (2001) [Erratum-*ibid.* *D* **66**, 059902 (2002)].
- [6] S. Godfrey and J. L. Rosner, *Phys. Rev. D* **66**, 014012 (2002).
- [7] N. Brambilla *et al.*, arXiv:hep-ph/0412158.
- [8] E. J. Eichten, K. Lane and C. Quigg, *Phys. Rev. D* **69**, 094019 (2004).
- [9] T. Barnes and S. Godfrey, *Phys. Rev. D* **69**, 054008 (2004).
- [10] E. J. Eichten, K. Lane and C. Quigg, *Phys. Rev. D* **73**, 014014 (2006) [Erratum-*ibid.* *D* **73**, 079903 (2006)].
- [11] T. Barnes, S. Godfrey and E. S. Swanson, *Phys. Rev. D* **72**, 054026 (2005).
- [12] E. Eichten, K. Gottfried, T. Kinoshita, J. B. Kogut, K. D. Lane and T. M. Yan, *Phys. Rev. Lett.* **34**, 369 (1975) [Erratum-*ibid.* **36**, 1276 (1976)]; E. Eichten, K. Gottfried, T. Kinoshita, K. D. Lane and T. M. Yan, *Phys. Rev. Lett.* **36**, 500 (1976); E. Eichten, K. Gottfried, T. Kinoshita, K. D. Lane and T. M. Yan, *Phys. Rev. D* **17**, 3090 (1978) [Erratum-*ibid.* *D* **21**, 313 (1980)]; *Phys. Rev. D* **21**, 203 (1980).
- [13] V. A. Novikov, L. B. Okun, M. A. Shifman, A. I. Vainshtein, M. B. Voloshin and V. I. Zakharov, *Phys. Rept.* **41**, 1 (1978).
- [14] T. Appelquist, R. M. Barnett and K. D. Lane, *Ann. Rev. Nucl. Part. Sci.* **28**, 387 (1978).
- [15] C. Quigg and J. L. Rosner, *Phys. Rept.* **56**, 167 (1979).
- [16] H. Grosse and A. Martin, *Phys. Rept.* **60**, 341 (1980).
- [17] S. F. Radford and W. W. Repko, arXiv:hep-ph/0701117.
- [18] C. Quigg and J. L. Rosner, *Phys. Lett. B* **71**, 153 (1977).

- [19] R. Van Royen and V. F. Weisskopf, *Nuovo Cim. A* **50**, 617 (1967) [Erratum-*ibid.* A **51**, 583 (1967)].
- [20] C. Quigg and J. L. Rosner, *Phys. Rev. D* **23**, 2625 (1981).
- [21] H. B. Thacker, C. Quigg and J. L. Rosner, *Phys. Rev. D* **18**, 274, (1978); *ibid.* **18**, 287 (1978); J. F. Schonfeld, W. Kwong, J. L. Rosner, C. Quigg and H. B. Thacker, *Annals Phys.* **128**, 1 (1980); W. Kwong and J. L. Rosner, *Prog. Theor. Phys. Suppl.* **86**, 366 (1986).
- [22] A. Gray *et al.*, *Phys. Rev. D* **72**, 094507 (2005).
- [23] J. L. Rosner *et al.* [CLEO Collaboration], *Phys. Rev. Lett.* **96**, 092003 (2006).
- [24] A. Messiah, "*Quantum Mechanics*", Dover Publications, Inc., Mineola, NY, USA (1999), p.554.
- [25] S. Bethke, arXiv:hep-ex/0606035. For a more recent review see S. Kluth, hep-ex/0609020, presented at XXXIII International Conference on High Energy Physics (ICHEP 06), Moscow, Russia, 2006, Proceedings edited by A. N. Sissakian and G. A. Kozlov, to be published by World Scientific, 2007.
- [26] M. Davier, A. Hoecker and Z. Zhang, arXiv:hep-ph/0701170.
- [27] C. T. H. Davies *et al.* [HPQCD Collaboration], *Phys. Rev. Lett.* **92**, 022001 (2004).
- [28] G. S. Bali, *Phys. Rept.* **343**, 1 (2001).
- [29] M. Koma, Y. Koma and H. Wittig, *PoS LAT2005*, 216 (2006) [arXiv:hep-lat/0510059]; Y. Koma and M. Koma, arXiv:hep-lat/0609078.
- [30] V. Zambetakis and N. Byers, *Phys. Rev. D* **28**, 2908 (1983).
- [31] H. Grotch, D. A. Owen and K. J. Sebastian, *Phys. Rev. D* **30**, 1924 (1984).
- [32] S. Godfrey and N. Isgur, *Phys. Rev. D* **32**, 189 (1985).
- [33] X. Zhang, K. J. Sebastian and H. Grotch, *Phys. Rev. D* **44**, 1606 (1991).
- [34] D. Ebert, R. N. Faustov and V. O. Galkin, *Phys. Rev. D* **67**, 014027 (2003).
- [35] T. A. Lahde, *Nucl. Phys.* **A714**, 183 (2003).
- [36] G. Feinberg and J. Sucher, *Phys. Rev. Lett.* **35**, 1740 (1975).
- [37] J. Sucher, *Rept. Prog. Phys.* **41**, 1781 (1978).
- [38] J. S. Kang and J. Sucher, *Phys. Rev. D* **18**, 2698 (1978).
- [39] P. Moxhay and J. L. Rosner, *Phys. Rev. D* **28**, 1132 (1983).

- [40] R. McClary and N. Byers, Phys. Rev. D **28**, 1692 (1983).
- [41] H. Grotch and K. J. Sebastian, Phys. Rev. D **25**, 2944 (1982).
- [42] A. J. F. Siegert, Phys. Rev. **52**, 787 (1937).
- [43] G. Karl, S. Meshkov and J. L. Rosner, Phys. Rev. D **13**, 1203 (1976); Phys. Rev. Lett. **45**, 215 (1980).
- [44] S. Godfrey, G. Karl and P. J. O'Donnell, Z. Phys. C **31**, 77 (1986).
- [45] K. J. Sebastian, H. Grotch and F. L. Ridener, Phys. Rev. D **45**, 3163 (1992).
- [46] A. Petrelli, M. Cacciari, M. Greco, F. Maltoni and M. L. Mangano, Nucl. Phys. B **514**, 245 (1998).
- [47] K. Gottfried, Phys. Rev. Lett. **40**, 598 (1978); G. Bhanot, W. Fischler and S. Rudaz, Nucl. Phys. B **155**, 208 (1979); M. E. Peskin, Nucl. Phys. B **156**, 365 (1979); G. Bhanot and M. E. Peskin, Nucl. Phys. B **156**, 391 (1979); M. B. Voloshin, Nucl. Phys. B **154**, 365 (1979).
- [48] T. M. Yan, Phys. Rev. D **22**, 1652 (1980).
- [49] Y. P. Kuang and T. M. Yan, Phys. Rev. D **24**, 2874 (1980).
- [50] W. E. Caswell and G. P. Lepage, Phys. Lett. B **167**, 437 (1986); G. T. Bodwin, E. Braaten and G. P. Lepage, Phys. Rev. D **51**, 1125 (1995) [Erratum-ibid. D **55**, 5853 (1997)]; M. E. Luke and A. V. Manohar, Phys. Rev. D **55**, 4129 (1997).
- [51] W. Buchmüller and S. H. H. Tye, Phys. Rev. Lett. **44**, 850 (1980).
- [52] L. S. Brown and R. N. Cahn, Phys. Rev. Lett. **35**, 1 (1975).
- [53] M. B. Voloshin, Phys. Rev. D **74**, 054022 (2006).
- [54] M. B. Voloshin, Sov. J. Nucl. Phys. **43**, 1011 (1986) [Yad. Fiz. **43**, 1571 (1986)]; Y. P. Kuang, S. F. Tuan and T. M. Yan, Phys. Rev. D **37**, 1210 (1988); Y. P. Kuang and T. M. Yan, Phys. Rev. D **41**, 155 (1990); Y. P. Kuang, Phys. Rev. D **65**, 094024 (2002); M. B. Voloshin, Phys. Lett. B **562**, 68 (2003); Y. P. Kuang, Front. Phys. China **1**, 19 (2006).
- [55] W. M. Yao *et al.* [Particle Data Group], J. Phys. G **33**, 1 (2006).
- [56] S. J. Brodsky, G. P. Lepage and P. B. Mackenzie, Phys. Rev. D **28**, 228 (1983).
- [57] J. J. Aubert *et al.* [BNL E598 Collaboration], Phys. Rev. Lett. **33**, 1404 (1974).
- [58] J. E. Augustin *et al.* [SLAC-SP-017 Collaboration], Phys. Rev. Lett. **33**, 1406 (1974).
- [59] V. M. Aulchenko *et al.* [KEDR Collaboration], Phys. Lett. B **573**, 63 (2003).

- [60] G. S. Adams *et al.* [CLEO Collaboration], Phys. Rev. D **73**, 051103 (2006).
- [61] B. Aubert *et al.* [BABAR Collaboration], Phys. Rev. D **69**, 011103 (2004).
- [62] J. Gaiser *et al.*, Phys. Rev. D **34**, 711 (1986).
- [63] J. J. Dudek, R. G. Edwards and D. G. Richards, Phys. Rev. D **73**, 074507 (2006).
- [64] N. Brambilla, Y. Jia and A. Vairo, Phys. Rev. D **73**, 054005 (2006)
- [65] Z. Li *et al.* [CLEO Collaboration], Phys. Rev. D **71**, 111103 (2005).
- [66] K. K. Seth, Phys. Rev. D **69**, 097503 (2004).
- [67] G. P. Lepage, CLNS-83/587, presented at the *1983 Int. Symp. on Lepton-Photon Interactions at High Energies, Ithaca, N.Y., August 4 – 9, 1983* using D. L. Scharre *et al.* [Mark II Collaboration], Phys. Rev. D **23**, 43 (1981).
- [68] F. Maltoni, arXiv:hep-ph/0007003, published in *Proceedings of “5th Workshop on Quantum Chromodynamics (QCD 2000)”, January 3 – 7, 2000, Villefranche-sur-Mer, France*, ed. H.M. Fried, B. Muller, and Y. Gabellini (World Scientific, Singapore, 2000), p. 301.
- [69] T. A. Armstrong *et al.* [E760 Collaboration], Phys. Rev. Lett. **68**, 1468 (1992).
- [70] M. Andreotti *et al.* [E835 Collaboration], Nucl. Phys. B **717**, 34 (2005).
- [71] M. Ablikim *et al.* [BES Collaboration], Phys. Rev. D **71**, 092002 (2005).
- [72] T. Appelquist, A. De Rujula, H. D. Politzer and S. L. Glashow, Phys. Rev. Lett. **34**, 365 (1975).
- [73] S. B. Athar *et al.* [CLEO Collaboration], Phys. Rev. D **70**, 112002 (2004).
- [74] N. E. Adam *et al.* [CLEO Collaboration], Phys. Rev. Lett. **94**, 232002 (2005).
- [75] W. Buchmüller and S. H. H. Tye, Phys. Rev. D **24**, 132 (1981).
- [76] S. N. Gupta, S. F. Radford and W. W. Repko, Phys. Rev. D **34**, 201 (1986).
- [77] M. Oreglia *et al.* [Crystal Ball Collaboration], Phys. Rev. D **25**, 2259 (1982).
- [78] M. Ambrogiani *et al.* [E835 Collaboration], Phys. Rev. D **65**, 052002 (2002).
- [79] D. Ebert, R. N. Faustov and V. O. Galkin, Mod. Phys. Lett. A **18**, 601 (2003).
- [80] S. Dobbs *et al.* [CLEO Collaboration], Phys. Rev. D **73**, 071101 (2006).
- [81] K. Abe *et al.* [Belle Collaboration], Phys. Lett. B **540**, 33 (2002).
- [82] M. Ambrogiani *et al.* [E835 Collaboration], Phys. Rev. D **62**, 052002 (2000).

- [83] M. Andreotti *et al.* [E835 Collaboration], Phys. Lett. B **584**, 16 (2004).
- [84] G. S. Abrams *et al.*, Phys. Rev. Lett. **33**, 1453 (1974).
- [85] T. A. Armstrong *et al.* [E760 Collaboration], Phys. Rev. D **47**, 772 (1993).
- [86] J. Z. Bai *et al.* [BES Collaboration], Phys. Lett. B **550**, 24 (2002).
- [87] M. Andreotti *et al.* [Fermilab E835 Collaboration], arXiv:hep-ex/0703012.
- [88] N. E. Adam *et al.* [CLEO Collaboration], Phys. Rev. Lett. **96**, 082004 (2006).
- [89] M. Ablikim *et al.* [BES Collaboration], Phys. Rev. D **70**, 012003 (2004).
- [90] M. Andreotti *et al.*, Phys. Rev. D **71**, 032006 (2005).
- [91] J. Z. Bai *et al.* [BES Collaboration], Phys. Rev. D **70**, 012006 (2004).
- [92] G. A. Miller, B. M. K. Nefkens and I. Slaus, Phys. Rept. **194**, 1 (1990).
- [93] B. L. Ioffe and M. A. Shifman, Phys. Lett. B **95**, 99 (1980); B. L. Ioffe and M. A. Shifman, Phys. Lett. B **107**, 371 (1981); Y. P. Kuang, S. F. Tuan and T. M. Yan, Phys. Rev. D **37**, 1210 (1988).
- [94] N. E. Adam *et al.* [CLEO Collaboration], Phys. Rev. Lett. **94**, 012005 (2005).
- [95] J. Z. Bai *et al.* [BES Collaboration], Phys. Rev. D **69**, 072001 (2004).
- [96] M. Ablikim *et al.* [BES Collaboration], Phys. Lett. B **619**, 247 (2005).
- [97] M. Ablikim *et al.* [BES Collaboration], Phys. Rev. D **70**, 112003 (2004).
- [98] M. Ablikim *et al.* [BES Collaboration], Phys. Rev. D **70**, 112007 (2004) [Erratum-*ibid.* D **71**, 019901 (2005)].
- [99] M. Ablikim *et al.* [BES Collaboration], Phys. Lett. B **614**, 37 (2005).
- [100] S. Dobbs *et al.* [CLEO Collaboration], Phys. Rev. D **74**, 011105 (2006).
- [101] R. A. Briere *et al.* [CLEO Collaboration], Phys. Rev. Lett. **95**, 062001 (2005).
- [102] T. K. Pedlar *et al.* [CLEO Collaboration], Phys. Rev. D **72**, 051108 (2005).
- [103] M. Ablikim *et al.* [BES Collaboration], arXiv:hep-ex/0610079.
- [104] J. L. Rosner *et al.* [CLEO Collaboration], Phys. Rev. Lett. **95**, 102003 (2005).
- [105] P. Rubin *et al.* [CLEO Collaboration], Phys. Rev. D **72**, 092004 (2005).
- [106] D. Cassel and J. L. Rosner, CERN Cour. **46N5**, 33 (2006).
- [107] M. Andreotti *et al.* [E835 Collaboration], Phys. Rev. D **72**, 032001 (2005).

- [108] F. Fang *et al.* [Belle Collaboration], Phys. Rev. D **74**, 012007 (2006).
- [109] T. Manke *et al.* [CP-PACS Collaboration], Phys. Rev. D **62**, 114508 (2000); M. Okamoto *et al.* [CP-PACS Collaboration], *ibid.* **65**, 094508 (2002).
- [110] J. Stubbe and A. Martin, Phys. Lett. B **271**, 208 (1991).
- [111] Y. P. Kuang, S. F. Tuan and T. M. Yan, Phys. Rev. D **37**, 1210 (1988).
- [112] C. Edwards *et al.* [Crystal Ball Collaboration], Phys. Rev. Lett. **48**, 70 (1982).
- [113] S. K. Choi *et al.* [Belle Collaboration], Phys. Rev. Lett. **89**, 102001 (2002).
- [114] K. Abe *et al.* [Belle Collaboration], Phys. Rev. Lett. **89**, 142001 (2002).
- [115] E. J. Eichten, K. Lane and C. Quigg, Phys. Rev. Lett. **89**, 162002 (2002).
- [116] D. M. Asner *et al.* [CLEO Collaboration], Phys. Rev. Lett. **92**, 142001 (2004).
- [117] B. Aubert *et al.* [BABAR Collaboration], Phys. Rev. Lett. **92**, 142002 (2004).
- [118] E. J. Eichten and C. Quigg, Phys. Rev. D **49**, 5845 (1994).
- [119] L. P. Fulcher, Phys. Rev. D **44**, 2079 (1991).
- [120] S. N. Gupta and J. M. Johnson, Phys. Rev. D **53**, 312 (1996).
- [121] J. Zeng, J. W. Van Orden and W. Roberts, Phys. Rev. D **52**, 5229 (1995).
- [122] A. Martin and J. M. Richard, Phys. Lett. B **115**, 323 (1982).
- [123] J. L. Rosner, Annals Phys. **319**, 1 (2005).
- [124] R. Chistov *et al.* [Belle Collaboration], Phys. Rev. Lett. **93**, 051803 (2004).
- [125] B. Aubert *et al.* [BABAR Collaboration], Phys. Rev. Lett. **96**, 052002 (2006).
- [126] M. Ablikim *et al.* [BES Collaboration], Phys. Rev. Lett. **97**, 121801 (2006).
- [127] M. Ablikim *et al.* [BES Collaboration], Phys. Lett. B **603**, 130 (2004).
- [128] R. A. Briere *et al.* [CESR-c Taskforce, CLEO-c Taskforce, and CLEO-c Collaboration], “CLEO-c and CESR-c: A New Frontier of Weak and Strong Interactions,” CLNS 01/1742 (unpublished) (2001).
- [129] D. Besson *et al.* [CLEO Collaboration], Phys. Rev. Lett. **96**, 092002 (2006).
- [130] Q. He *et al.* [CLEO Collaboration], Phys. Rev. Lett. **95**, 121801 (2005) [Erratum-*ibid.* **96**, 199903 (2006)].
- [131] M. Ablikim *et al.* [BES Collaboration], Phys. Lett. B **641**, 145 (2006).
- [132] M. Ablikim *et al.* [BES Collaboration], arXiv:hep-ex/0612056.

- [133] M. B. Voloshin, Phys. Atom. Nucl. **68**, 771 (2005) [Yad. Fiz. **68**, 804 (2005)] [arXiv:hep-ph/0402171].
- [134] J. L. Rosner, Phys. Rev. D **64**, 094002 (2001).
- [135] Y. P. Kuang, Phys. Rev. D **65**, 094024 (2002).
- [136] R. A. Briere *et al.* [CLEO Collaboration], Phys. Rev. D **74**, 031106 (2006).
- [137] Y. P. Kuang, Front. Phys. China **1**, 19 (2006) [arXiv:hep-ph/0601044].
- [138] J. Z. Bai *et al.* [BES Collaboration], Phys. Lett. B **605**, 63 (2005).
- [139] T. E. Coan *et al.* [CLEO Collaboration], Phys. Rev. Lett. **96**, 182002 (2006).
- [140] G. S. Adams *et al.* [CLEO Collaboration], Phys. Rev. D **73**, 012002 (2006).
- [141] Y. S. Zhu for the BES Collaboration, presented at the *11th International Conference on Hadron Spectroscopy (Hadron05)*, Rio de Janeiro, Brazil, 21 – 26 August, 2005, AIP Conf. Proc. **814**, 580 (2006).
- [142] M. Ablikim *et al.* [BES Collaboration], Phys. Rev. D **70**, 077101 (2004).
- [143] D. Cronin-Hennessy *et al.* [CLEO Collaboration], Phys. Rev. D **74**, 012005 (2006).
- [144] G. S. Huang *et al.* [CLEO Collaboration], Phys. Rev. Lett. **96**, 032003 (2006).
- [145] K. K. Seth, Phys. Rev. D **72**, 017501 (2005).
- [146] S. Eidelman *et al.* [Particle Data Group], Phys. Lett. B **592**, 1 (2004).
- [147] T. Barnes, Int. J. Mod. Phys. A **21**, 5583 (2006).
- [148] T. E. Coan *et al.* [CLEO Collaboration], Phys. Rev. Lett. **96**, 162003 (2006).
- [149] J. L. Rosner, 25th International Symposium on Physics in Collision (PIC 05), AIP Conf. Proc. **815**, 218 (2006).
- [150] S. Godfrey, in *Proceedings of the Fourth International Conference on Flavor Physics and CP Violation (FPCP 2006)*, April 9 - 12, 2006 Vancouver, B.C., Canada, eConf **C060409**, 221 (2006) [arXiv:hep-ph/0605152].
- [151] E. Swanson, presented at the *Conference on the Intersections of Particle and Nuclear Physics (CIPANP 2006)*, Rio Grande, Puerto Rico, May 30 – June 3, 2006, AIP Conf. Proc. **870**, edited by T. M. Liss, p. 349.
- [152] S. K. Choi *et al.* [Belle Collaboration], Phys. Rev. Lett. **91**, 262001 (2003).
- [153] B. Aubert *et al.* [BaBar Collaboration], Phys. Rev. D **71**, 071103 (2005).
- [154] D. Acosta *et al.* [CDF II Collaboration], Phys. Rev. Lett. **93**, 072001 (2004).

- [155] V. M. Abazov *et al.* [D0 Collaboration], Phys. Rev. Lett. **93**, 162002 (2004).
- [156] B. Aubert *et al.* [BaBar Collaboration], Phys. Rev. D **71**, 031501 (2005).
- [157] S. Dobbs *et al.* [CLEO Collaboration], Phys. Rev. Lett. **94**, 032004 (2005).
- [158] B. Aubert *et al.* [BaBar Collaboration], Phys. Rev. Lett. **96**, 052002 (2006).
- [159] B. Aubert *et al.* [BaBar Collaboration], Phys. Rev. D **74**, 071101 (2006).
- [160] K. Abe *et al.* [Belle Collaboration], Belle report BELLE-CONF-0540, arXiv:hep-ex/0505037, paper no. LP-2005-175, contributed to the *XXII International Symposium on Lepton-Photon Interactions at High Energy*, Uppsala, Sweden, June 30 – July 5, 2005.
- [161] B. Aubert *et al.* [BABAR Collaboration], Phys. Rev. Lett. **93**, 041801 (2004).
- [162] G. Gokhroo *et al.* [Belle Collaboration], Phys. Rev. Lett. **97**, 162002 (2006).
- [163] C. Cawlfeld *et al.* [CLEO Collaboration], Phys. Rev. Lett. **98**, 092002 (2007).
- [164] J. L. Rosner, Phys. Rev. D **70**, 094023 (2004).
- [165] K. Abe *et al.* [Belle Collaboration], Belle report BELLE-CONF-0541, arXiv:hep-ex/0505038, paper no. LP-2005-176, contributed to the *XXII International Symposium on Lepton-Photon Interactions at High Energy*, Uppsala, Sweden, June 30 – July 5, 2005.
- [166] A. Abulencia *et al.* [CDF Collaboration], Phys. Rev. Lett. **98**, 132002 (2007).
- [167] H. Marsiske, in *Proceedings of the Fourth International Conference on Flavor Physics and CP Violation (FPCP 2006), April 9 - 12, 2006 Vancouver, B.C., Canada*, eConf **C060409**, 211 (2006) [arXiv:hep-ex/0605117].
- [168] I. Kravchenko, in *Proceedings of the Fourth International Conference on Flavor Physics and CP Violation (FPCP 2006), April 9 - 12, 2006 Vancouver, B.C., Canada*, eConf **C060409**, 222 (2006) [arXiv:hep-ex/0605076].
- [169] D. Ebert, R. N. Faustov and V. O. Galkin, Phys. Lett. B **634**, 214 (2006).
- [170] F. E. Close and P. R. Page, Phys. Lett. B **578**, 119 (2004); N. A. Tornqvist, arXiv:hep-ph/0308277; E. S. Swanson, Phys. Lett. B **588**, 189 (2004); *ibid.* **598**, 197 (2004).
- [171] S. Uehara *et al.* [Belle Collaboration], Phys. Rev. Lett. **96**, 082003 (2006).
- [172] Barnes, Godfrey, and Swanson [11] obtain similar results when the 2^3P_2 mass is rescaled to 3930 MeV. See E. Swanson, AIP Conf. Proc. **814**, 203 (2006) [Int. J. Mod. Phys. A **21**, 733 (2006)].

- [173] T. Barnes, Oak Ridge National Laboratory Report No. ORNL-CCIP-92-05; Invited paper at *Int. Workshop on Photon-Photon Collisions, La Jolla, CA, March 22 – 26, 1992*.
- [174] K. Abe *et al.* [Belle Collaboration], Phys. Rev. Lett. **94**, 182002 (2005).
- [175] H. Severini *et al.* [CLEO Collaboration], Phys. Rev. Lett. **92**, 222002 (2004).
- [176] K. Abe *et al.* [Belle Collaboration], Phys. Rev. Lett. **98**, 082001 (2007).
- [177] B. Aubert *et al.* [BaBar Collaboration], Phys. Rev. Lett. **95**, 142001 (2005).
- [178] Q. He *et al.* [CLEO Collaboration], Phys. Rev. D **74**, 091104 (2006).
- [179] K. Abe *et al.* [Belle Collaboration], arXiv:hep-ex/0612006.
- [180] B. Aubert *et al.* [BABAR Collaboration], Phys. Rev. D **73**, 011101 (2006).
- [181] B. Heltsley for the CLEO Collaboration, presented at the *2006 Quarkonium Working Group Meeting*, Brookhaven Natl. Lab., June 27 – 30, 2006.
- [182] B. Aubert *et al.* [BABAR Collaboration], Phys. Rev. D **73**, 012005 (2006).
- [183] S. J. Gowdy, presented at the *41st Rencontres de Moriond: QCD and Hadronic Interactions*, La Thuile, Italy, 18 – 25 March 2006, arXiv:hep-ex/0605086.
- [184] S. Ye for the BaBar Collaboration, presented at the *2006 Quarkonium Working Group Meeting*, Brookhaven Natl. Lab., June 27 – 30, 2006.
- [185] F. J. Llanes-Estrada, Phys. Rev. D **72**, 031503 (2005).
- [186] L. Maiani, V. Riquer, F. Piccinini and A. D. Polosa, Phys. Rev. D **72**, 031502 (2005).
- [187] S. L. Zhu, Phys. Lett. B **625**, 212 (2005).
- [188] F. E. Close and P. R. Page, Phys. Lett. B **628**, 215 (2005).
- [189] E. Kou and O. Pène, Phys. Lett. B **631**, 164 (2005).
- [190] See, for example, T. Barnes, F. E. Close and E. S. Swanson, Phys. Rev. D **52**, 5242 (1995), and references therein.
- [191] P. Lacock, C. Michael, P. Boyle and P. Rowland [UKQCD Collaboration], Phys. Lett. B **401**, 308 (1997).
- [192] C. McNeile, C. Michael and P. Pennanen [UKQCD Collaboration], Phys. Rev. D **65**, 094505 (2002)
- [193] J. L. Rosner, Phys. Rev. D **74**, 076006 (2006).

- [194] X. Liao and T. Manke, Columbia University Report No. CU-TP-1063, arXiv:hep-lat/0210030.
- [195] B. Aubert *et al.* [BaBar Collaboration], presented at *33rd International Conference on High Energy Physics (ICHEP 06)*, *op. cit.* SLAC Report SLAC-PUB-12155, arXiv:hep-ex/0610057, submitted to Phys. Rev. Letters.
- [196] M. Artuso *et al.* [CLEO Collaboration], Phys. Rev. Lett. **94**, 032001 (2005).
- [197] G. Peter Lepage, Ann. Phys. **315**, 193 (2005).
- [198] D. Besson *et al.* [CLEO Collaboration], Phys. Rev. D **74**, 012003 (2006).
- [199] C. Cawfield *et al.* [CLEO Collaboration], Phys. Rev. D **73**, 012003 (2006).
- [200] B. Aubert *et al.* [BABAR Collaboration], Phys. Rev. Lett. **96**, 232001 (2006).
- [201] A. Sokolov *et al.* [Belle Collaboration], arXiv:hep-ex/0611026, to appear in Phys. Rev. D (Rapid Communication).
- [202] G. S. Adams *et al.* [CLEO Collaboration], Phys. Rev. Lett. **94**, 012001 (2005).
- [203] T. Skwarnicki for the CLEO Collaboration, presented at *40th Rencontres de Moriond On QCD and High Energy Hadronic Interactions*, 12 – 19 March 2005, La Thuile, Aosta Valley, Italy, arXiv:hep-ex/0505050.
- [204] D. Besson *et al.* [CLEO Collaboration], Phys. Rev. Lett. **98**, 052002 (2007).
- [205] L. P. Fulcher, Phys. Rev. D **42**, 2337 (1990).
- [206] A. Grant and J. L. Rosner, Phys. Rev. D **46**, 3862 (1992).
- [207] D. Cinabro *et al.* [CLEO Collaboration], arXiv:hep-ex/0207062, CLEO-CONF-02-07, ICHEP-02-ABS-949, contributed to *31st International Conference on High Energy Physics (ICHEP 2002)*, Amsterdam, The Netherlands, 24 – 31 July, 2002.
- [208] G. Bonvicini *et al.* [CLEO Collaboration], Phys. Rev. D **70**, 032001 (2004)
- [209] V. Fonseca *et al.* [CUSB Collaboration], Nucl. Phys. **B242**, 31 (1984).
- [210] I. C. Brock *et al.* [CLEO Collaboration], Phys. Rev. D **43**, 1448 (1991).
- [211] M. B. Voloshin, Mod. Phys. Lett. A **19**, 2895 (2004).
- [212] F. Butler *et al.* [CLEO Collaboration], Phys. Rev. D **49**, 40 (1994).
- [213] B. Aubert *et al.* [BABAR Collaboration], Phys. Rev. D **72**, 032005 (2005).
- [214] M. B. Voloshin, JETP Lett. **21**, 347 (1975) [Pisma Zh. Eksp. Teor. Fiz. **21**, 733 (1975)].

- [215] M. Aoki for the CDF Collaboration, presented at *2006 Quarkonium Working Group Meeting*, Brookhaven Natl. Lab., June 27 – 30, 2006, updating W. Wester, Nucl. Phys. B Proc. Suppl. **156**, 240 (2006); A. Abulencia *et al.*, Phys. Rev. Lett. **96**, 082002 (2006).
- [216] I. F. Allison, C. T. H. Davies, A. Gray, A. S. Kronfeld, P. B. Mackenzie and J. N. Simone [HPQCD Collaboration], Phys. Rev. Lett. **94**, 172001 (2005).
- [217] L. P. Fulcher, Phys. Rev. D **60**, 074006 (1999).